Visualize the Intrinsic and Extrinsic Processes that Determine the Patterns of Human Mortality

Ting Li

A dissertation
submitted in partial fulfillment of the
requirements for the degree of

Doctor of Philosophy

University of Washington

2011

Program Authorized to Offer Degree:
Quantitative Ecology and Resource Management

University of Washington
Graduate School

This is to certify that I have examined this copy of a doctoral dissertation by

Ting Li

And have found that it is complete and satisfactory in all respects,
and that any and all revisions required by the final
examining committee have been made.

Chair of the Supervisory Committee:

_____
James J. Anderson

Reading Committee:

_____
James J. Anderson

_____
Peter Guttorp

_____
Samuel Clark

Date:_____.

In presenting this dissertation in partial fulfillment of the requirements for the doctoral degree at the University of Washington, I agree that the Library shall make its copies freely available for inspection. I further agree that extensive copying of the dissertation is allowable only for scholarly purposes, consistent with "fair use" as prescribed in the U.S. Copyright Law. Requests for copying or reproduction of this dissertation may be referred to ProQuest Information and Learning, 300 North Zeeb Road, Ann Arbor, MI 48106-1346, 1-800-521-0600, to whom the author has granted "the right to reproduce and sell (a) copies of the manuscript in microform and/or (b) printed copies of the manuscript made from microform."

Signature _____

Date _____

University of Washington

Abstract

Visualize Intrinsic and Extrinsic Processes that Determine the Patterns of Human Mortality

Ting Li

Chair of the Supervisory Committee:
Professor James J. Anderson
Quantitative Ecology and Resource Management

Over life, the accumulation of small day-to-day processes associated with behavior, nutrition, health care, stress and other events contribute, in sum, to mortality. A biology-motivated framework is developed in this work to quantify these contributions through two stochastic processes: an intrinsic process defining the survival capacity (i.e. vitality) of an organism declines stochastically to a zero-boundary, and an extrinsic process representing the occurrence of external stresses. Each of the two components is represented parsimoniously using relations that strongly reflect the general mechanisms underlying the killing processes. The model is demonstrated to be able to fit the mortality data of entire human life, provide biologically meaningful explanations for the observed mortality patterns, and conduct mechanism-based mortality partition. Finally, the ability to analyze historical mortality patterns through process-based parameters and explain the irregular patterns from other models (i.e. Strehler and Mildvan general theory of aging and mortality) helps address fundamental questions in demography, such as how the dynamics of environmental and physiological interactions change over time.

TABLE OF CONTENTS

LIST OF FIGURES

LIST OF TABLES

ACKNOWLEDGEMENTS

The author wishes to thank the Bonneville Power Administration and the Center of Statistics and Social Science at University of Washington who fund this work, and the program of Quantitative Ecology and Resource Management who provides extended long-term resource and support for this work. In particular, I would like to express sincere appreciation to my mentor Professor James J. Anderson for his vast reserve of patience, knowledge, and help in all aspects of my Ph. D. studies. Also, this dissertation would never have been completed without the encouragement and devotion of my family and friends.

Chapter I: Introduction

1.1 In Search for a Law

In the past 200 hundred years, history has witnessed so many great achievements attained by human beings. Perhaps one of the most exciting achievements is that the average life expectancy of human beings has doubled from about 35 years to 70 years (Gurven and Fenelon 2009). This accomplishment is so inspiring that great efforts have been put into investigating the reasons behind such a dramatic improvement (Acsádi and Nemeskéri 1970; Kunitz 1984; Hacker 1997; Cutler, Deaton et al. 2006). More interestingly, we are eager to know whether there is a limit to the extension of human longevity (Manton, Stallard et al. 1991; Oeppen and Vaupel 2002; Bongaarts 2006; Vaupel 2010). However, answering these questions relies on a fundamental issue: why death and senescence happen?

As one of the greatest mysteries in the human history, the mechanisms underlying death and senescence attract scholars from a wide range of fields. The focus have unique to the individual fields. Biochemists have explored the free radical theory as a cause of senescence, molecular biologists have focused on telomere attrition, evolutionary biologist have investigated the age dependent forces of natural selection, and demographers have concentrated on illuminating functional forms underlying survivorship curves. In the field of demography, interests in age-specific mortality trajectory of human beings are largely aroused by its highly regular yet complex pattern, which is believed to be informative, reflecting the combined effects of natural aging with environmental insults (Neafsey 2008).

Characterizing and understanding how the pattern of human mortality changes with age has been of great interest since the astronomer Edmond Halley (1694) constructed age-specific life tables for the city of Breslau in Silesi, now the city of Wrochlaw in Poland. After that the modern life table developed by the early British actuaries helped further reveal an approximately exponential increase in mortality with age (Gompertz 1825), in particular between age 30 and 80. With the advance of mathematical techniques and the improvement in the accuracy of death registration, the age-specific mortality pattern can be represented in more details. It is astonishing that the general features in this pattern have persisted over the centuries, in spite of the significant increase in human longevity.

In particular, the pattern of human survival in both cohort and period lifespan data can be characterized by four visually distinct features when the log of the age-specific mortality rate $\log(\mu)$ is plotted against age x (Fig. 1.1). The most dominant feature is the slope in curve which is typically characterized as linear, such that the mortality rate increases exponentially with age. The other persistent features of the curve characterize departures from the linear slope. An early age "hook" in the curve characterizes higher child mortality, an "elbow" characterizes a distinct increase in the curve slope at middle age and a "plateau" characterizes a leveling off of the mortality rate at old age. Besides these primary features, the curve sometimes has a pronounced secondary feature, a "hump", known as the mortality peak at young adulthood (Fig. 1.1B). It is classified as a secondary feature, because, albeit widely observed, the pattern is not evident in all populations (Gage and Mode 1993). To resolve the mortality pattern, endeavors in two perspectives are essential. One is to fit the important elements of mortality curves and the

other is to explain the shape through biologically meaningful processes. Historically, a variety of models or so called theories and laws have been developed to address the mortality patterns emphasizing one or both of the perspectives.

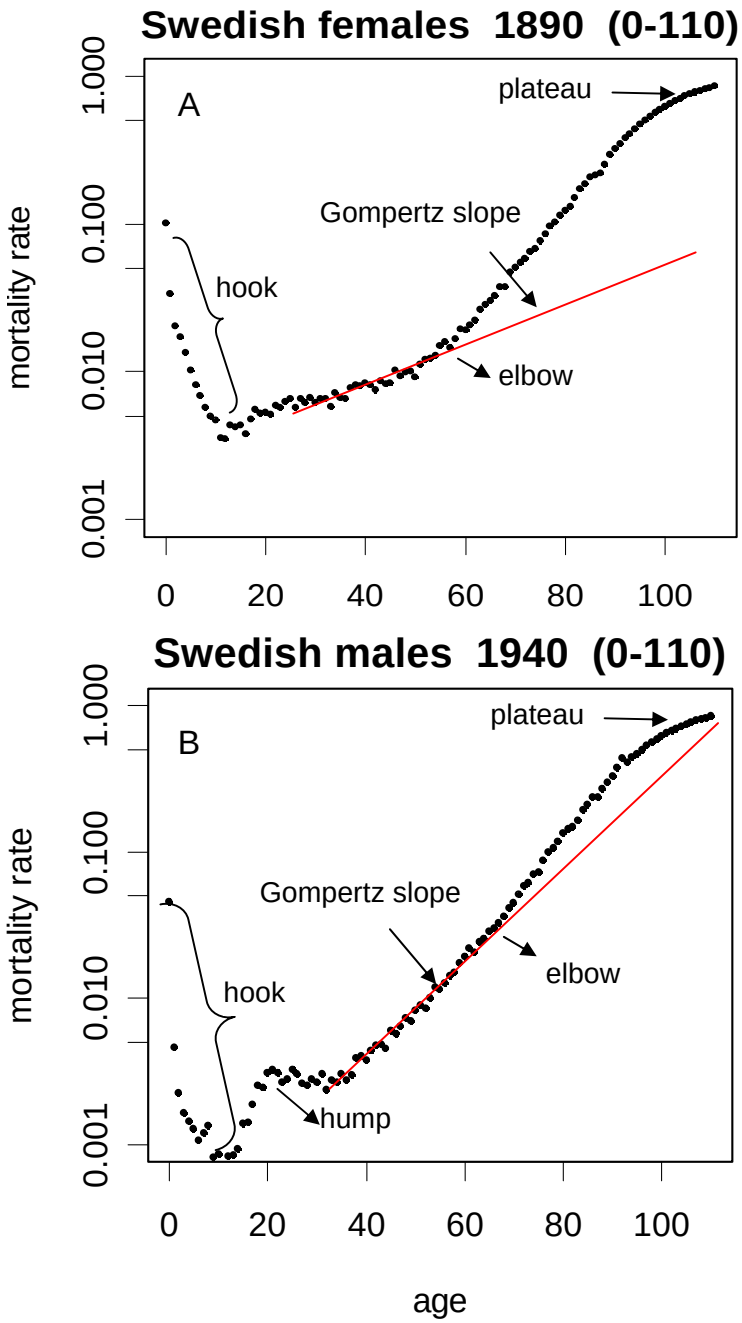

Figure 1.1: Mortality rate in log scale against age for period Swedish females at year 1890 (A) and period Swedish males at year 1940 (B) (data source: Human mortality database (HMD 2010)). The general trend in mortality can be described by a linear increase with age, designated here the "Gompertz slope". Deviations from the linear slope can characterized by three primary anomalies: an early age "hook", middle age "elbow" and old age "plateau" and a second feature, young adult "hump", significantly evident in the plot (B) only.

Gompertz (1825) was the first to consider the pattern of mortality and proposed that to a reasonable degree the mortality rate can be expressed as an exponential function of age as $\mu(x) = a\exp(bx)$. The log form, $\log \mu(x) = \log a + bx$, yields the first feature of Fig. 1, a linear increase in log mortality with slope *b*. The major contributions of Gompertz were in defining the increase in mortality with age which usually occurs within middle age span and proposing that there exists a general mechanism behind death. So fundamental were these ideas that his model was assumed to be the law of mortality. It quickly became a paradigm and to this day it is widely applied to mortality data due to its simplicity and universal applicability. The model is generally applied to truncated human mortality data starting from age 30 or 40 to avoid addressing the childhood "hook". However, in spite of, or because of, its simplicity and stature, controversies have surrounded the law since it was proposed 175 years ago (Carnes, Olshansky et al. 1996; Olshansky and Carnes 1997). The Gompertz law, based on the instantaneous rate of mortality, is challenged as lacking a plausible mechanism (Bonneux 2003; Rauser, Mueller et al. 2006). Although Gompertz suggested at the same time that an unspecific force might destroy the material of organization necessary for life, the connection between this force and mortality rates is vague and makes the concept of an instantaneous mortality rate elusive and biologically tenuous (Aalen and Gjessing 2001; Li and Anderson 2009). Most importantly, a focus on the mortality event itself implicitly disregards the fact that, as Aalen and Gjessing (2001) note, "apart from pure accidents, mortality events do not happen out of the blue, they are the endpoint of some process that develops with age". Additionally, the observed anomalies away from the exponential increase, in particular, the old age "plateau" limit the universality of the Gompertz

equation (Golubev 2009). However, despite its inadequacies, the law remains highly influential and has stimulated a variety of studies that have attempted to either improve the model or propose alternative theories for the senesces and death (Olshansky and Carnes 1997).

The first significant improvement to the Gompertz law was made by Makeham (1860) who added a constant term to the age-dependent mortality rate. The Makeham-Gompertz model $\mu(x) = A + a\exp(bx)$ efficiently increases the goodness-of-fit to empirical mortality data. The Makeham term accounts for the up-bending trend for the truncated mortality curve (starting from age 30), and thus partially explains the "elbow" (Fig.1.1). Nevertheless, the biological sense of the constant term is largely unresolved (Carnes, Olshansky et al. 1996; Golubev 2004; Carnes, Holden et al. 2006; Golubev 2009). The initial interpretation, treating the constant term as accidental mortality independent of age and the other part as senescence related mortality (Makeham 1860), lacks biological justification and thus is considered as inappropriate (Carnes, Olshansky et al. 1996; Carnes, Holden et al. 2006).

The Strheler-Mildvan (SM) general theory of mortality and aging (Strehler and Mildvan 1960) proposes a biological explanation for the Gompertz law, though the theory is not designed to improve the model fit. To overcome the inadequacy in the theory of the Gompertz law, Strehler and Mildvan (1960) used an analogy to chemical kinetics (Golubev 2009) in which the increase in the age-specific mortality rate results from the interaction between the internal energy reserves of the organism and the external energy demands from environmental insults. They defined the term "vitality" as the organism's capacity to remain alive and assumed that vitality declined linearly with age.

Death occurs when the external challenge exceeds the remaining vitality and the distribution of challenge magnitudes is assumed to follow a Maxwell-Boltzmann distribution. An essential finding of the SM theory, known as the SM correlation, is a negative correlation between the Gompertz parameters *a* and *b*. Despite the fact that the SM theory has appealing and intuitive elements, it does not resolve the arguments surrounding the Gompertz law. Firstly, because the SM theory is based on the Gompertz equation, the dimensionality of the model is simply too small. Artificial constraints must be put on some of the underlying coefficients to estimate the others, e.g. the vitality decline rate (this will be illustrated in later chapters in detail). The Gompertz parameters derived for recent mortality data exhibit significant deviations from the SM correlation (Krementsova and Konradov 2001; Yashin, Begun et al. 2001; Yashin, Begun et al. 2002) and Yashin et al. (2001) has suggested that this new trend "requires a revision of traditional gerontological concepts". Secondly, the SM theory is only designed to interpret the exponential rise in age-specific mortality rate and thus is inadequate to address the pattern over the entire lifespan. Finally, since the vitality in SM theory is defined in a deterministic way, it is unable to account the heterogeneity of a population which has a significant effect on patterns of mortality with age (Vaupel, Manton et al. 1979; Vaupel, Carey et al. 1998; Zens and Peart 2003; Benton, Plaistow et al. 2006; Saccheri and Hanski 2006; Anderson, Gildea et al. 2008; Li and Anderson 2009).

To specifically address how heterogeneity affects population mortality, the concept of frailty, which denotes the susceptibility to death, was introduced by Vaupel et al. (Vaupel, Manton et al. 1979). The idea is that individuals possess different frailties at birth which results in the more frail individuals tending to die earlier and the less frail, i.e.

robust, individuals surviving to old age. One substantial achievement of the frailty model is its ability to capture the mortality "plateau". The slowing down of mortality at old ages is explained as the consequence of systematic selection of robust individuals in old age. However, the shape of the mortality curve and the occurrence of the plateau depend on the distribution of fragility at birth. In the frailty model, this distribution is expressed by describing the Gompertz parameter, *a*, through a gamma distribution which further improves the model fit to the age-specific mortality rate at old ages, and provides new insight into the mortality process. But as an affiliate to an existing model, the frailty framework is not a completely independent theory that explains why mortality happens. In addition, the heterogeneity is incorporated into the population as a fixed level, such that the frailty model is inadequate to represent the survival differences evolving with age.

The Heligman-Pollard model (1980) is one of the best known models that attempt to model mortality over all ages (Thiele 1872; Wittstein 1883; Siler 1979; Gage 1988; Gage 1993). In the Heligman-Pollard model, the mortality pattern is divided into three stages: childhood, young adult and old age, each of which is characterized by 2 or 3 parameters making a total of 8 parameters. The model successfully fits the general mortality pattern including the childhood "hook", the middle age "elbow" and the old age "plateau". It also captures secondary features such as the mortality "hump" observed in young adult stage of period data mostly in the first half of 20^{th} century. In spite of its extraordinary performance in fitting data, the model does not explain the mortality patterns, because it lacks a biological basis connecting the model parameters to the mechanism of death. Besides, the gradual disappearance of the mortality "hump" in the

data of recent years makes it hard for the model to differentiate the stages of young adult and old age designed by its original structure (Heligman and Pollard 1980).

The models discussed above are formulated differently, but all take the Gompertz approach which characterizes the change of mortality rate with age. Meanwhile, several non-Gompertzian models or theories also make significant contributions in describing the temporal nature of mortality. Nevertheless, they mainly focus on a biological interpretation of the rise in mortality rate starting from middle ages along with an explanation for the old age mortality "plateau".

The reliability theory makes an analogy between biological aging and system failure (Gavrilov, Gavrilova et al. 1978; Gavrilov and Gavrilova 1991; Gavrilov and Gavrilova 2001; Gavrilov and Gavrilova 2004). The term "redundancy" is introduced as a key for understanding the systemic nature of aging. In systems with redundant irreplaceable elements, the elements deteriorate over time, even if they are built of non-aging elements. Within this framework, the exponential rise of mortality rates with age is explained by taking into account initial flaws in newly formed system and the late-life mortality deceleration is explained in terms of the loss of redundant elements over the life course.

The evolutionary theory for aging can be traced back to as early as 1891, when Weismann proposed that aging was a product of evolution (Weismann 1891). Modern theories of evolutionary aging (Hamilton 1966; Haldane 1990; Rose 1991; Rose, Burke et al. 2008) express the temporal increase in mortality as the declining force of natural selection. In addition, the old age deceleration in mortality is interpreted as the

consequence that “natural selection does not discriminate among genetic effects that act at very late ages which have had no impact on fitness during the evolutionary history of a population” (Rose, Burke et al. 2008).

Finally, a group of models based on a killing Markov process provides an alternative theory for understanding age-specific mortality patterns. Those models express mortality through the process point-of -view. They characterizes the first passage time of a random abstract measure of survival capacity, i.e. vitality, to an absorbing boundary representing death. Thus, the age-dependent increase in mortality results from the stochastic depletion of survival capacity. The model was first proposed half a century ago (Sacher 1956) and used to address some other applications (Chhikara and Folks 1989). Anderson (Anderson 1992; Anderson 2000; Anderson, Gildea et al. 2008) was the first to apply the concept in organism survival incorporating with a vitality-independent random killing. This expresses mortality in terms of an intrinsic process (vitality) and an extrinsic process (vitality-independent). The intrinsic vitality-only part of the model was also independently proposed by Weitz and Frazer (2001) and Aalen and Gessing (2001). Its mathematical properties have been further developed by Steinsaltz and Evans (2004; Steinsaltz and Evans 2007) and Anderson et al. (2008). The recent advance is suggested by Li and Anderson (2009) to include the initial population heterogeneity. Under this framework, the mortality plateau is then represented as the genetic consequence of Markov process reaching a quasistationary distribution (Weitz and Fraser 2001; Steinsaltz and Evans 2004; Steinsaltz and Evans 2007; Li and Anderson 2009).

Although all the developments since the Gompertz provide their own insights to the mortality process, none of them attempt to consider the pattern of human mortality

over the entire life span, i.e., to account for the exponential increase, or Gompertz rise, as well as the three primary anomalies (hook, elbow, plateau). Compared to the old age mortality "plateau", the childhood "hook", is deliberately avoided by many studies via left truncating mortality curves, whereas the middle age "elbow" is largely under-addressed. The "hook" and "elbow" deserve explanations in their turn. It is argued that the early stage mortality is mainly caused by external force (Carnes, Holden et al. 2006), and thus carries less information regarding to the aging process. However, the mortality curve as a whole should consistently reflect the interaction between the internal and the external forces. The early death pattern plays an important role in differentiating effects from senescence and environmental insults which are often comingled. Moreover, information obtained from the truncated mortality curves is biased by excluding a significant portion of the lifespan where natural selection acts, i.e. in childhood. Since the individuals who die at early life stage may be internally frailer, the physiological properties, e.g. the degree of frailty of the population, summarized from the incomplete mortality curve may be biased. Last but not least, any shifts in the mortality patterns result from continuous changes at both physiological and non-physiological levels, such that simply truncating the curve disconnects the underlying associations.

1.2 The Goal of the Work

In general, it is necessary to search for a new framework that expresses mortality through biologically meaningful processes, consistently accounts for the patterns through the entire life period, and especially has logical explanations for all the features. The goal of this work is to develop such a model that helps better understand the process of aging and mortality. The new framework does not necessarily come out of the blue, but could be

developed from historical works, which have their essential merits from a certain perspective. In particular, the Markov killing process model with constant extrinsic mortality rate (vitality model) developed by Anderson (1992; 2000; 2008) and Li and Anderson (2009) not only explicitly expresses the intrinsic process, but also sets up a two-process view to look at the death dynamics. However, the reason that the model fails to capture the early-age hook and middle-age elbow is probably because its extrinsic killing process is too simple. Meanwhile, the SM theory, in spite of a simple and unrealistic intrinsic form, provides a logical connection between the intrinsic and extrinsic forces. Therefore, the idea of further developing the stochastic vitality model by including an extrinsic process of SM style emerges naturally. Nevertheless, it will not be simply a version of adding the two models together, but a multi-process view to understand and quantify mortality into two processes: the intrinsic vitality process and the extrinsic challenge process which work simultaneously to shape the population mortality trajectory. I designate this model the Intrinsic-Extrinsic-Vitality model (IEV).

The rest of the dissertation is organized by five chapters. Chapter II explicitly illustrates the construction of the IEV model and explores some of the model properties including the ability of explaining the primary characteristics of age-specific human mortality patterns. Chapter III further demonstrates two unique features of the model as well as their applications: the heterogeneity structure and the mortality partition. Chapter IV exhibits how the model parameters can be used to resolve the complexity of mortality and help explore the historical patterns of survival through biological meaningful perspectives. Chapter V compares the IEV model with other established mortality models such as the Siler model (Siler 1979), the Heligman-Pollard (HP) mortality law (Heligman

and Pollard 1980) and the Strheler-Mildvan (SM) general theory of mortality (Strehler and Mildvan 1960). Chapter IV explores the potential misspecifications of the model and assesses how that would affect the estimated parameter patterns. And the final chapter discusses the limitations, the potential extensions and the future directions of the model.

Chapter II: Model Construction and Model Properties

2.1 The Concept of Vitality

First of all, a fundamental term needs to be clarified. Both the SM theory and Markov killing models are constructed on an abstract concept, *vitality*, which is a single variable summarizing the actions of many mechanisms working together. It is an ensemble measure of the degenerative and rebuilding processes that occur with age and result ultimately in senescence and death (Anderson 2000). The assumption that vitality declines with age relies on ample biological evidences. Shock (1957) has made extensive cross-sectional studies on physiological functions of man at different ages (Shock 1957; Strehler and Mildvan 1960). These studies conclude that most of the functions decrease approximately linearly with age in a rate between 0.5 and 1.3 percent per year, including nerve cell velocity, basal metabolic rate, cardiac output, glomerular filtration rate, standard plasma flow of the kidney, and vital capacity and maximal breathing capacity of lung. With the advance of science, the aging related degradations were further examined at molecular level such as the accumulation of faulty cells due to the mistranscription of messenger RNA (Wiegel, Beier et al. 1973), free radicals that produce oxidative damage (Beckman and Ames 1998; Ashok and Ali 1999; Ungvari, Kaley et al. 2010), minute impairments to the immune and neuronal endocrine systems (Yin and Chen 2005), shortening of telomeres important for chromosome replication and protection (Passos, Saretzki et al. 2007), and activation of a gene controlling proliferation of stem cells involved with tissue repair and regeneration (Janzen, Forkert et al. 2006).

Representing the day-to-day damage accumulations as a single variable, i.e. *vitality*, has the advantage of not needing to explicitly consider the individual

mechanisms and how they affect senescence and death. Summarizing the aging related effects together makes the model mathematically tractable. Therefore, the introduction of the term vitality makes sense at both biological and modeling levels. Note another term usually used in the literature is *frailty* (Yashin and Iachine 1997; Fried, Tangen et al. 2001; Mitnitski, Graham et al. 2002). In some ways this is a converse concept to the vitality and represents the "increasing loss of reserves and resilience, lack of energy and inability to function" (Crimmins, Kim et al. 2010). The two terms essentially represent the same processes in physiological system but in opposite directions. Here I adopt *vitality* because it sets up an absorption boundary that defines the intrinsic death. In contrast, frailty has no upper boundary for representing death.

2.2 Intrinsic-Extrinsic Vitality Model

A valuable model construction should represent in a plausible, but tractable manner, the underlining pathways leading to death. Since death has many causes, it is extremely difficult to find an appropriate but relatively simple way to separate the multitude of causes into reasonable categories that can be addressed in a single mathematical framework (Carnes, Olshansky et al. 1996; Carnes, Holden et al. 2006). However, taking a step back from the detail consideration helps us gain a broader vision that mortality is generally determined by the accumulated conditions up to the death moment (Aalen and Gjessing 2001) and the instantaneous conditions at the death moment. Therefore, it makes sense to quantify the contribution of mortality as coming from two sources, one of which is a cumulative process often involving natural aging and the other is an instantaneous process largely affected by environmental interventions. Following the

terminology of Carnes and Olshansky's (1996), we refer to these as intrinsic and extrinsic processes respectively.

2.2.1 Intrinsic Process

In the terminology of Carnes et al. (2006), intrinsic mortality arises from inside an organism and is associated with senescence, but the exact processes are not specified. The Markov killing models, as introduced before, explicitly express a cumulative process as a diffusion process to a killing boundary. The concept that describes the stochastic rate of loss of survival capacity, vitality, to a killing boundary is heuristic enough to be used to approximate the intrinsic process. The biological sense of considering aging as day-to-day damage accumulation, as discussed previously, is based on ample evidences, such as the age-dependent decreases in DNA repair, control of metabolic by-product generation, detoxication, protection from reactive oxygen and carbonyl species (Kirkwood and Austad 2000). Although the details of the aging processes are not specified, intrinsic death can be defined as the collapse of the physiological system resulting from the accumulation of natural damages to a critical point, such as organ failure or malfunction.

The intrinsic vitality process assumes each individual in a population starts with an initial amount of vitality, v_0', which then declines stochastically with age until intrinsic death occurs when the vitality reaches the zero boundary (Fig. 2.1) or when an extrinsic killing event occurs. The random trajectory of vitality, v', between v_0' and 0 is described by the Wiener process:

$$dv'/dx = -\rho + \sigma\varepsilon_x \tag{2.1}$$

where x is age, ρ is the mean value of the rate of vitality loss, σ is the magnitude of the stochastic component and ε_x is a white noise rate process. To reflect the effects of the initial vitality, eq. (2.1) is scaled according to v_0':

$$dv / dx = -r + s\varepsilon_x \tag{2.2}$$

In this case, $v = v' / v_0'$ is the normalized vitality with initial value equaling 1, $r = \rho / v_0'$ indicates the fraction of vitality loss per unit time and $s = \sigma / v_0'$ represents the normalized spread rate. Noted that the normalized equation (eq. (2.2)) implies that each normalized vitality trajectory starts at v = 1, however, the differences in the actual initial values are reflected in the spread term s. To be specific, s demonstrates the averaged combined variation from both inherent (initial) and acquired (evolving) sources per unit time. I will discuss the issues about normalization in a separate section below.

Derivation of population mortality due to the absorption of vitality requires the probability distribution of the first arrival time of vitality to the zero-boundary, $f(x)$, which is an inverse Gaussian distribution produced by a Wiener process (eq. (2.2)) (Cox and Miller 1965):

$$f(x) = \frac{1}{s\sqrt{2\pi}} x^{-2/3} \exp\left(-\frac{(1 - rx)^2}{2s^2 x} \right) \tag{2.3}$$

By definition, the fraction of total population that has not died from intrinsic causes at age x, is equivalent to the probability that the individual's vitality has not reached zero by x. The survival pattern resulting from the intrinsic process $l_i(x)$ can be expressed as (Cox and Miller 1965)

$$l_i(x) = 1 - \int_0^x f(x)dx = \Phi\left(\frac{1-rx}{s\sqrt{x}}\right) - \exp\left(\frac{2r}{s^2}\right)\Phi\left(-\frac{1+rx}{s\sqrt{x}}\right) \tag{2.4}$$

The intrinsic mortality rate is derived from eq. (2.3) and eq. (2.4):

$$\mu_i(x) = -\frac{1}{l_i(x)}\frac{dl_i(x)}{dx} = -\frac{1}{l_i(x)}\frac{d\left(1-\int_0^x f(t)dt\right)}{dx} = \frac{f(x)}{l_i(x)} \tag{2.5}$$

The intrinsic mortality is characterized by two parameters: the mean rate *r* which determines the fraction of vitality loss per unit time and the variance term *s* which determines the fraction of vitality spread per unit time. Both parameters are assumed to be constant with age or in another sense, represent the average decline and spread force at each time unit. Meanwhile, because the model is usually applied to population survival data, the two parameters characterize the average properties of the population, i.e., indicate the mean values of the measures across the population.

The conditional vitality distribution evolving with time can also be formulated analytically (Anderson, Gildea et al. 2008)

$$f_v(v_x \mid v_0 = 1) = \frac{p_v(v_x \mid v_0 = 1)}{\int_0^\infty p_v(v_x \mid v_0 = 1)dv} = \frac{p_v(v_x \mid v_0 = 1)}{l_i(x)} \tag{2.6}$$

where $l_i(x)$ is eq. (2.4) the intrinsic survival rate at age *x* and v_0 and v_x are normalized vitality levels at ages 0 and *x* respectively and

$$p_v(v_x \mid v_0 = 1) = \frac{1}{\sqrt{2\pi x s^2}}\exp\left(-\frac{(v_x - 1 + rx)^2}{2xs^2}\right)\left[1 - \exp\left(-\frac{2v_x}{xs^2}\right)\right] \tag{2.7}$$

is the absolute density function of the vitality which evolves from an initial Dirac distribution into a Gaussian distribution and then a quasistationary gamma-like distribution that is finally absorbed into the zero-vitality boundary (Anderson, Gildea et al. 2008).

Note that the SM model (Strehler and Mildvan 1960) uses a similar approach in that the senescence process reflects an intrinsic physiological decline, but there are important differences between vitality and the SM model. The SM model does not presume intrinsic killing while the vitality model defines intrinsic death from the absorption of the vitality trajectory (Anderson 1992). In addition, instead of a deterministic linear decrease, the vitality model includes randomness in the decline process and hence naturally builds in population heterogeneity. Despite the fact that the frailty model (Vaupel, Manton et al. 1979; Yashin and Iachine 1997) also includes variation in the survival capacity, it is at the expense of adding complexity to relate the rate of mortality to conditions that occurred prior to the time of the mortality event itself.

Issues on vitality normalization

Eq. (2.1) assumes that individuals in the population share a common ρ and σ. The trajectory for each organism is characterized by three values: the initial vitality, v_0', the rate of vitality loss ρ and the rate of vitality spread σ. However, if all individuals start from a single value of v_0', the distribution of first arrival time only depends on two of the three properties. Hence, from a statistical point of view, there are only two free parameters (Aalen and Gjessing 2001). We can use $r = \rho / v_0'$ and $s = \sigma / v_0'$ to represent the normalized rate of vitality loss and vitality spread. But in reality, individuals within a

population are endowed with different initial values of vitality as from genetic heterogeneity. To simplify this complexity first, postulate that v_0' follows a normal distribution $N(\mu, \tau)$. Then there are two ways to normalize the vitality trajectory.

The first method is to divide the vitality trajectory v' by the mean value of v_0', which we call, μ. Therefore, the initial vitality distribution is rescaled to a new normal distribution with an initial mean value of 1 and an initial standard deviation $u = \tau/\mu$ (Fig. 2.1A). Under this scenario, the first arrival time to the zero-boundary is determined by three parameters $r_1 = \rho/E(v_0') = \rho/\mu$, $s_1 = \sigma/E(v_0') = \sigma/\mu$ and $u_1 = \tau/E(v_0') = \tau/\mu$. Eq. (2.1) becomes $dv/dx = -r_1 + s_1\varepsilon_x$ where $v = v_0'/\mu$. Through this approach, the initial heterogeneity in the vitality distribution is maintained in the normalized parameter standard deviation, u, and the expected deviation of vitality trajectory from the mean at age x is equivalent to $u + s_1 x$.

The second method considers normalizing each vitality trajectory according to its own initial value v_0', such that the rescaled vitality trajectories all start from the same value 1 (Fig. 2.1B). Here let ρ / v_0' and σ / v_0' denote the fraction of vitality loss and spread per unit time. But since these values are different for each individual, the aggregation of the individual values for population level parameters are approximated as $r_2 = \rho E\left(1/v_0'\right)$ and $s_2 = \sigma E\left(1/v_0'\right)$ respectively. Under this method, the expected deviation of vitality trajectory from the mean at a given age x is equivalent to $s_2 x$.

Note, r_2 and s_2 are different than r_1 and s_1 in their exact meanings. The two definitions of parameters represent different sequences in averaging and normalization.

While r_1 and s_1 indicate the normalized mean rate of vitality loss and spread (average first and then rescale), r_2 and s_2 represent the mean fraction of vitality loss and spread per unit time (rescale first and then average). Sometimes we are more interested in the average fraction than the normalized rate and these values are also different for the two methods. Although v_0' has a normal distribution, there is no analytical solution for the probability density function (pdf) of the reciprocal of normal distribution, i.e. $E(1/v_0')$. Thus, the expectation of $1/v_0'$ cannot be determined through a closed form. However, by simulation we can still approximate $E(1/v_0')$. Within the parameter range $0 \le \tau/\mu \le 0.4$, the ratio $E(1/v_0')/(1/\mu)$ is greater than 1 and increases as τ increases. Both r_2 and s_2 are larger than r_1 and s_1 by the ratio $E(1/v_0')/(1/\mu)$ which carries the information of initial heterogeneity. Therefore, s_2 reflects both initial and evolving heterogeneity in the population while s_1 reflects only the evolving heterogeneity. Note the first method of normalization was implicitly used in the models of Anderson (1992; 2000), and Anderson et al. (2008). In Li and Anderson (2009), the first method was used and the initial distribution was defined explicitly with a normal distribution.

Studies suggest that only about 20% of the variation in human survival is heritable (Gavrilov and Gavrilova 1991; McGue, Vaupel et al. 1993; Herskind, McGue et al. 1996), which implies that the initial heterogeneity τ is relatively small for human beings. Therefore, the two approaches, even without an explicit initial distribution of heterogeneity, should yield very similar parameter estimates.

In general, the two normalization methods lead to slightly different models and explanations for the vitality parameters. The first method coupled with a normal

distribution of initial heterogeneity was successfully applied to ecological data to differentiate the effects of the initial and evolving heterogeneity on survival (Li and Anderson 2009). However, for the IEV model the first method of normalization fails to disentangle the two sources of heterogeneity because the extrinsic processes, which are developed below, confound the separation of initial and evolving heterogeneity. Therefore, the current IEV model normalizes the parameters using the second method in which the initial heterogeneity and the heterogeneity that evolves with age are combined...

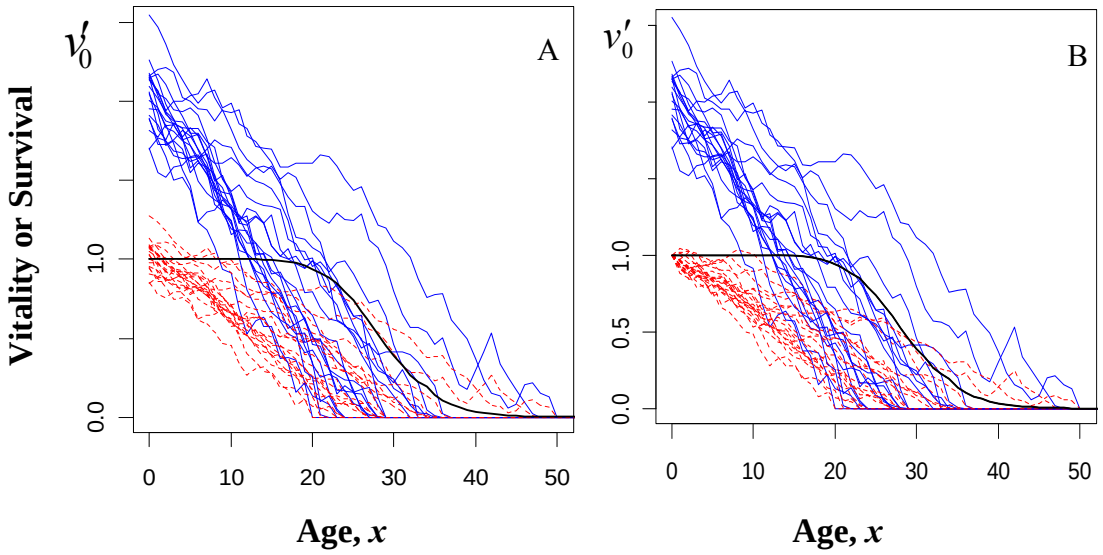

Figure 2.1: Individual vitality trajectories and population survival (eq. (2.4)) from two normalization schedules. A: vitality is normalized by the mean initial value. B: vitality is normalized by each individual's initial value. Solid lines depict original vitality trajectories (eq. (2.1)); dashed lines depict scaled vitality trajectories (eq. (2.2)); bold line depicts the intrinsic survival function calculated from the proportion of non-absorbed vitality trajectories at age x. The survival function is the same for both cases because the death age distribution is the same in both cases.

2.2.2 Extrinsic Process

Extrinsic killing is usually considered as death that is "relatively preventable and treatable", including "mortality mainly from infections and accidents" (Shryock, Siegel et

al. 1980). Makeham (1860) first suggested using the age-independence as the criterion to distinguish extrinsic mortality from intrinsic mortality. In Anderson's first model (1992), extrinsic mortality was independent of the vitality process and constant with age. This model yields a good fit when applied to survival data from animals such as nematode, medfly, yellow perch and sheep (Anderson 1992; Anderson 2000; Anderson, Gildea et al. 2008; Li and Anderson 2009), but does not fit well when applied to human mortality data. Human beings have a more complex life pattern than laboratory animals, such that the extrinsic mortality process is likely determined by both the dynamics of aging and environmental challenges. But how the intrinsic and extrinsic processes interact is complex, and no simple theoretical explanations seem forthcoming. However, evidence suggests that the extrinsic mortality has increasing probability with age, especially for human beings. For instance, the immune system declines in function with age (Makinodan and Adler 1975; Miller 1996; Grubeck-Loebenstein and Wick 2002), which weakens the organism's capacity of resisting external stresses and thus leads to a higher extrinsic mortality with age. Carnes et al. (2006) partitioned U.S. 1996 mortality data into intrinsic and extrinsic categories according to their criterion. They found an age-dependent increasing trend in extrinsic mortality which was defined as death not arising from within the organism. Finally, as developed below, including an age/vitality-dependent extrinsic mortality results in a significant improvement in the goodness-of-fit to human data.

For the IEV model, let Y_x with $x \geq 0$ be a random point process with rate λ to represent the occurrence of instantaneous extrinsic challenges such as a natural disaster or infection. In essence, λ measures the frequency of extrinsic challenges. For each extrinsic

event, a magnitude variable Z_x with a cumulative distribution function $\varphi(z)$ denotes the intensity of the challenge. Assume that when the challenge magnitude Z_x exceeds the current vitality level v'_x, the challenge results in death, i.e. death occurs when $P(Z_x \geq v'_x)$. We can also view Z_x as an instantaneous and momentary drop in vitality and once experienced, the organism returns to its previous vitality level unless the drop results in zero or negative vitality and therefore death. Fig. 2.2 depicts the extrinsic process. This assumption couples the risk of death from external forces to the intrinsic age-dependent vitality level of the individual and insures that the effect of the extrinsic challenge changes with age. For instance, the outcome of twenty and eighty year-old persons falling down a stairs can be very different: the younger person might suffer a bruised hip and limp for a day, while the older person is more likely to break a hip which could lead to death. Assuming that Y_x is a history-independent Poisson process (Finkelstein 2007), the extrinsic mortality rate for each individual is

$$m_e(x) = \Pr(Z_x \geq v'_x)\lambda = (1-\varphi(v'_x))\lambda \tag{2.8}$$

Further assume that the magnitudes of the events are exponentially distributed such that most are small and the probability of large events declines relative to their magnitude. Then the cumulative distribution function is $\varphi(z) = 1 - e^{-z/D}$, where D is a scale parameter. Now the rate of extrinsic mortality for an individual with absolute vitality v'_x becomes

$$m_e(x) = \lambda e^{-v'_x/D} = \lambda e^{-v_x/\beta} \tag{2.9}$$

Because we only know vitality relative to the initial vitality, we normalize vitality characterizing the extrinsic rate by the initial value giving, $v_x = v'_x / v'_0$. Furthermore, the challenge magnitude scalar is normalized to the initial vitality as $\beta = D / v'_0$ and thus characterizes the environmental deleteriousness relative to the initial condition of the organism. In essence, a larger β implies that high magnitude challenges occur more frequently. Also, note that eq. (2.9) implies that the susceptibility to extrinsic death depends on an individual's survival capacity and β is a scalar, which expresses the intuition that the effect of stressors varies with age and vitality.

The aggregated extrinsic mortality rate at the population level equals

$$\mu_e(x) = \int_0^\infty \lambda e^{-v_x/\beta} f'(v_x \mid v_0 = 1) dv \tag{2.10}$$

where $f'(v_x \mid v_0 = 1)$ is the conditional vitality distribution at time x when starting with a normalized single value 1 at $x = 0$. Note that it is different from eq. (2.7). Because the extrinsic process unequally eliminates individuals from the total population, it changes the original vitality distribution. In addition, the change in the vitality distribution will also influence the intrinsic mortality by altering the absorbing probability.

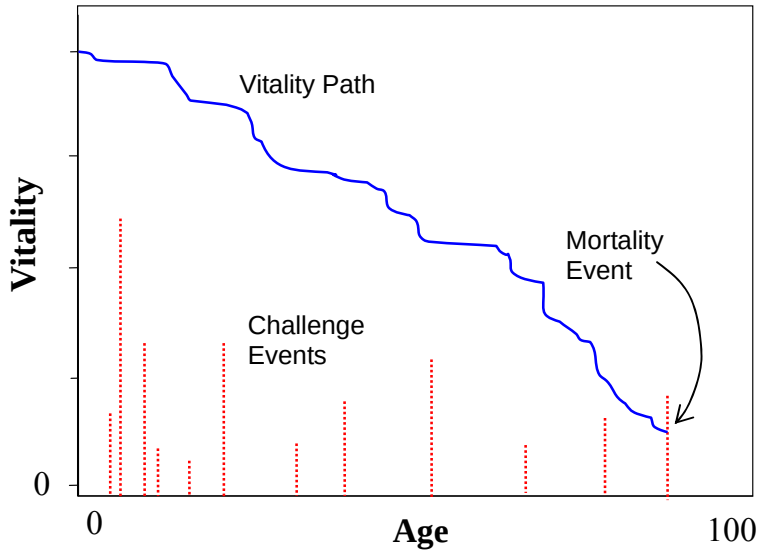

Figure 2.2: Extrinsic vitality challenges (dotted line) momentarily decrement intrinsic vitality (solid line) and cause death when the challenge magnitude exceeds the remaining vitality. Challenges do not affect the trajectory of vitality itself.

Model approximation

In making the extrinsic mortality dependent on vitality, the density distribution of vitality no longer has a closed analytical form, so we approximate v_x in eq. (2.10). The approximation has two steps. First, assume the v_x can be approximated by the mean vitality $\bar{v}_x$. Second, note that the mean vitality without extrinsic killing declines approximately linearly with age when the population variation term s is small (Anderson, Gildea et al. 2008) and can be approximated as $\bar{v}_x \approx 1 - rx$. The extrinsic mortality rate then becomes

$$\hat{\mu}_e(x) = \lambda e^{-(1-rx)/\beta} \tag{2.11}$$

For human mortality data, s is relatively small, which guarantees eq. (2.11) a good approximation over most of the life time. There are several advantages of eq. (2.11).

Firstly, it simplifies the equation and yields an approximately analytical solution for the mortality rate, which assures that the estimation algorithm rapidly converges to a solution. Secondly, since most classical models express mortality rates as a function of age, it provides a way to interpret the traditional results in terms of a vitality process. Finally, empirically $1-rx$ is a better approximation than $\bar{v}_x$ to the original eq. (2.10), which will be used later to simplify the model further.

Childhood mortality

High child death rate is consistently observed through all human age-specific mortality data. According to the statistics from United Nations Children's Fund (UNICEF 2010), the leading cause of death for children is the infectious disease including acute respiratory infections, diarrhea, malaria and etc., which account about two-thirds of the total death under 5. Therefore, the deaths at childhood can be mostly classified as extrinsic mortality in the context of the IEV model. The shape of child mortality is conventionally represented as an exponential decreasing function with age, i.e., $\mu_c = \mu_0 e^{-\alpha x}$, in some models, such as the Siler model (Siler 1979), which makes a reasonable approximation to the empirical data. The IEV model can add the same expression to account for the child mortality part, but the vitality framework is able to visualize how the exponential decreasing function can be derived from the intrinsic and extrinsic processes that alter the mortality schedules at childhood.

Firstly, we consider the influence from the extrinsic process. Many forms of age-dependency in challenge frequency can be incorporated into the model to capture complex changes in extrinsic stresses with aging. For the purpose of modeling the overall

survival of a cohort, consider the challenge frequency more in the nature proposed by Yashin et al. (2002) which assumes that an organism is capable of modulating the frequency of stressful challenges by devoting a fraction, *p*, of its resources to protecting against environmental challenges. Assume this resource partitioning is age dependent and express the frequency of the challenges in a generic manner as $\lambda = (1-p)\lambda^*$ where p characterizes the efficiency of defensive mechanisms and the total challenge frequency from the environment is λ^*. The age dependency of resource partitioning could have both physiological and behavioral components. In a physiological context, as an immune system develops it is expected that infant susceptibility to disease challenges decreases with age (Chandra 1997; Holt and Jones 2000). In a behavioral context, individuals learn through experimentation and experience to avoid accidents and again we expect the effective frequency of external challenges to decrease with age. Details how individuals avoid challenges is multifaceted and complex, but in principle it is reasonable to assume that the challenge frequency asymptotically decreases with age and can be expressed as an exponential function

$$\lambda(x) = \lambda + (\lambda_0 - \lambda)e^{-\theta x} \tag{2.12}$$

where λ_0 is the challenge frequency at age zero, λ is the frequency at adulthood and θ is the rate of decline of challenge frequencies with age at childhood. Secondly, the intrinsic process may also contribute to the high child mortality. For example, children could experience an increase in vitality as the development of their internal systems, which would affect their ability to recover from a challenge event. Additionally, variation in initial vitality at birth may be skewed such that a few newborns have very low initial

vitality due to low birth weight and congenital malformations. Mortality of such individuals would be expected to be high and we speculate that the extrinsic killing process at very beginning would remove more such individuals leaving the average vitality across the entire population increasing merely due to the selection effects. In both cases, the trajectory of mean vitality would not follow a monotonic decline, but could first increase over a short period $(0, x_0)$ and then decline (Fig. 2.3). We could introduce a function $R(x)$ to indicate the proportion of reduction in mean vitality from its optimal trajectory (i.e., a monotonic decline). To reduce the complexity, $R(x)$ can be assumed to be a step function

$$R(x) = \begin{cases} R_0 & x < x_0 \\ 1 & x \geq x_0 \end{cases} \tag{2.13}$$

such that the vitality is represented with an average reduction, R_0 (R_0<1), to the scheduled track previous to age x_0 and back to its original track afterwards.

Thus, the extrinsic mortality rate incorporating both mechanisms from intrinsic and extrinsic processes at childhood can be expressed as

$$\begin{aligned} \widehat{\mu}_e(x) &= \left(\lambda + \left(\lambda_0 - \lambda\right)e^{-\theta x}\right)e^{-(1-rx)R(x)/\beta} = \lambda e^{-(1-rx)R(x)/\beta} + \left(\lambda_0 - \lambda\right)e^{-\theta x-(1-rx)R(x)/\beta} \\ &= \begin{cases} \lambda e^{-(1-rx)R_0/\beta} + \left(\lambda_0 - \lambda\right)e^{-\theta x-(1-rx)R_0/\beta} & x < x_0 \\ \lambda e^{-(1-rx)/\beta} + \left(\lambda_0 - \lambda\right)e^{-\theta x-(1-rx)/\beta} & x > x_0 \end{cases} \end{aligned} \tag{2. 14}$$

However, in a short period $(0, x_0)$ $\lambda e^{-(1-rx)R_0/\beta} \approx \lambda e^{-(1-rx)/\beta}$, because λ is small compared to λ_0 - λ and a reduction in vitality would not induce more deaths. In addition, when $x>x_0$, $\left(\lambda_0 - \lambda\right)e^{-\theta x-(1-rx)/\beta} \approx 0$. Hence eq. (2.14) can be further reduced:

$$\begin{aligned}\widehat{\mu}_e(x) &\approx \lambda e^{-(1-rx)/\beta} + (\lambda_0 - \lambda) e^{-\theta x - (1-rx)R_0/\beta} \qquad x > 0 \\ &= \lambda e^{-(1-rx)/\beta} + (\lambda_0 - \lambda) e^{-R_0/\beta} e^{-(\theta - rR_0/\beta)x} \\ &= \lambda e^{-(1-rx)/\beta} + \mu_0 e^{-\alpha x}\end{aligned} \tag{2.15}$$

Eq. (2.15) has the general form for child mortality as proposed by the Siler model (1978), but it has a biological justification Nevertheless, the model is still inadequate to differentiate the contributions from the two processes, i.e., high challenge frequency and low recovery chance at childhood. As suggested by eq. (2.15), the child mortality function only possesses two free parameters. $\mu_0 = (\lambda_0 - \lambda) e^{-R_0/\beta}$ indicates the additional child mortality rate at age 0 containing information from both intrinsic and extrinsic processes, while $\alpha = \theta - rR_0 / \beta$ denotes the rate of decline in child mortality which is mainly determined by the rate of decline in challenge frequency with age, since rR_0/β is small.

In general, we speculate that the high child mortality could result from the effects of high selection pressure (extrinsic force) on the low internal survival capacity (intrinsic force) due to the immaturity of the immune system and other physiologic functions. However, the real underlying mechanisms of the child mortality are very complex involving multifaceted processes. It is impossible to model everything in detail, but here we conceptually approximate some of the complexity in a mathematically tractable way through the vitality framework. Although the second component in eq. (2.15) cannot be used to disentangle the effects of high challenge frequency from the low recovery chance, it is the most parsimonious model that could fit the early age “hook”. Other empirical works such as the Siler model (Siler 1979) have long used the same shape to model child

mortality.

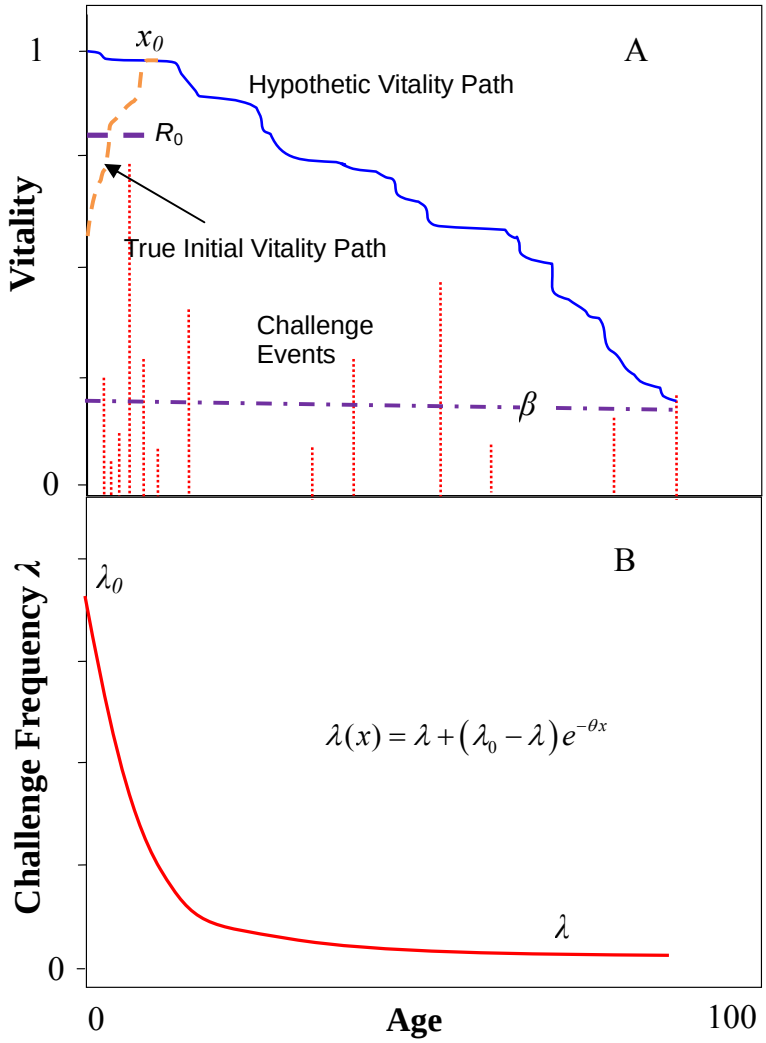

Figure 2.3: (A). Vitality process of extrinsic mortality includes the schedule of high child mortality rate. Solid line: the hypothetic mean vitality path following a monotonic decline; dashed line: the true initial mean vitality path at childhood which merges to the hypothetic trajectory later and an approximation to the true path by a constant line (R_0) dotted line: extrinsic challenges; dotted-dashed line: average mean challenge magnitude (β). (B). challenge frequency following an approximately exponential decrease with age.

2.2.3 Complete model

The final model presumes two sources of death: an extrinsic killing and an intrinsic killing expressed as a boundary absorption process. By approximating the extrinsic

mortality as a function of age with eq. (2.11) or eq. (2.15), the extrinsic hazards have a uniform killing force on the population at each age. To be specific, the extrinsic killing does not change the vitality distribution so that it does not affect the intrinsic mortality rate, i.e., the absorption rate to the zero-vitality boundary. Therefore, the total mortality rate is expressed as the sum of the two forces:

$$\mu(x) = \mu_i(x) + \hat{\mu}_e(x) \tag{2.16}$$

The corresponding survival function is

$$l(x) = l_i(x) l_e(x) = \exp\left(-\left(\mu_i(x) + \hat{\mu}_e(x)\right)\right) \tag{2.17}$$

The generic form combining eq. (2.5) and eq. (2.11) has 4 parameters r, s, λ and β where the challenge frequency is constant with age. And the implicit form combining eq. (2.5) and eq. (2.15) expands the model to 6 parameters: r, s, λ, β, μ_0 and α to include the child mortality schedule. In contrast to Gompertz-type model, the parameters are all process-based and specify both the population vitality and mortality trajectories.

Note that the aging related process, which determines the intrinsic mortality, also reflects the influence from environment and behavior, e.g. nutrition level and smoking status, which have long-term effects in altering the vitality trajectory and thus modify the aging process. In that sense, the vitality parameters r and s, which characterize the intrinsic process, can also be modified by the extrinsic challenges. Furthermore, the extrinsic parameters λ and β do not measure the absolute environmental deleteriousness but reflect the external hazards relative to the physiological condition of the individuals as measured by vitality. For instance, λ measures the frequency of challenges that can

get through the body defensive system and thus reveals the physiological robustness as to the environment, while β measures the average magnitude of challenges relative to the initial vitality level. In conclusion, both intrinsic and extrinsic mortality result from interactions between the force of aging and the interventions of environment. Thus, the parameters cannot be simply determined as influenced by internal or external factors but rather reflect chronic and acute effects that contribute to the mortality process.

2.3 Parameter Estimation and Evaluating the Model Approximation

2.3.1 Parameter Estimation

The vitality parameters r, s, λ and β (or the expanded version r, s, λ, β, μ_0 and α) are estimated from fitting to the age-specific survival fraction data. The method is similar to that used in Li and Anderson (2009). The estimation problem is cast as a maximum likelihood optimization, as developed by Salinger et al. (2003) to deal with interval-censored data, in which mortalities are counted at the end of each time period rather than continuously. The likelihood function is constructed from the multinomial distribution based on the proportion of deaths in each time period.

$$\text{LogLik} = \sum_x \left(d_x \ln q_x + (n_x - d_x) \ln(1 - q_x) \right) \tag{2.18}$$

where d_x is the number of deaths at age x, n_x is the number of population at the beginning of age x, and q_x is the probability of death at age x. The probability of death is derived from eq. (2.17) $q_x = 1 - l(x+1)/l(x)$. The algorithm estimates standard errors thorough the estimated variance matrix. Specifically, standard errors are obtained by taking the

square root of the diagonal elements in the inverse of the Hessian of the negative log-likelihood, evaluated at the parameter estimates (Kendall, Stuart et al. 1977).

2.3.2 Evaluating the Model Approximation

The model assumes that the extrinsic mortality does not affect the distribution of vitality as determined by the intrinsic process, which is in fact not the case. The bias of this approximation was evaluated through simulation. Using a numerical form of the vitality model, survival curves were generated for a range of specified model parameters. The parameters were then estimated with the estimation algorithm described in section 2.3.1 and the simulated (true) and estimated parameters were compared.

Survival curve generation

The survival curves were simulated from the vitality process. Each population member was assumed to have a vitality of 1 at time 0. The vitality for each individual was calculated for a single time step as

$$v_x = v_{x-1} - r_a + s_a \times W \qquad x=1, 2, 3\ldots \tag{2.19}$$

where W is the white noise calculated by selecting a random number from a normal distribution. Note that this generation uses a simplified random walk with drift to approximate the continuous process described in eq. (2.2). From eq. (2.19), 10,000 vitality trajectories are generated to represent a population. At each time x, death from intrinsic and extrinsic process are recorded. The intrinsic mortality occurs when the individual vitality trajectory v_x drops below zero. Mortality from extrinsic challenges are defined by a probability distribution where the probability of dying from extrinsic process

in age interval (x-1, x) equals $1-e^{-\int_{x-1}^{x}\lambda e^{-\beta v_m}dm} \approx 1-e^{-\lambda(e^{-\beta v_{x-1}}+e^{-\beta v_x})/2}$. A binomial random variable is generated to determine whether the individual is killed from external forces according to the probability. When either intrinsic or extrinsic death occurs, the vitality trajectory is excluded from further calculation. Thus, survival curves are generated from the fraction of vitality trajectories left at each time point.

Evaluation and correction

To evaluate the model approximation, we use simulated survival curves as described above. Since the approximation procedure has limited influence on the child mortality parameters: μ_0 and α, the 4-parameter model is used for simplicity. However, the parameter space still has too many dimensions, such that it is almost impossible to analytically track the change of one parameter under approximation based on the entire spaces of the other three parameters. Fortunately, we only need to determine the parameter values for human mortality data which follow certain patterns and change within relative small ranges. Preliminary studies (Table 2.1) revealed that r and β have little bias under approximation and s and λ are overestimated by less than 40% of their true values. To efficiently investigate the bias of parameters estimated from human mortality data, I conduct simulations based on parameters obtained from period mortality data of Swedish females (1800-2007) (HMD 2010) using the approximation. For each period year, a set of parameters (r, s, λ and β) were estimated from the mortality curve of Swedish female using the algorithm described in section 2.3.1. Thus, there are 208 baseline parameter sets for simulation. 3 additional values are picked randomly for each s and λ separately within a range from 60% to 100% of their baseline values, which gives

in total 3328=208×4×4 true parameter sets. I generate 3328 curves from the underlining process and obtain 3328 estimated parameter sets from eq. (2.16) under approximation.

The simulation results are summarized in fig.2.4. The ratios of the estimated parameters over the true parameters are plotted against the estimated $\hat{\beta}$. Ratios of $\hat{\beta}/\beta$ are flat and close to 1, indicating that β is robust under approximation. $\hat{r}/r$ slightly increases with $\hat{\beta}$, and the ratio is near 0.95. Both $\hat{s}/s$ and $\hat{\lambda}/\lambda$ decline with $\hat{\beta}$, but the variance of $\hat{\lambda}/\lambda$ is relative large compared to the other ratios. The strong linear relationships between the estimated and true parameters can be used to correct the bias in the approximation. According to the fitting results in fig. 2.4, the true underlining parameters can be approximated as $r \approx \frac{\hat{r}}{0.94+0.094\hat{\beta}}$, $s \approx \frac{\hat{s}}{1.39-1.03\hat{\beta}}$, $\lambda \approx \frac{\hat{\lambda}}{1.57-1.55\hat{\beta}}$ and $\beta \approx \frac{\hat{\beta}}{1.02}$. Note that because uncertainties are introduced by the correction, variance for adjusted parameters is larger than that directly obtained from the maximum likelihood algorithm.

In conclusion, the model slightly underestimates *r* and overestimates *s* and λ, but a correction can be applied to those parameters according to the strong relationships between the true and estimated parameters.

Table 2.1: Results from the pioneer studies. Parameters are chosen to be close to the values estimated from the morality data of Swedish females (Human mortality database).

	r	s	λ	β
true parameter	0.01200	0.01000	0.02500	0.50000
estimated parameter	0.01183	0.01006	0.02516	0.50001
s.e.	0.00001	0.00017	0.00113	0.01849
true parameter	0.01200	0.01000	0.04000	0.40000
estimated parameter	0.01170	0.01081	0.04287	0.39096
s.e.	0.00004	0.00024	0.00199	0.01135
true parameter	0.01200	0.00900	0.08000	0.20000
estimated parameter	0.01145	0.01027	0.09606	0.19887
s.e.	0.00006	0.00031	0.00634	0.00437
true parameter	0.01200	0.00900	0.08000	0.15000
estimated parameter	0.01144	0.01149	0.09982	0.14989
s.e.	0.00001	0.00031	0.00968	0.00372
true parameter	0.01100	0.01000	0.05000	0.30000
estimated parameter	0.01065	0.01107	0.05302	0.30112
s.e.	0.00005	0.00030	0.00300	0.00809
true parameter	0.01100	0.01000	0.05000	0.20000
estimated parameter	0.01046	0.01201	0.06419	0.19422
s.e.	0.00007	0.00028	0.00556	0.00534
true parameter	0.01100	0.00800	0.06000	0.20000
estimated parameter	0.01064	0.00883	0.06990	0.19804
s.e.	0.00004	0.00020	0.00409	0.00425
true parameter	0.01100	0.00800	0.08000	0.15000
estimated parameter	0.01037	0.01049	0.11773	0.14455
s.e.	0.00008	0.00034	0.01241	0.00363

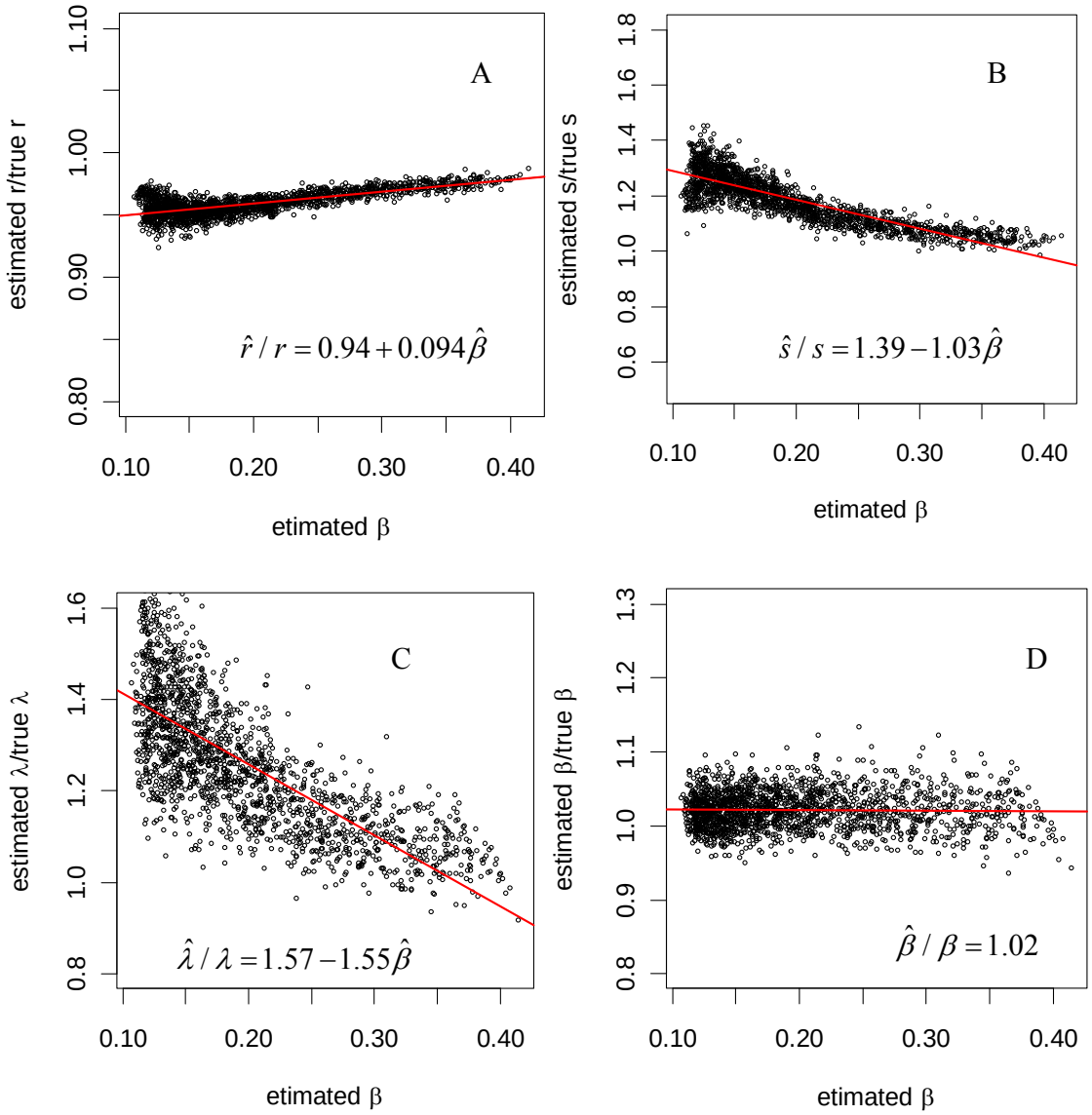

Figure 2.4: the ratio of estimated parameters over the true values against estimated β.

Comparing $\bar{v}_x$ to 1-rx

We next compare the effect of approximating $\bar{v}_x$ with $1-rx$ in eq. (2.10). As stated before, one reason to choose $1-rx$ is because it yields a better overall fit than $\bar{v}_x$. To illustrate their differences, we begin with the vitality distribution changing with age.

Simulations show that although extrinsic killings affect the vitality distribution, within the parameter range for humans, the influence is small and $f'(v_x \mid \overline{v}_0 = 1)$ is similar to eq. (2.7). Therefore, at early ages $f'(v_x \mid \overline{v}_0 = 1)$ follows a Gaussian-like distribution (purple line in fig. 2.5) and $\overline{v}_x$, the same as the distribution mode, approximately equals 1-*rx*, while at old ages $f'(v_x \mid \overline{v}_0 = 1)$ has a gamma-like distribution (red line) and $\overline{v}_x$ is located at the right of the distribution mode. Furthermore, the true aggregated extrinsic mortality rate at population level equals the exponential function of vitality integrating over the space of vitality distribution, i.e. $\mu_e(x) = \int_0^\infty \lambda e^{-v_x/\beta} f'(v_x \mid \overline{v}_0 = 1) dv_x$. Demonstrated in Fig. 2.5, $\mu_e(x)$ can be derived from the weighted value of the solid line (blue), where the weight functions are determined by the schedule of the dashed lines (red or purple). For early ages, $\mu_e(x)$ can be well represented by point *a*. However, for old ages by taking $\overline{v}_x$, $\mu_e(x)$ is approximated by the value of point *b*, which obviously leads to an underestimation, since the blue line is a declining function within the calculation interval and the left part of point *b* takes more than 50% of the weights. The bias becomes more serious as the distribution of vitality gets more skewed toward zero-boundary at very old ages. At the same time, 1-*rx* is a good approximation for $\overline{v}_x$ for early ages, but tends to underestimate $\overline{v}_x$ at the very end. In effect, 1-*rx* shifts the dashed line to the left indicated in Fig. 2.5 and approximates $\mu_e(x)$ by the value of point *c* and thus yields a better fitting.

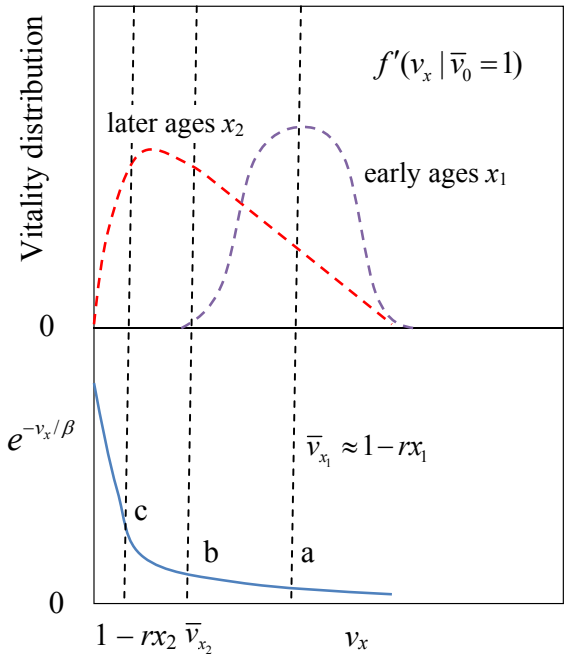

Figure 2.5 An illustration of why 1 - *rx* yields a better fit than $\overline{v}_x$ for $\mu_e(x)$ at old ages. The upper plot demonstrates the vitality distribution at both early (x_1) and old ages (x_2) and the lower plot depicts the exponential decrease function of v_x.

2.4 Fitting to Human Mortality Data

A good fit to data is a goal for any model and also an important way to validate the model structure. As discussed in the introduction, the Gompertz model cannot capture the early-age "hook", middle-age "elbow" and old-age "plateau" observed in all human mortality patterns. These respectively refer to the anomalously high infant death rate, the middle age acceleration of increase in death rate and old age leveling off in death rate (Carey, Liedo et al. 1992; Vaupel, Carey et al. 1998; Vaupel 2004). Neither the Gompertz nor the Gompertz-Makeham models fit all of these features, and consequently the classical models are typically applied to human mortality between the ages of 35 and 85. These discrepancies are well known, but because the classical models fit the majority of the

human lifespan, they are routinely applied and considered sufficient for many analyses. Alternatively, models have been applied to phases of the human mortality curve. For example, the Heligman-Pollard model (Heligman and Pollard 1980) schedules of mortality in three parts: the childhood, adulthood and old age, each of which is characterized by 2 or 3 parameters making a total parameter of 8. Milne (Milne 2010) divides the mortality curve into five phases and applies a model based on redundancy decay and interactive risk individually to each phase. The Milne model also has 8 parameters which individually apply to specific age intervals. In contrast, the 6-parameter IEV model acts across the entire lifespan and so there is no ad hoc designations of stages. Moreover, the vitality parameters are process-driven and thus are biologically plausible. The next section discusses model characteristics and illustrates the model fit to survival data.

The IEV model is applied to mortality data from Swedish females (data source: human mortality database (HMD 2010)). Fig. 2.6 and 2.7 illustrate the model fit to period survival and mortality data for years 1820, 1890, 1960 and 2006. The model fits all the mortality data very well expect for the very old age (>85) at period years 1820 and 1890 where the estimated trajectories fall below the data. The potential reasons for the underestimation are addressed further on. In essence, the primary features of mortality curves are well captured by the model.

2.4.1 Mortality Plateaus

The mortality plateau is a well-established phenomenon in populations from insects to humans (Carey, Liedo et al. 1992; Horiuchi and Wilmoth 1998; Vaupel, Carey et al. 1998). While there has been debate on the processes responsible for the plateau (Rauser,

Mueller et al. 2006), I believe the most propitious explanation is based on hidden Markov-type models, of which the vitality model has been the most explored. A number of authors have noted that vitality-type models, in which death is represented by the absorption of the remaining survival capacity into a zero-vitality boundary produce mortality plateaus. Weitz and Evans (2001) proposed that a mortality plateau is a generic consequence of considering death in terms of first passage time processes undergoing a random walk with drift. Aalen and Gjessing (2001) explored these first passage time models and noted that such models develop a quasi-stable probability distribution in the vitality-like property in which the frail individuals die first leaving the more robust ones. Steinsaltz and Evans (2004; 2007), explored the property further noting that the convergence to a mortality plateau is, in fact, the natural property of a Markov-process model convergence to a quasistationary distribution where the shape of the probability mass is stable, and the level of distribution sinks proportionately at every location. Although explicit solutions would be difficult, Steinsaltz and Evans (2004) established a general case of Brownian motions including both extrinsic killing and boundary killing to approach a quasistationary distribution, which theoretically proved that the two-process vitality model, being a general Markov-process model, was able to capture the mortality plateau.

2.4.2 Mortality Hook

The early age "hook" has not been fully resolved previously except by piecing together independent mortality stages. The IEV model, though ends up with a similar additional component to produce the hook, has a mechanism to explain the emergence of hook in terms of the same processes that act across the entire lifespan. In contrast, other models

restrict the additional component to the childhood stage only. In the IEV model, we derive the hook from the combined effects of an age-dependent challenge frequency term $\lambda(x)$ and a building process of vitality at early ages. To be specific, an exponentially decreasing function of $\lambda(x)$ is used to denote the change of selection pressure and a lower value of R_0 is used to approximate the average lower recovery ability caused by a lower mean vitality away from the hypothetic trajectory at the early stage of life. As discussed above, there is a biological sense under the assumption. We speculate that due to the immature of the internal defense system (Beisel 1996), children tend to have a much higher susceptibility rate to diseases in comparison with adults and because of the large variation in acquired initial vitality and the development of physiologic functions, children also possess an average low capacity of recovering from a challenge.

2.4.3 Mortality Elbow

The "elbow", indicating an acceleration of the increase rate in log mortality with age occurs at the transition period from middle to old ages. This deviation from a linear increase is observed in almost all period and cohort data, over the past two centuries, though the up-bending trend becomes less prominent in recent years. As demonstrated in Fig. 2.7, the age at which the "elbow" occurs increases over time: in Swedish females ages 50, 55, 60 and 70 for period years 1820, 1890, 1960 and 2000.

Compared with the other features, the mortality "elbow" has not been thoroughly explored. Makeham (1860) attempted to account for the change in Gompertz slope by including a constant term in the exponential increase in mortality rate. The resulting Makeham-Gompertz model mortality function is $\mu(x) = A + ae^{bx}$. Later models such as the Siler model (Siler 1979) and the Heligman-Pollard mortality law (Heligman and

Pollard 1980), include a Makeham-Gompertz model form with some additional complex structures, to fit the entire mortality curve. The Makeham term indeed increases the goodness of model fit, especially for data when the "elbow" occurs at relatively younger ages (e.g. year 1820 and 1890). Nevertheless, the explanation of the Makeham term has a questionable biological foundation (Carnes, Olshansky et al. 1996; Golubev 2004; Carnes, Holden et al. 2006; Golubev 2009). The initial interpretation, treating the constant term, A, as the accidental mortality independent of age and the Gompertz part as senescence related mortality (Makeham 1860), has been long considered inappropriate (Carnes, Holden et al. 2006). Besides the lack of a biological justification, the Makeham term does not sufficiently improve the fit for recent period year data, because it is unable to capture the "elbow" when it occurs at older ages (e.g. year 1960 and 2000).

In contrast, the IEV model provides a natural explanation to the "elbow" as the age at which the intrinsic mortality begins to have an important contribution to mortality schedule. The vitality model smoothly fits the change of mortality schedules, because it tracks intrinsic and extrinsic mortalities separately. Although the location of "elbow" cannot be analytically calculated, the change in the location through period or cohort years reflects improvements, i.e. delays, in the aging processes that lead to intrinsic death. Therefore, the vitality model not only fits data better, but also provides a biologically plausible interpretation to the elbow in the mortality rate curve.

In addition to capturing the early-age hook and the old-age plateau, the ability to capture the middle-age elbow further supports the model. Though fitting to mortality data is not the ultimate goal, it does provide support for the utility and biological basis of the model.

2.4.4 Mortality Hump

Though not shown in Fig. 2.7, the young-adult mortality "hump" is classified as a secondary feature of the mortality curve. It is usually observed between ages 10 and 25 in many data sets, particularly for males. The 8-parameter Heligman-Pollard model (Heligman and Pollard 1980) has special design to fit the pattern and thus yields a better fit to data with a significant "hump". It would be possible to capture the pattern in the IEV framework by including parameters to increase the challenge frequency during the late-child to young adult period. Plausible mechanisms for an increase in challenge frequency include war and immature risky behavior. The hump is not included in this dissertation because it does not exist in all the data sets and has significantly diminished in recent years. For instance, the curves for Swedish females shown in Fig. 2.7 do not exhibit prominent "humps". The important point here is the IEV model provides a framework in which to consider transient mortality events that have specific causes.

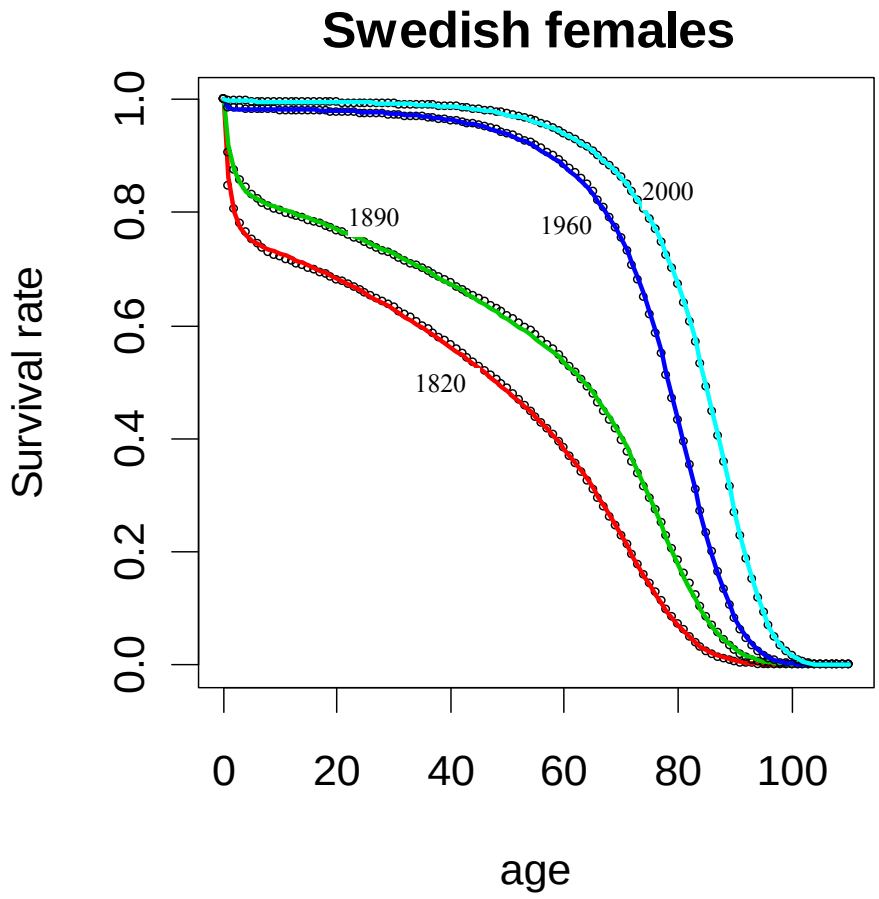

Figure 2.6: vitality model fits to Swedish female survival curves at period year 1820, 1890, 1960 and 2000 respectively. Circle: original data from human mortality database; solid line: fitted lines from the vitality model.

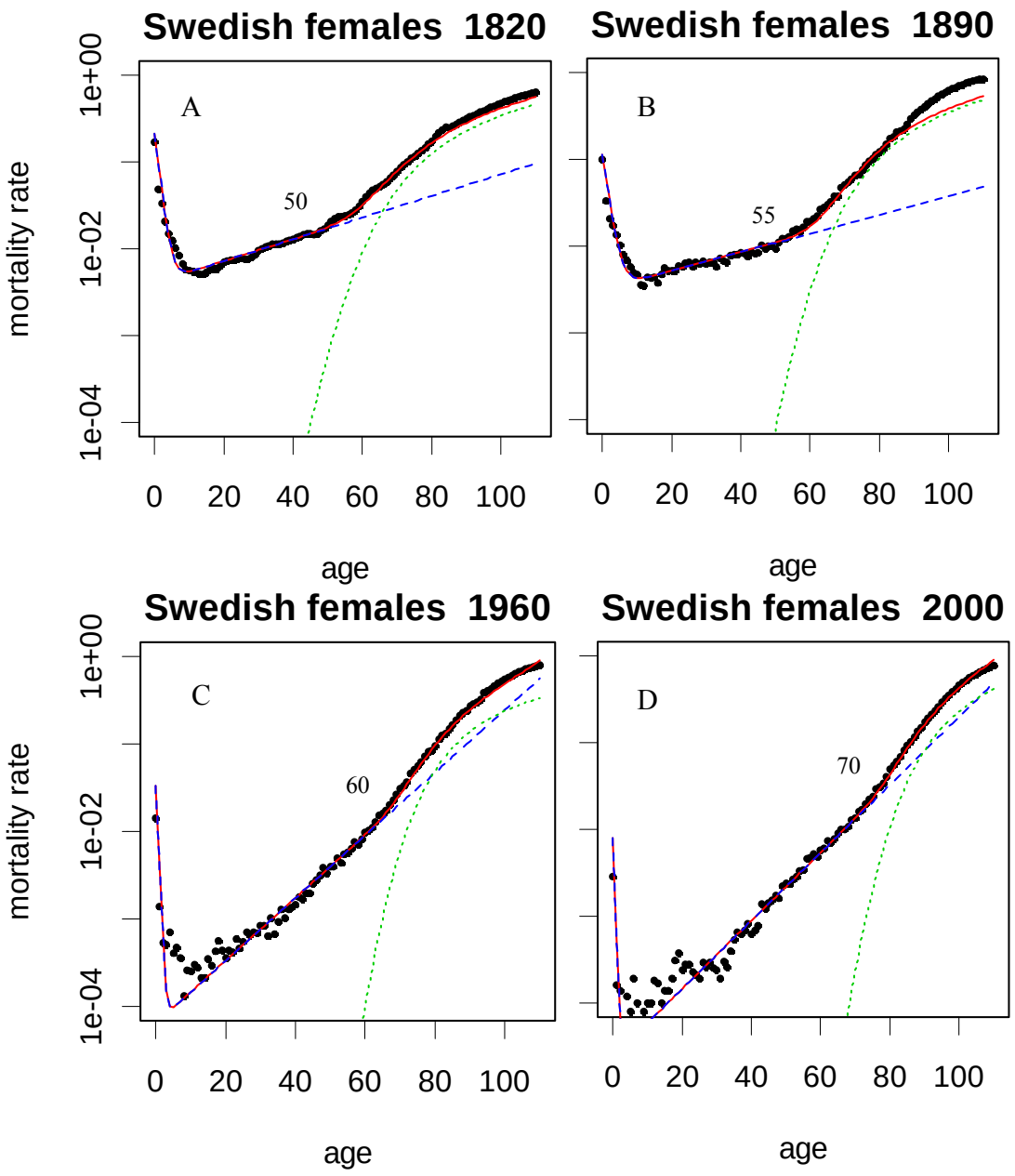

Figure 2.7: vitality model fits to Swedish female mortality rate in log scale at period year 1820, 1890, 1960 and 2000 respectively (A-D) corresponding to the four survival curves in Fig. 2.6. Dot: original data from human mortality database; solid line: total mortality trajectory fitted from the vitality model; dashed line: extrinsic mortality trajectory; dotted line: intrinsic mortality trajectory.

2.5 Sensitive Analysis for IEV Parameters

Although a structure has been established between the inputs, i.e. the vitality parameters, and the outputs, i.e. survival rate or mortality rate, the IEV model does not lead itself to a straightforward understanding of the relationship between the parameters and the output rates. To be specific, the aim is to know how the mortality trajectory behaves in response to changes respectively in vitality loss rate, population heterogeneity, challenge frequency and challenge magnitude. It is not only important for better understanding the model properties but also essential for validating the model structure. In this section, I numerically evaluate the shape of both intrinsic and extrinsic mortality under different parameter sets. Because the child mortality parameters μ_0 and α only affect a short life period and their effects on mortality patterns are straightforward, here we only assess the other four parameters which control the post-childhood mortality.

The parameter sets are chosen within reasonable ranges for human mortality. Both intrinsic and extrinsic mortality rates are obtained from simulation as discussed in section 2.3. That is, vitality trajectories are generated and extrinsic mortality is produced probabilistically when challenges exceed the vitality and intrinsic mortality is produced when vitality reaches zero. Intrinsic and extrinsic mortality rates can be calculated separately by recording the status of each vitality trajectory. Figs. 2.8 and 2.9 show the effects of individual parameters on the progression of intrinsic and extrinsic mortality rates with age. In each plot the other parameters are fixed.

2.5.1 Fraction of Vitality Loss per Unit Time *r*

The parameter *r*, measuring the fractional loss of vitality per unit time, affects both intrinsic and extrinsic mortality trajectories. Indicated by Fig. 2.8.A and Fig. 2.9.A, *r*

positions of intrinsic and extrinsic mortality rate curves with age but does not change their general shape. In effect, a decline in vitality loss rate, *r*, does not result in significant change in the mortality rate at young ages, but does decrease the mortality rate in older ages. Essentially, lowering *r* improves survival capacity in all age groups; however, the effect on mortality is not evident until old age

2.5.2 Population Heterogeneity *s*

In contrast to *r*, *s* which reflects the population heterogeneity has cross-over effects on both intrinsic and extrinsic population mortalities (Fig. 2.8B and Fig. 2.9B). The crossover indicates a phenomenon that two trajectories change their upper-down positions at certain time point. In this case, a lower value in *s* benefits population survival at early ages but leads to a higher average killing force at old ages. Given other IEV parameters, in particular *r*, fixed, a more heterogeneous cohort consists of a few more individuals with relatively low vitality trajectories and a few more individuals with relatively high vitality trajectories. Both intrinsic and extrinsic killings eliminate weaker individuals at early ages leaving the average vitality across the population higher than a uniform cohort at the same old age. Thus, the average survival chance for a less homogeneous cohort would be better later after a stronger selection process occurring early in the life period (Li and Anderson 2009).

The phenomenon of crossovers is widely observed among the age-specific mortality trajectories of different sexes and races (Coale and Kisker 1986; Johnson 2000). For example, the observed mortality rates for blacks are higher than whites for middle and early old ages, but at very old ages blacks are observed to have favorable mortality risks compared with whites (Berkman, Singer et al. 1989). The population heterogeneity

in susceptibility to death is one primary hypothesis to explain the crossover (Coale and Kisker 1986; Johnson 2000). However, it is very difficult to test the hypothesis because seldom models are able to specifically address the variation among a population. The parameter *s* in the IEV model provides a way to further examine the phenomenon. In conclusion, the population heterogeneity is a fundamental component in shaping age-specific population mortality curves, such that more and more attention should be paid to it in considering the mortality patterns.

2.5.3 Environmental Parameters λ and β

λ and β mainly measure the acute effects on mortality from extrinsic challenges. As defined in previous sections, λ and β indicate challenge frequency and the average challenge magnitude respectively. Although these challenge parameters also affect the intrinsic absorption rate by changing the distribution of vitality, the influence is small and does not significantly change the shape of the intrinsic mortality process with age. Simulations show that within the parameter range for humans, the intrinsic mortality trajectories are almost indistinguishable under different challenge parameters. So I only display how the extrinsic mortality trajectories change according to λ and β.

Suggested by Fig. 2.9.C and D, λ and β shape the extrinsic mortality curve in different manners. A decline in the frequency term tends to benefit the old age group more than the early age group, whereas the advantage of lower average challenge magnitudes, as expressed by lower β, is diminished with age. It is not difficult to understand the distinct characteristics of the two parameters on mortality. In early life, when vitality is high, more frequent challenges do not cause a significant increase in the mortality rate because most challenges do not exceed the individual's vitality. In contrast,

more frequent challenges promote the chance of death at later ages when vitality levels are low and low magnitude challenges can exceed the remaining vitality and thus result in death. Therefore, λ, which controls the frequency of challenges, is a key to determine the level of mortality rate in this case. Correspondingly, a high average challenge magnitude β has a notable impact on survival in early time but not at later ages since most challenges would exceed the remaining vitality and thus kill the individual no matter what the magnitude is.

In general, the IEV model provides a framework to make intuitive statements on mortality shape.

2.5.4 Issues on the Identifiability of IEV Parameters

The identifiability of parameters is of concern in model validation. The sensitivity analysis above demonstrates that the four adult parameters shape mortality trajectories differently, which, to a certain degree suggests that their effects on mortality are distinguishable. In empirical model fitting, the middle-age "elbow" provides key information for disentangling intrinsic and extrinsic mortality rates. Prior to the "elbow", most death is from extrinsic process. Thus, the extrinsic mortality, which maintains an exponential increase with age across life is defined $\lambda \exp\left((1-rx)/\beta\right) = a\exp(bx)$, and a and b can be estimated from the linear portion of the log mortality curve prior to the mortality elbow (See Fig. 2.7). The intrinsic mortality is then derived as the total mortality minus the extrinsic mortality. r and s are independently estimated from the intrinsic mortality trajectory and the estimated r is used to disentangle λ from β in the extrinsic part based on $\beta = r/b$ and $\lambda = a\exp(1/\beta)$.

However, the differentiability between λ and β relies on the assumption that the parameters are constant across life. To be specific, λ and β can be only accurately separated if they are completely independent of age. But in reality, both parameters are expected to have age structures, especially for the challenge frequency term λ. To fit data it is necessary to have a higher value of λ at childhood and young adulthood, therefore it is plausible that the frequency of challenges varies over other life stages. Also, λ could possibly increase with age suggesting a higher susceptible rate to challenge for very old ages. But the model would allocate all the age-dependent components to exponential part, i.e. $\exp\left((1-rx)/\beta\right)$, and consequently change the estimated value of β. In other sense, the estimated λ would always represent the part that is non-monotonically changed with age.

Moreover, the model also has identifiability issues on mortality in the childhood stage when additional information of intrinsic survival is not available. While expressing child mortality as an exponentially decreasing mortality rate provides a reasonable fit to the data, it does not resolve the contributions of intrinsic and extrinsic processes. Irrespective of these issues, the assumption on λ yields a reasonably good fit to mortality data, and in particular for recent data.

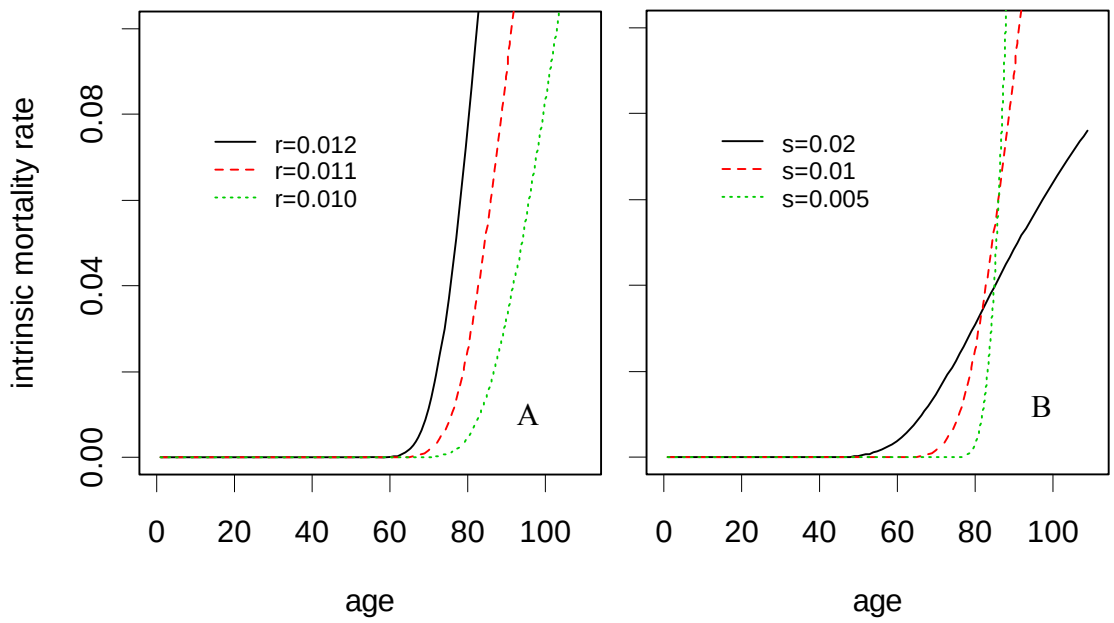

Figure 2.8: age-specific intrinsic mortality rate under different IEV parameters. (A). *r* varies, while s, λ and β are fixed at 0.01, 0.05 and 0.2 respectively. (B). *s* varies, while r, *λ* and *β* are fixed at 0.011, 0.05 and 0.2 respectively.

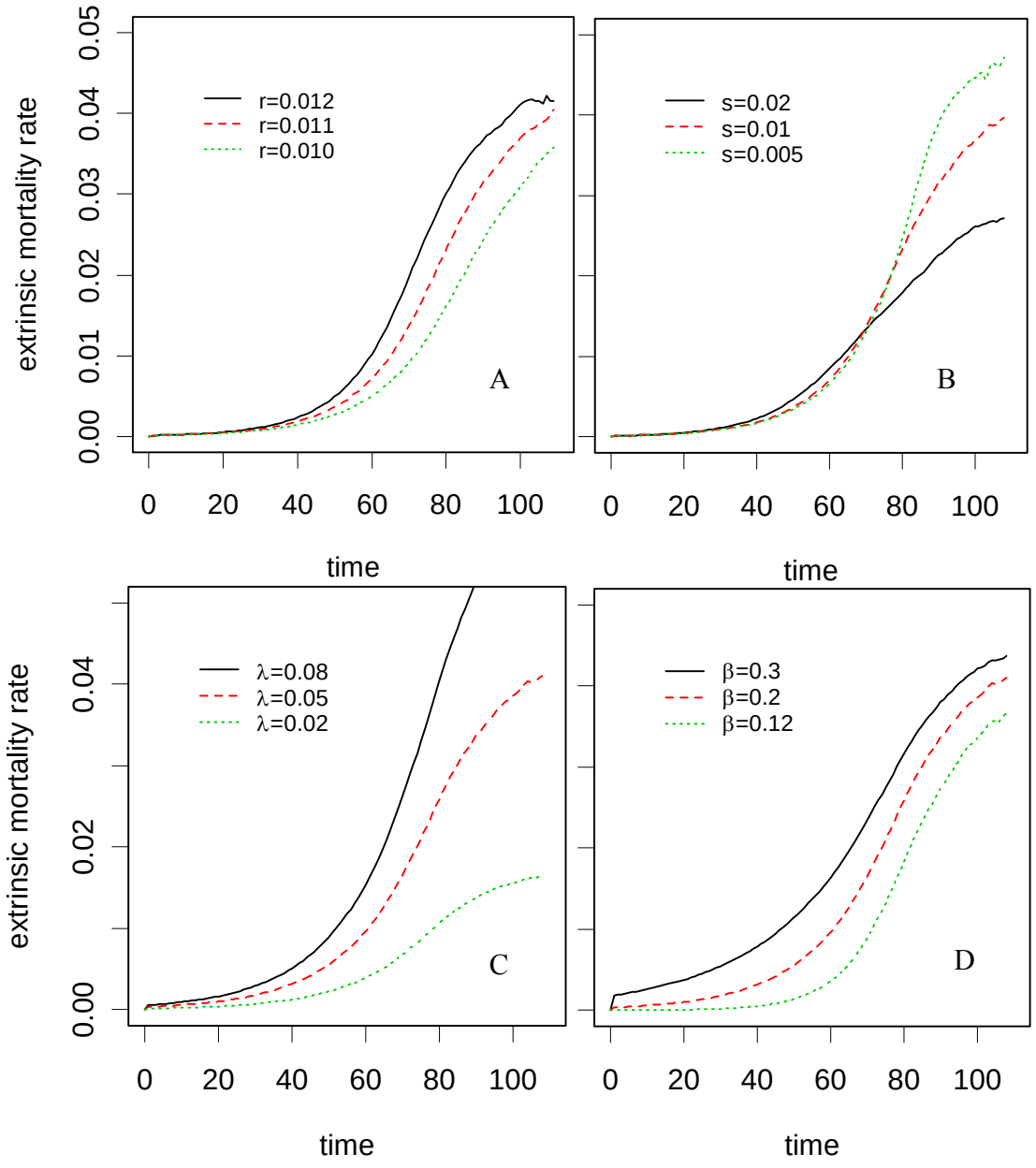

Figure 2.9: age-specific extrinsic mortality rate under different IEV parameters. (A). *r* varies, while *s*, λ and β are fixed at 0.01, 0.05 and 0.2 respectively. (B). *s* varies, while *r*, λ and β are fixed at 0.011, 0.05 and 0.2 respectively. (C) λ varies, while *r*, *s* and β are fixed at 0.01, 0.01 and 0.2 respectively. (D). β varies, while *r*, *s* and λ are fixed at 0.01, 0.01 and 0.2 respectively.

Chapter III: Heterogeneity structure of the IEV model and Mortality Partition

Compared to other models, the IEV framework has two prominent advantages in that it explicitly considers population heterogeneity and quantifies mortality from two sources. In this chapter, we further address these features and show how they can be used for understanding mortality patterns.

3.1 Heterogeneity Structure of the IEV Model

It is understood that individuals even within a population are different at birth and differentiate further over time because of their unique experiences and innate capabilities. These differences are generically attributed to heterogeneity, which is an important factor in determining features of population survival. These include the time to starvation, response to stress, expected life span etc. However, little attention was paid to the issue of heterogeneity in demography until the discovery of mortality plateaus: a widely observed tendency for the rate of mortality to level off at old ages (Carey, Liedo et al. 1992; Horiuchi and Wilmoth 1998; Vaupel, Carey et al. 1998) which was against the well-accepted Gompertz law (Gompertz 1825). There are at least two possible explanations for the mysterious phenomenon: the heterogeneity hypothesis and the individual-risk hypothesis (Khazaeli, Xiu et al. 1995). According to the heterogeneity hypothesis, the deceleration in the mortality rate is a statistical effect of selection through the attrition of weak individuals at early ages while strong ones survive longer, finally leading to a decline or leveling off of mortality rate at old ages. Alternatively, the individual-risk

hypothesis postulates that because the age-related increase of mortality at individual level slows down at older ages, the mortality drops.

Based on the first hypothesis of heterogeneity, a few models and theories have invoked a demographic stochasticity in which variability in survival and reproduction rates are expressed as random events within population age classes (Vaupel, Manton et al. 1979; Fox and Kendall 2002; Engen, Lande et al. 2003; Boyce, Haridas et al. 2006). Heterogeneity is then formally admitted. In popular demographic heterogeneity theories, heterogeneity is explicitly expressed in the mortality rate of a Gompertz model, by either assuming the distribution of mortality coefficients (Vaupel, Manton et al. 1979; Service 2000; Service 2004) or identifying the coefficients of subpopulations (Yashin, Ukraintseva et al. 2001). These models successfully explain the mortality plateau. In addition, Service (2000) used them to interpret the bell-shape of the age-specific patterns of variance in mortality rates. However, these heterogeneity models have been criticized from different aspects: Pletcher et al. (1998) first pointed out that in order to explain the mortality plateau, unrealistic variance in mortality rate parameters is required for these models and the deceleration is still observed even when great care is taken to reduce phenotypic variation. Then Mueller et al. (2003) questioned the results of Service (2000) and speculated that binomial sampling was sufficient to explain the bell shape of age-specific variance instead of considering within-line demographic heterogeneity which was suggested by Service (2000). Although Service (2004) responded, the problem still exists that these models are unable to distinguish the true heterogeneity effect from the statistical sampling effect.

If heterogeneity theories have value, to respond these criticisms mentioned above, a new way to model variation in population mortality is needed. Heterogeneity should be formulated more naturally and the model should also be able to show the heterogeneity effects without the disturbance of sampling effects. The IEV model proposed in this work can potentially solve the dilemma, since it has a biologically realistic form of heterogeneity. Moreover, the model explicitly considers the processes that produce heterogeneity which is not the case in many other heterogeneity models. For instance, the well-known frailty model, proposed by Vaupel et al. (1979; 1985) expresses an individual's survival capacity in terms of the deviation of its mortality rate from a cohort baseline. The model provides insight into survival processes but somewhat at the expense of added complexity to relate the rate of mortality to conditions that occurred prior to the time of the mortality event itself. In addition, it is unable to capture the change of population heterogeneity as time is evolving.

The previous chapter illustrates how the IEV model explains mortality plateaus. In this section, I will further explore the feature of mortality leveling off based on simulation results, with emphasis on demonstrating how the IEV model characterizes the bell shape of age-specific variance in mortality.

3.1.1 Heterogeneity Structure

Different from other heterogeneity models, the IEV model represents mortality variation in terms of the heterogeneity in vitality. Therefore, it is necessary to understand the variance structure of the vitality first. Similar to early version of the vitality models (Anderson 1992; Anderson 2000; Aalen and Gjessing 2001; Weitz and Fraser 2001; Anderson, Gildea et al. 2008), heterogeneity acts directly on vitality process in an

evolving manner which is manifested as a linear increase in the variance of the vitality distribution with time expressed as $E = s^2 t$. In reality, the variance in vitality comes from two sources: an initial heterogeneity, which results from genetic and epigenetic differences in individuals, is constant through life, and an evolving heterogeneity, which is an acquired difference that increases with age (Li and Anderson 2009). As discussed in the section of vitality normalization (2.2.1), the IEV model summaries variances from both sources into a single variable, *s*, indicating the fraction of vitality spread per unit time. Because the contribution from genetic variation is relatively small (Gavrilov and Gavrilova 1991; McGue, Vaupel et al. 1993; Hacker 1997), using a single variable *s* to reflect the combined effects of the two kinds of variations averaged in each age interval still yields a good approximation, but in a parsimonious way.

One point that needs to be emphasized is that in the IEV model only the intrinsic vitality process produces heterogeneity in vitality, while both intrinsic and extrinsic mortality processes reduce the total variability by removing individuals from the population. Intuitively, the variance in vitality starts to increase under the force of evolving heterogeneity and reaches the maximum value when the effect of killing process imposed on population surpasses that from the stochastic diffusion. Consequently, the age-specific variance in vitality has a natural bell-shape. Meanwhile, since extrinsic mortality has a monotonic relationship with vitality implied by eq. (2.7), the age-specific variance in mortality rate follows a similar shape. Mathematical statements will be presented to explain the age-specific patterns of heterogeneity in mortality rate.

3.1.2 Mortality Plateaus Revisit

One of the most interesting phenomena in demographical studies is the mortality plateau which is believed to be critical for explaining the dynamics of senescence. The mortality plateau, as defined previously, is a fundamental problem that "the supposedly tenets of ageing, namely the exponential growth of mortality rates proposed by Gompertz (Gompertz 1825), may fail to describe the behavior of observed populations adequately" (Weitz and Fraser 2001). More specifically, studies using different animals and humans demonstrate that mortality rates tend to level off and even decease at later stages of life (Carey, Liedo et al. 1992; Horiuchi and Wilmoth 1998; Vaupel, Carey et al. 1998). As explicitly addressed in the previous chapter, the IEV model naturally achieves a mortality plateau as a consequence of Markov-process model convergence to a quasistationary distribution. From the perspective of heterogeneity, the variance structure in vitality ensures some individuals die early and some die late. The slowing down of the average rate of vitality loss leads to the leveling off of mortality. Compared to other heterogeneity theories, the Markov-type model produces variance following a natural random process and thus no artificial selection process is required.

Although an analytical solution for the mortality plateau is not available, we can still assess its properties through simulations, such as the time when the plateau is achieved and the asymptotic mortality rate at the plateau stage. Since the plateau is mostly determined by the intrinsic vitality process, the parameters r and s play a major role in shaping the plateau. In contrast, the extrinsic parameters λ and β have limited impact. Therefore, we can illustrate the two features of the plateau mentioned with respect to variations in r and s only, while fixing λ and β. The procedure of simulation

follows the method described in Chapter II. Each mortality curve is constructed from population vitality trajectories under a desired parameter set. Mortality curves in log scale are then plotted against age (Fig. 3.1).

Mortality plateaus result under all simulated parameter sets and both *r* and *s* influence the time and the height of the plateau. Increasing *r* leads to earlier, and higher plateaus (Fig. 3.1A), while increasing *s* results in lower plateaus but does not significantly change the time to reach them (Fig. 3.1B). It is interesting that the level at which mortality is stabilized is fully determined by the ratio of *s* to *r* as suggested by Fig. 3.1C and D. In recent work, Vaupel (2010) displayed that the observed mortality rates at extremely old ages were very similar across years. This phenomenon could be explained under the IEV framework when *r* and s decline at a similar pace across all periods.

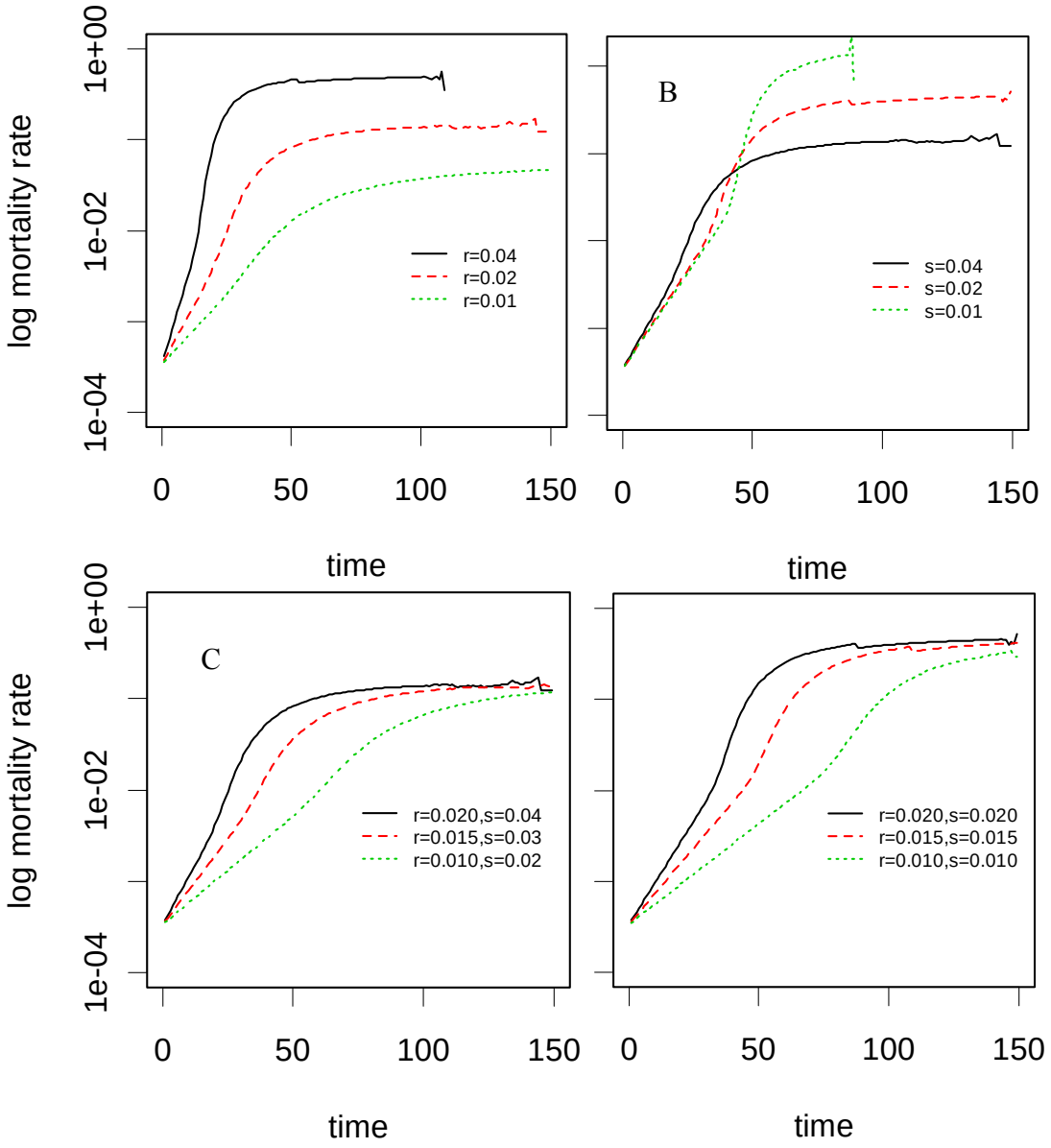

Figure 3.1: Log mortality against time (age). (A) *r* varies, while *s* is fixed at 0.02; (B) *s* varies, while *r* is fixed at 0.02; (C) *s*/*r* are fixed at 2; (D) *s*/*r* are fixed at 1. λ and β are fixed at 0.05 and 0.2 for all plots. Each curve is obtained through a simulated population with desired parameter values.

3.1.3 The Age-specific Patterns of Variance in Mortality Rate

Although age-specific patterns of variance in mortality rate are not as visually evident or noticeable as mortality plateaus, the pattern in variance gives an opportunity to compare

different demographic theories, like heterogeneity theory, evolutionary theory and others. Promislow et al. (1996) and Pletcher et al. (1998) first examined this rate variance in *Drosophila* experiments. A bell shape was observed for the variance in logarithmic scale of mortality rate: it was high or increased in early and intermediate ages and declined in old ages. This pattern was not predicted by theory, until Service (2000) proposed that the within-line demographic variation from heterogeneity theories might be responsible. This conclusion was questioned by Mueller et al. (2003), who suggested that the sampling effects could explain the pattern in heterogeneity. In spite of a quick response from Service (2004), heterogeneity theories still have to face a severe challenge that the model cannot isolate the effects of heterogeneity from that of statistical sampling. In the previous models heterogeneity has been expressed in terms of a parametric distribution, such that variance in mortality rate can only be obtained by repeated sampling, whereas the IEV model treats mortality rate as a random variable, which allows us to theoretically assess its variance directly in terms of the analytically derived probability distribution of vitality.

The individual level mortality rate $m(x)$ has two parts: the intrinsic mortality expressed as the absorption rate of vitality and the extrinsic mortality related to the individual vitality level. At each age, the former is constant while the latter is a random variable. Therefore, the only source of age-specific variation is from the extrinsic part, i.e. $m_e(x) = m_e(v_x) = \lambda e^{-v_x/\beta}$ (eq. (2.7)).

The delta method can be applied to approximate the variation at age *x*:

$$\mathrm{var}\left[m(v_x)\right] = \mathrm{var}\left[m_e(v_x)\right] \approx \left(\frac{dm_e(v_x)}{dv_x}\right)^2\Bigg|_{E(v_x)} \times \mathrm{var}\left(v_x\right) = \frac{\lambda^2}{\beta^2}\exp\left(-2\frac{\overline{v}_x}{\beta}\right)\mathrm{var}\left(v_x\right) \quad (3.1)$$

where the average vitality rate $\overline{v}_x$ and $\mathrm{var}(v_x)$ cannot simply be calculated from the Wiener Process, since vitality distribution is modified by the extrinsic death process. Although analytical forms for $\overline{v}_x$ and $\mathrm{var}(v_x)$ do not exist, numerical computations are possible. Although simulation is still used to examine the age-specific variance patterns in mortality, the IEV model does not require repeat sampling to generate mortality curves, but only relies on an approximation of the vitality distribution. Thus, no statistical effects are introduced.

In articles mentioned above (Promislow, Tatar et al. 1996; Pletcher, Houle et al. 1998; Service 2000; Service 2004) instead of mortality rate itself, the logarithmic scale is generally used. Also, in Service's (2000) opinion, the choice of logarithmic form influences the shape of variance. So the variance in the logarithmic form needs to be considered explicitly. By the delta method:

$$\mathrm{var}\left[\log(m(v_x))\right] \approx \left(\frac{1}{E\left[m(v_x)\right]}\right)^2 \mathrm{var}[m_e(v_x)] = \left(\frac{1}{\mu_e(x)+\mu_i(x)}\right)^2 \mathrm{var}[m_e(v_x)] \qquad (3.2)$$

where $\mu_e(x)$ and $\mu_i(x)$ indicate the extrinsic and intrinsic mortality at population level respectively and $\mathrm{var}[m_e(v_x)]$ is derived from eq. (3.1). Therefore, we can assess the age-specific shape of both variance of mortality in original and logarithmic scale through simulation.

Fig. 3.2 and 3.3 show the variance of mortality rates in normal and logarithmic form separately against age under different parameter sets. For the variance of mortality

itself, not all the parameter sets yield an obvious peak, but all of the curves tend to increase first and then decline. The plots illustrate that the bell-shape of age-specific variance in mortality can be explained by the vitality structure. The location and the height of the maximum variance are affected by all of the parameters. Under both scales in mortality, s, λ and β mainly influence the height of the maximum variance, where r determines both location and height. Intuitively, the larger the s term is, the higher the maximum variance is. A lower value in r imposes a smaller killing force, such that the time for the accumulation of variance is longer. Interestingly, λ and β have counteracting effects on the maximum variance. A larger λ increases maximum variance whereas a larger β reduces it.

Compared to the variance pattern in the normal mortality scale, the log transformation makes the bell shape more prominent, which corresponds to what observed in Promislow et al. (1996) and Pletcher et al. (1998)'s experiments. Hence, it supports the conclusion from Service (2000; 2004) that the reduction in variance of mortality rates at later ages is partially due to the choice of a logarithmic scale. Nevertheless, the bell shape essentially stems from the interaction between the stochastic aging process, which produces heterogeneity, and the death process including both boundary and extrinsic killing, which removes individuals from the population and thus reduces population variation.

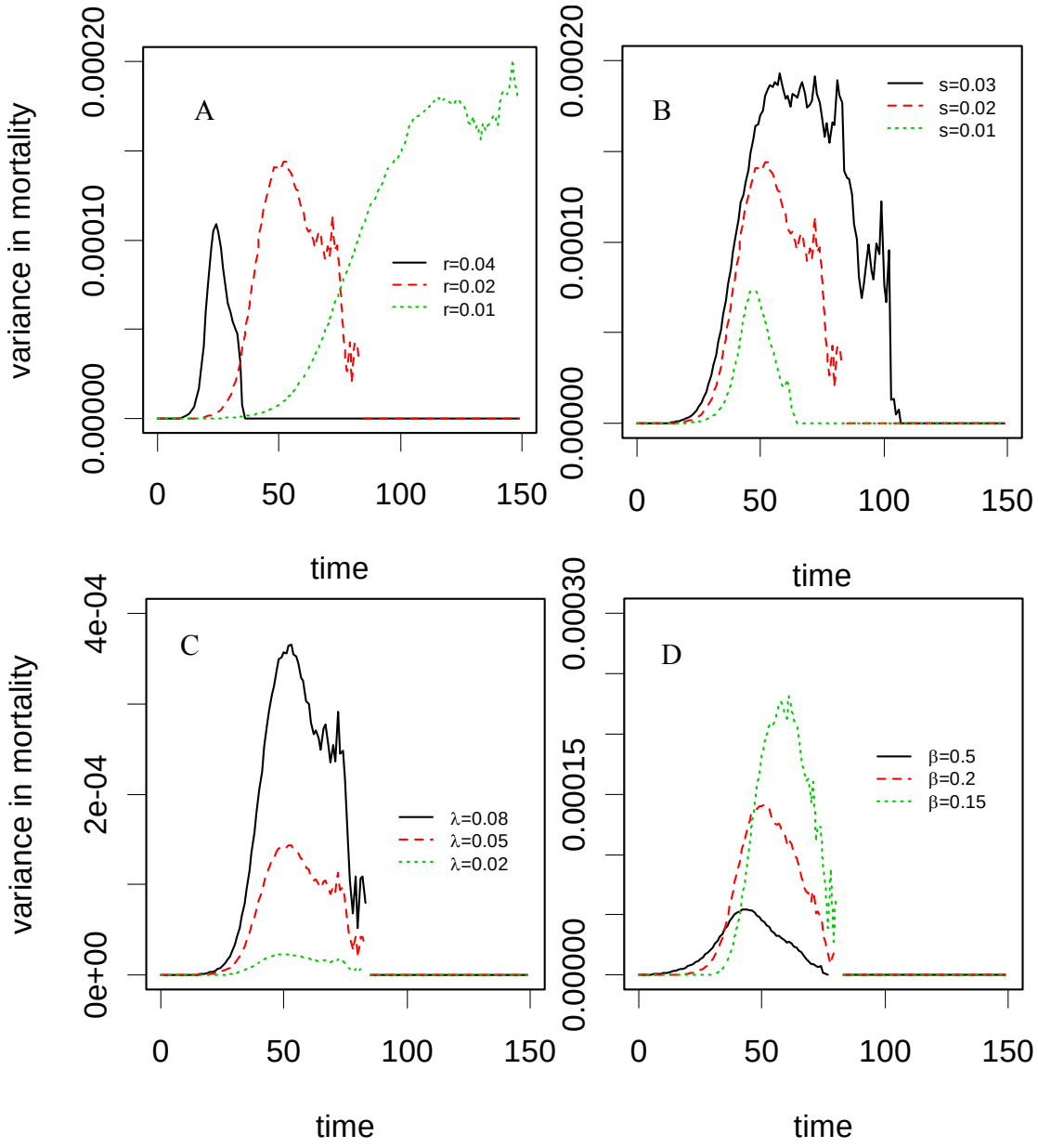

Figure 3.2: Age-specific variance in mortality rates under different parameter sets. (A) only r varies while $s = 0.02$, $\lambda = 0.05$ and $\beta = 0.2$. (B) only s varies while $r = 0.02$, $\lambda = 0.05$ and $\beta = 0.2$. (C) only λ varies while $r = 0.02$, $s = 0.02$ and $\beta = 0.2$. (D) only β varies while $r = 0.02$, $s = 0.02$ and $\lambda = 0.05$.

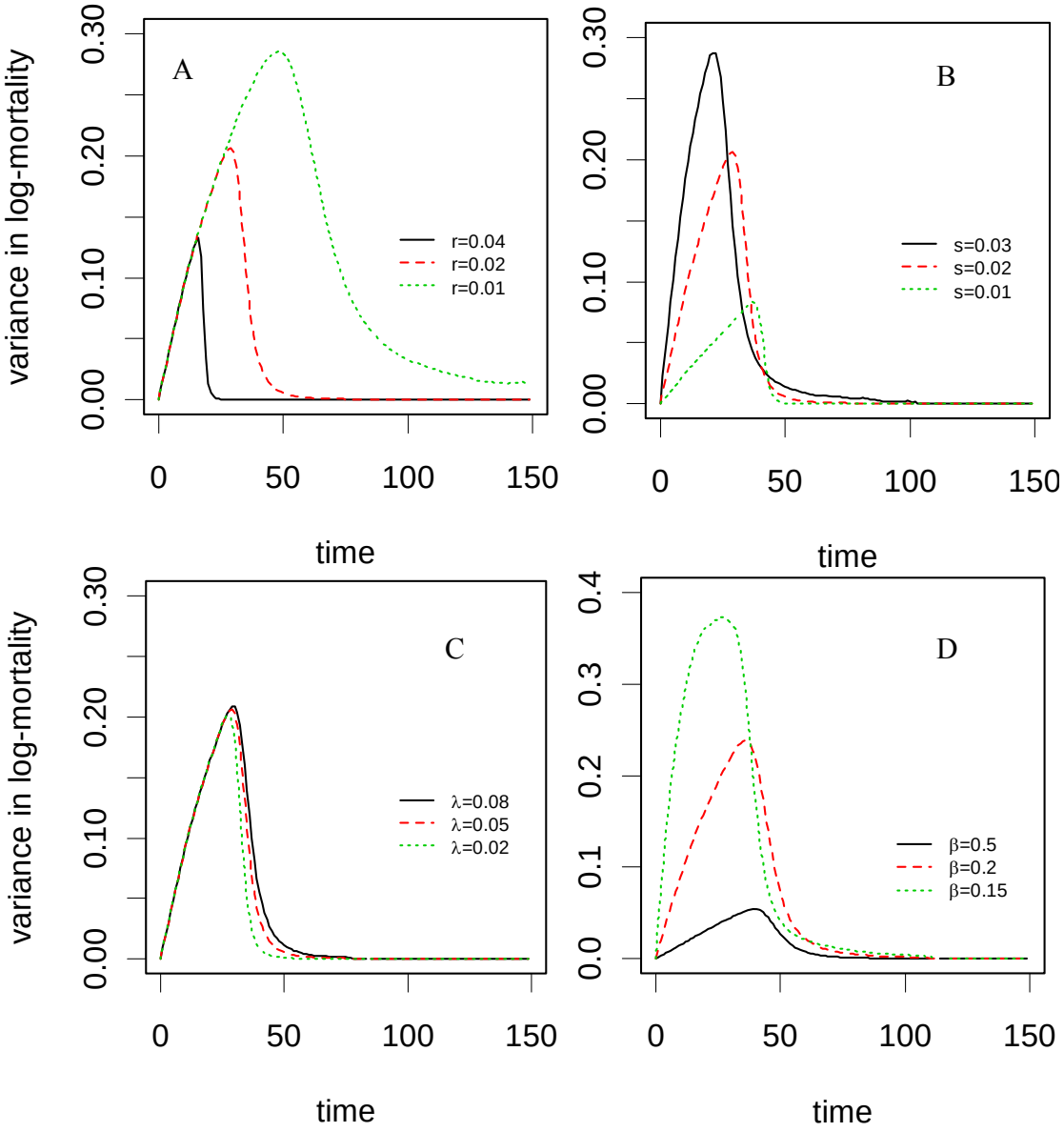

Figure 3.3: age-specific variance in logarithm mortality rates under different parameter sets which are chosen to be the same as figure 11. (A) only r varies while $s = 0.02$, $\lambda = 0.05$ and $\beta = 0.2$. (B) only s varies while $r = 0.02$, $\lambda = 0.05$ and $\beta = 0.2$. (C) only λ varies while $r = 0.02$, $s = 0.02$ and $\beta = 0.2$. (D) only β varies while $r = 0.02$, $s = 0.02$ and $\lambda = 0.05$. The bell-shape of variance has been remarked by the logarithmic transformation of the mortality rates. The curves yield significant peaks among for all parameter sets.

3.2 Mortality Partition

Because death has many causes, most scientists focus on subsets of causes, i.e. disease, suicide, alcohol. In spite of the success in each subfield, focusing on a single death category usually blocks the view of understanding mortality as a consequence of senescence (Carnes, Holden et al. 2006).

As early as 200 years ago, scientists began thinking about an informative standardized way to partition mortality (Carnes, Olshansky et al. 1996). Although there is no consensus, it is generally agreed that mortality can be divided into a senescence relevant part identified as "actual death" and the accidental part identified as "avoidable death" (McGlnnis and Foege 1993). Following Carnes et al. (1996), we denote the former intrinsic mortality and the latter extrinsic mortality which together correspond to the two death processes of the IEV model. Exploring the senescence process is believed to be a useful focus for understanding questions of primary concern, such as why organisms grow old, whether there is a way to slow down senescence, and what the life limitation is for human beings. At the same time, "the focus on intrinsic mortality does not mean that the extrinsic mortality is unimportant or of no interest" (Carnes, Holden et al. 2006). To the contrary, the extrinsic process plays a central role in the evolutionary theories of senescence (Kirkwood and Holliday 1979) and also expresses the environment that population experiences. Thus, an intrinsic/extrinsic partition of mortality is meaningful and most important, biologically motivated.

A model based partition was first attempted by Makeham (1860) by adding an age-independent term to the traditional Gompertz model (1825). By doing this, the causes of death were actually partitioned into: 1) a subset responsible for the age-dependent

increases in mortality that characterized the “Gompertz law”, and 2) a subset ascribed to ‘‘accidental circumstances’’ that do not depend on age. The problem with this approach is that since the method is based on the Gompertz law, which represents death as an instantaneous mortality, the concept is ambiguous. In other words, because of lacking a biologically meaningful process, the partition is usually unconvincing. For instance, Makeham has been criticized for using the age-independent part as the extrinsic mortality, as there is no visual evidence to indicate that the extrinsic mortality is constant with age (Carnes, Holden et al. 2006).

Due to the difficulties of formulating the partition mathematically, information on the causes of death has become more important. Non-model based approaches of partition have been widely adopted with increasing knowledge of disease mechanisms. Researchers, drawing on specific studies of mortality, have developed mortality partitions. For instance, Clarke et. al (1950) divided total mortality into anticipated deaths (“accident, disease or any other cause, which are anticipations of the natural termination of life”) and senescent deaths (principally “arteriosclerosis, cardiovascular diseases, renal diseases, bronchitis and bronchopneumonia, and senile decay”) and assumed that the proportion of total mortality attributable to senescent causes increased from 5% at age 20, to 100% above age 80. Benjamin (1959), on the other hand, classified all deaths before age 55 as accidental, and all deaths after age 76 as senescent. A recent classification criterion of intrinsic and extrinsic mortality established by Carnes et.al (2006) is based on whether the primary cause of death does, or does not, originate from within the organism. Through this standard, they conducted a mortality partition relying on the 6th, 9th and 10th Revisions of the International Classification of Diseases (ICD) published by the

World Health Organization (WHO). Although these approaches used the knowledge available, a perfect partition could not be achieved for several reasons. Firstly, many diseases have unknown etiological mechanisms. Secondly, humans may die from multiple causes, which makes it difficult to classify the death. Thirdly, sometimes death from a particular disease may be categorized differently. For example, lung cancer can be naturally originated from within the organism but can also be raised due to the exposure to mutagens or carcinogens. According to the criterion of Carnes et. al. (2006), the former death is defined as intrinsic while the latter is considered as extrinsic. Even if errors are allowed in the partition, these methods are inadequate for examining mortality patterns and conducting survival prediction, because they highly depend on the death information from the data which is usually unavailable.

The two-process model developed here provides a natural partition to the mortality into extrinsic and intrinsic parts without additional information on the exact cause of death and thus provides a judgment-free partition on which to base analyses of mortality patterns. In contrast to Makeham's model and any later improvements, the IEV models takes the process point of view in which the two processes are built on a common concept of individual's survival capacity, *vitality*. Since both intrinsic and extrinsic deaths are based upon meaningful processes, the method is biologically robust.

3.2.1 Intrinsic Mortality

The intrinsic mortality in the IEV model refers to death from vitality absorption into the zero boundary. It is the endpoint of aging process when the organism exhausts its survival capacity. According to the previous definition, each individual starts with certain amount of vitality that declines stochastically with age. Intrinsic death happens when the

vitality trajectory hits the zero-boundary as the consequence of aging. Although the real mechanisms for aging are highly complex, including fundamental changes in both physiologic functions and cells that are unable to be explicitly defined, the intrinsic death can be represented in a tractable way: the collapse of internal system when the natural damages are accumulated to a certain point such as organ failure or malfunction under the vitality framework. The parameters r and s are designed to characterize the intrinsic mortality, among which r is the mean fraction of vitality loss per unit time so $1/r$ measures the approximate average death time from the intrinsic mortality, and s is the heterogeneity parameter which stochastically spreads the vitality trajectories and ultimately shapes the population variance in intrinsic death time (Anderson 2000; Anderson, Gildea et al. 2008; Li and Anderson 2009).

Despite the fact that intrinsic mortality primarily reflects death originated from inside the body, it can be largely modified by external interventions. Harsh environmental conditions, bad nutrition supplies and unfavorable habits all might substantively raise the vitality loss rate and thus change the intrinsic mortality. On the contrary, a better living condition and healthy life style could extend life expectancy through slowing down the chronic vitality process. As suggested in chapter 2, the schedule of intrinsic death helps reveal the chronic survival conditions of organisms which can be affected by both internal and external factors.

Note that in a hypothetical environment where infectious diseases, aggression, fatal accidents, etc are totally removed, the population would theoretically achieve the average potential life span $1/r$ with variance expressed in s. In other words, $1/r$ defines the survival capacity under the average chronic conditions of the population.

3.2.2 Extrinsic Mortality

Probably, an easier way to define the intrinsic mortality is through the extrinsic mortality, in the sense that intrinsic causes of death are those that remain after excluding the total extrinsic causes of death. On the other hand, the extrinsic mortality can be defined as deaths occurring through processes other than natural damage accumulation. Thus, whether originating from within organisms, or not, is not a satisfying definition of extrinsic mortality. In our opinion, extrinsic mortality is relatively avoidable, preventable and treatable including mortality mainly from infections, accidents and even internal pathological changes (challenges) that cause unnatural collapses of organism's survival system. As stated before, the extrinsic mortality is not necessarily independent of age, on the contrary, it is highly likely to be associated with age, as suggested from previous discussion. Under the vitality framework, extrinsic mortality accounts for most of the early-age deaths whereas intrinsic deaths largely occur at old ages. It is difficult to determine whether a specific disease belongs to the intrinsic or extrinsic category, but expressing the partition through the statistical fit to data avoids problems involved with an artificial classification based on the assumed cause. Considering the previous example, the model would likely classify an early-age lung cancer death from smoking as an extrinsic event which is the consequence of exposure to carcinogens, while at old age, death from the same cancer would likely be classified as intrinsic which is probably caused from the malfunction of lung due to damage accumulation.

Extrinsic mortality is characterized by three factors: the frequency and average magnitude of challenges and the vitality level, but the extrinsic process only controls the first two. The extrinsic mortality is considered as an instantaneous event or process

occurring over a relatively short period. Compared to intrinsic parameters, the extrinsic parameters characterize the acute conditions of environment. In a generic form, both the frequency and the average magnitude of challenges can be modeled as constants across all age groups to represent the mean effects. However, more complexity can be added to capture the pattern of high child mortality. I model the challenge frequency as an exponentially declining function with age, implying that early ages have higher chances to encounter external strikes or pathological changes. It is understandable that the instability of a newborn's system may induce high-frequency pathological changes that attack its own organism and lead to unnatural failures (Chandra 1997; Holt and Jones 2000). The children may also have a lower recovery chance, indicated by a lower vitality as compared to young adult. I approximate the combined effects of increased frequency and reduced vitality in childhood by an exponentially decreasing function as mortality rate determined by death rate at age zero, μ_0, and the rate of mortality decline α.

Essentially, the intrinsic-extrinsic partition easily deals with age-specific events, such as the ability of explaining the consistently observed mortality "elbow" as the large presence of intrinsic mortality.

3.2.3 Mortality Partition Applied to Human Data

With the intrinsic-extrinsic framework, mortality partitioning can be applied to human mortality data for examining the patterns of both chronic and acute deaths. All age-specific mortality data are obtained from the Human mortality database (HMD 2010) with time interval of 1 year. Age-specific intrinsic and extrinsic mortality rate are abstracted from the IEV model fit to the empirical data. To be specific, I estimate the

parameters first and then portray the intrinsic and extrinsic mortality trajectories predicted by the estimated parameters.

Firstly, I compare US death rates classified by sex for period year 1945, 1970 and 2000 to see if humans exhibit changes in partitioned death rates over that broad time periods. Across all the years, extrinsic mortality dominates before age 50 and intrinsic mortality becomes dominant after age 50. Indicated by Fig. 3.4A and B, females have consistent improvements in both intrinsic and extrinsic mortality over almost all the ages from year 1945 to 2000, although the differences among the three years diminish at the extreme old ages. As discussed in the section of mortality plateau, the asymptotic mortality rate at plateau is determined by the ratio of the fraction of vitality spread (s) to the fraction of vitality loss per age (r). Therefore, the convergence of intrinsic mortality at plateau is suggested by similar values of s over r among the three period years. For males, the patterns are more complicated. The age-specific intrinsic mortality rate is significantly lower in 2000 than in 1945 but for 1970 intrinsic mortality is higher than either 1945 or 2000 for individuals less than 65 year age. This anomalously high rate for 1970 is mostly likely due to high death rates associated with a high incidence of smoking in the previous two decades (Preston and Wang 2006; Wang and Preston 2009). The lower intrinsic mortality rate in 1970 for males > 65 may be partially attributed to the larger selection effects imposed by smoking status at middle ages that remove frailer individuals. The male extrinsic mortality shows a consistently decline from 1945 to 2000 for almost all the ages (except the very old ages). The ratios of s to r are more heterogeneous among the three years for males (1.12, 1.82, 0.93) than for the females

(1.04, 0.95, 0.87), and thus the male mortality trajectories are less likely to converge to a single value.

A general improvement in survival has been observed through the second half of the 20th century for both sexes in the U.S, but the partition between extrinsic and intrinsic mortality reveals useful insights into the mechanisms of change in mortality patterns.

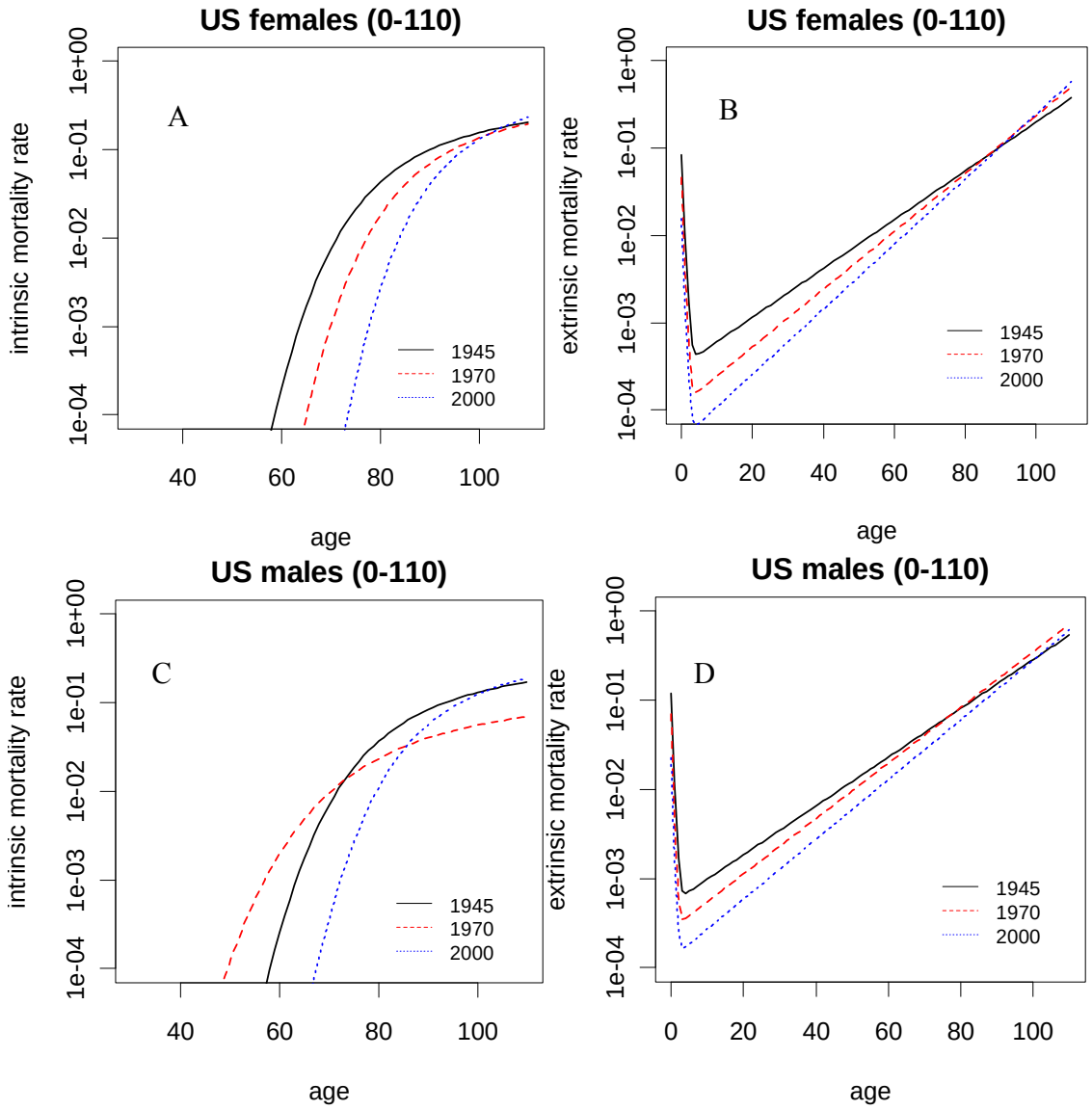

Figure 3.4 A comparison of age-specific death rates for intrinsic (A. females C. males) and extrinsic (B. females and D. males) mortality among period year 1945, 1970 and 2000.

Besides understanding the separate trajectories of intrinsic and extrinsic mortality, it is also interesting to explore the ratio of intrinsic mortality over the total rate, in particular when both absolute rates keep declining.

The ratio of the intrinsic mortality rate to the total rate is depicted in Fig. 3.5 for Sweden, Japan and the U.S. from selected period years. All countries and sexes exhibit

the same general trend; the ratio of intrinsic rate is zero up to middle age > 50, rises to a peak in old age, ~ 80, and declines at extreme old age, > 90. The onset of intrinsic mortality, i.e. non-zero values, has steadily increased across years indicating that the onset of senescence related process is being delayed. The decline of ratios at extreme old age may be an artificial effect caused by approximation to the extrinsic mortality. According to the original model setting, both intrinsic and extrinsic mortality would reach a plateau at very old age, such that the ratio of intrinsic rate should also level off. However, the extrinsic mortality is approximated as an increasing function with age here and thus the pattern at very old age exhibits an artificial decline.

For the patterns across different period years, there seems to be an increasing trend in the proportion of intrinsic deaths at very old ages through year 1800 to 1900 (indicated by Swedish population) implying the overall improvement of extrinsic mortality exceeds the improvement from intrinsic, and thus more and more individuals survive to old ages and die from intrinsic causes during this period. However, the entire 20th century shows an opposite trend with decreasing percentages of intrinsic mortality at old ages. The decline in the percentage (or the increase of proportion in extrinsic mortality) is likely to be the consequence of the large delay of extrinsic mortality to old ages and the simultaneous improvement in senescence-related rate (Fries 2005). The third period starts from year 2000 showing a reversal in the trend of intrinsic mortality percentage at old ages, although the onset time for intrinsic mortality has not changed too much especially for the Japanese population. It is not clear whether the recent trend is artificial or not. The patterns for the proportion of intrinsic mortality over the total one are complicated and involve many factors. We only conduct a preliminary examination

here and a thorough investigation needs further information regarding to the change of social, biological, environmental factors and so forth.

It is also possible to compare patterns among countries and genders. In contrast to Sweden and Japan, the U.S. has consistently lower proportion of intrinsic mortality through the entire lifetime uniformly across all the selected period years. In other words, extrinsic mortality always accounts for the major deaths even at very old ages for the U.S. With regard to the gender, males have a consistently high proportion of extrinsic mortality, suggesting they are more vulnerable to environmental challenges.

In summary, this cursory analysis suggests that the age-specific partition between intrinsic and extrinsic mortality rates reflects subtle changes in mortality processes across time, cultures and gender.

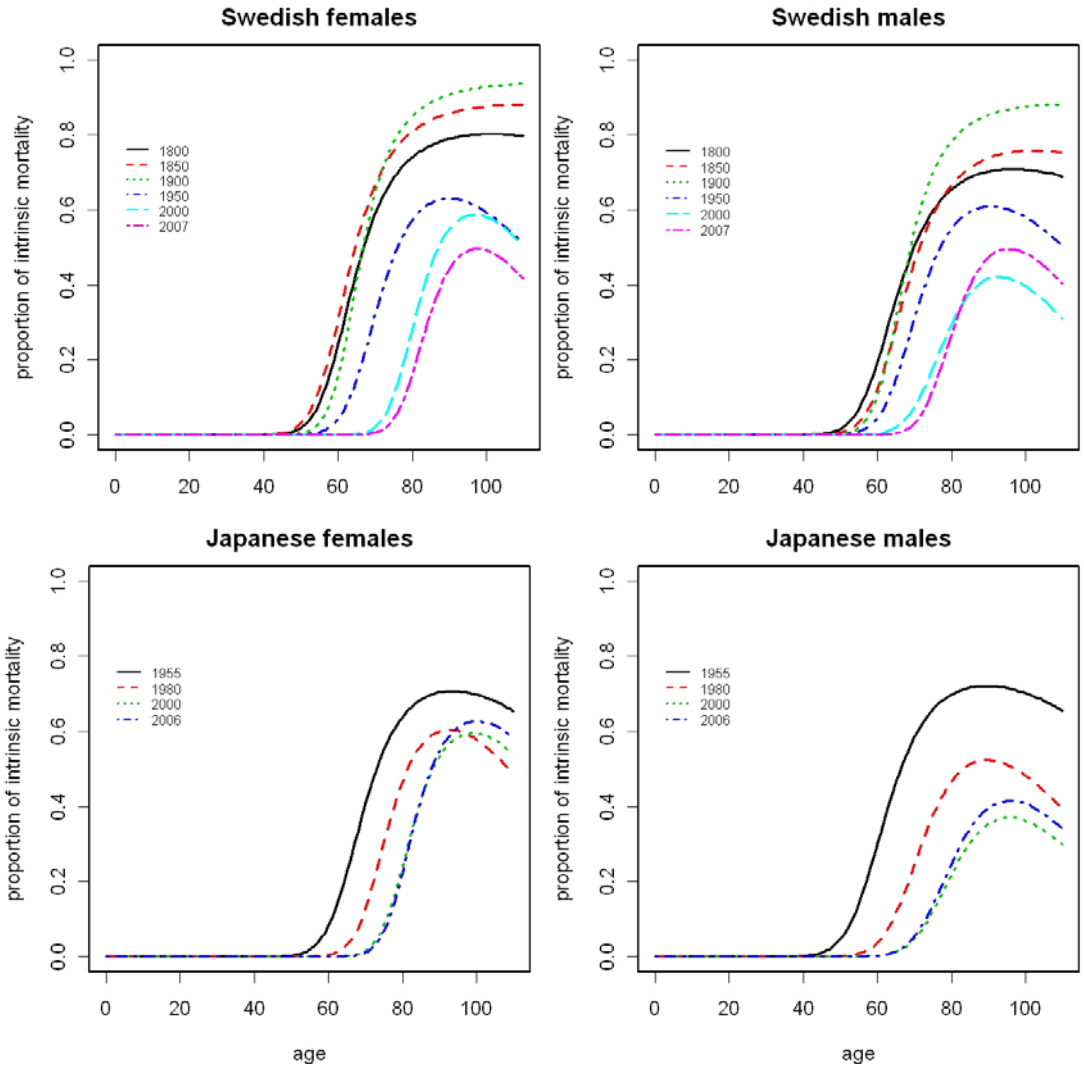

Figure 3.5: Proportion of intrinsic mortality rate in the total mortality rate against ages for Swedish, Japanese and the U.S. populations with selected period years.

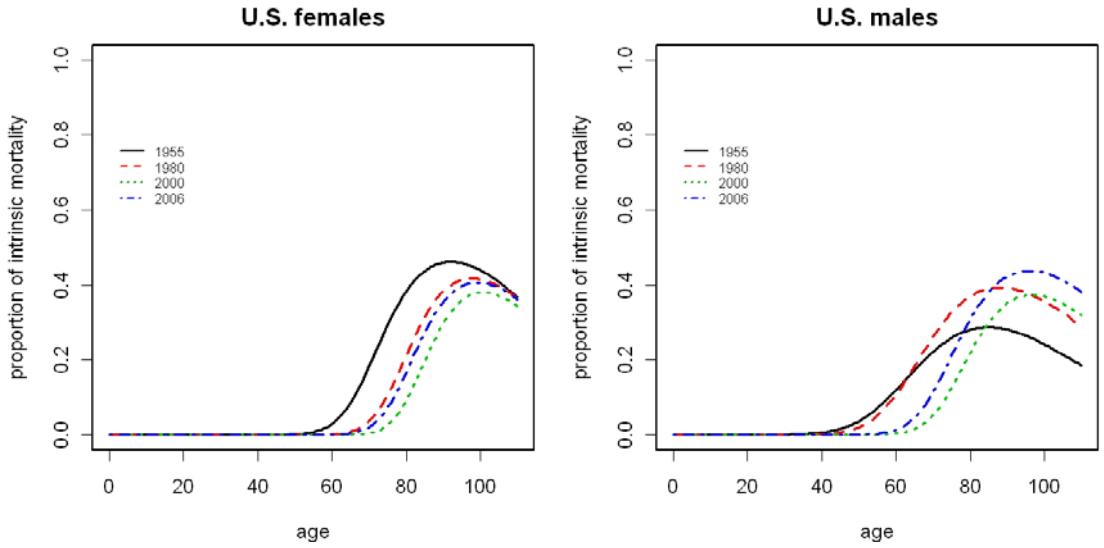

Figure 3.5 (cont.): Proportion of intrinsic mortality rate in the total mortality rate against ages for Swedish, Japanese and the U.S. populations with selected period years.

3.2.4 Interspecies Comparison of Intrinsic Mortality Patterns

As suggested by Carnes et al. (1996; 2006) mortality partitions also should be useful in interspecies comparisons of mortality patterns. Comparing survival across different species is very difficult, not only because their average life spans are, varying from days for insects to decades for humans and some large mammals, but also life history strategies are highly diverse across species. Consequently the patterns of intrinsic and extrinsic mortality rates can be quite different across species. For instance, the IEV model developed here postulates that the human extrinsic mortality is approximately an exponentially decreasing function of age, whereas the previous vitality models with a constant extrinsic killing rate, the extrinsic rate fits survival data from laboratory animals very well (Anderson 1992; Anderson 2000; Anderson, Gildea et al. 2008; Li and Anderson 2009). Even within a species, animals living in the wild typically do not reach their potential life expectancy because of predation and accidents imposed by the harsh

surroundings. In contrast laboratory groups are likely to survive longer with abundant food supplies and protection from natural predators. The mortality partition provides a way to separate the intrinsic mortality from the complex interventions of environment and narrows the comparison within intrinsic schedules. Because scientists are largely interested in how similar senescence-related mortality profiles are among different species, in particular, whether the variable intrinsic mortality signatures of humans resemble those of other animals in the controlled environments. Such comparisons are believed to be important for understanding the natural selection on population survival (Eakin and Witten 1995; Eakin and Witten 1995; Carnes, Olshansky et al. 1996; Carnes and Olshansky 1997; Carnes, Holden et al. 2006).

Carnes et al. (2006) compared the intrinsic mortality of human beings derived from their information-based partition with the mortality of laboratory mice and dogs. They scaled the survival curves by the median age at death to remove life-span effects and found that the intrinsic mortality patterns among different species had far more similarities than differences. They specifically introduced a statistic, the relative interquartile rate (%IQR), to measure the population variation in death time which was not affected by any proportional scaling of time and thus reflected the true differences in intrinsic mortality schedules among these populations. %IQR is computed as the difference between the 75^{th} and 25^{th} percentiles of the intrinsic survivorship distribution expressed as a percent of the median. A smaller %IQR means the survival curve is more compressed, in other words, the relative population heterogeneity is smaller. By comparing %IQR, Carnes et al. (2006) concluded that human beings and some laboratory animals share a similar relative variation in intrinsic death time.

The whole analysis can be redone in the framework of the vitality model which proposes a biologically meaningful partition to mortality. This model-based classification, not relying on detailed information on cause of death and artificial criterions, is more robust for comparisons. The mean survival time implied by $1/r$ provides a more intuitive way to scale survival curves and s serves as the direct measurement of population variation in intrinsic death time. In addition, since the information of causes of death is usually not available for laboratory animals, Carnes et al. (2006) might have slightly overestimated the intrinsic mortality level for those groups without eliminating the possible extrinsic interventions. In contrast, the IEV model can also be applied to animal data and thus helps disentangle the pure effects of intrinsic and extrinsic mortalities for laboratory animals.

From the point of view of the IEV model, the similarity between human and other animals on scaled survival curve is not surprising at all, because the intrinsic death time always follows an inverse Gaussian distribution defined by the model. The inverse Gaussian distributions only differ in scaled variance parameter characterized by s/r for different populations. s/r is the measure of the relative variation (RV) analogous to the coefficient of variation (CV). As discussed previously, RV is an important variable to determine the magnitude of mortality in the plateau.

Fig. 3.6 illustrates the clustering of RV by species and includes Swedish females and males at selected period years (1800, 1900 and 2000) from (HMD 2010) and laboratory studies on survival in *Drosophila* (Min and Tatar 2006), medfly (Carey and Liedo 1995), nematode (Wu, Cypser et al. 2009) and mice (Sprott 1997). The figure illustrates that the heterogeneity in RV among species is larger than that within a species.

The laboratory mice have the lowest RV compared to others, while insects have higher RVs and human beings are in between.

This study suggests that different animals may have distinct signatures of intrinsic mortality even after survival curves are normalized to the same scale. In particular, the intrinsic variation structures indicated by RV vary from species to species. It is not clear whether the differences are caused by the laboratory environment or the natural characteristics of different species. This question is beyond the scope of the dissertation. The main point is that the IEV model provides a useful tool for mortality partitions that can be applied to a broad range of fields such as biology and ecology.

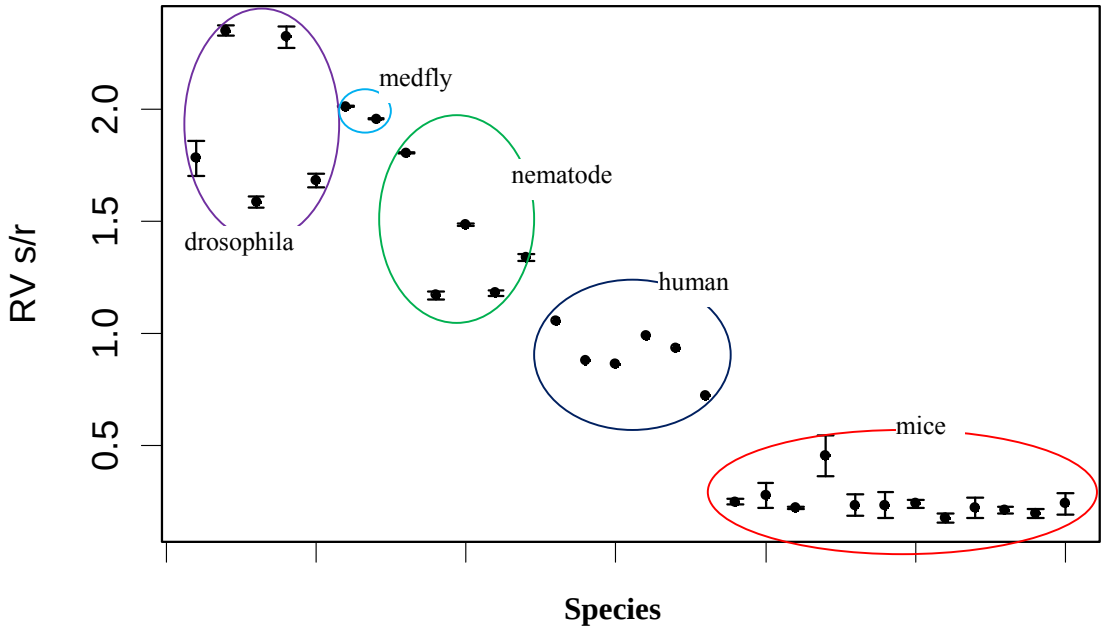

Figure 3.6: The relative variation (RV) calculated from different laboratory species and human population (Swedish females and males). 95% Confidence interval (CI) for RV are marked as bars. Note that because the population size of human is very large compared to the other animal populations used here, the CI is very small for humans and not visible in this plot.

Chapter IV: Historical Exploration of Human Mortality Patterns through Vitality Parameters

The health transition, which describes the reduction of mortality in the long run (Lerner 1973; Frenk, Bobadilla et al. 1991), has many causes (Schofield, Reher et al. 1991; Riley 2001). However, identifying the leading factors in different historical stages is very appealing to scholars from many disciplines (McKeown 1976; Kunitz 1986; Chesnais 1992). One way to explore the problem is through understanding the mortality patterns over time. The parametric methods may provide a way to examine the patterns which have many advantages for describing mortality, including "smoothness, parsimony, interpolation, comparison, trends and forecasting and analytic manipulation" (Congdon 1993; Dellaportas, Smith et al. 2001). Moreover, the longitudinal patterns in model parameters are likely to informatively reflect the health transition occurring over the past two centuries. These parameter patterns across years, in particular for developed countries, have been widely studied but based on different model specifications. For instance, Riggs and Millecchia (1992) explained mortality trends in industrialized countries using the Gompertz-Strehler model, Pireto et al. (Prieto, Llorca et al. 1996) analyzed Spanish adult mortality from both Gompertz and Weibull models, Heligman and Pollard (1980) tracked the Australian mortality over the 20th century based on the Heligman-Pollard model and Gage (1993) decomposed the mortality patterns of England of Wales by the Siler model (Siler 1979). Nevertheless, analyzing longitudinal data through the IEV model has advantages over these methods in its ability to succinctly summarize historical transitions in mortality dynamics through its biologically meaningful parameters. To be specific, the IEV model facilitates a time-series approach

in which the historical change in the pattern of human mortality can be decomposed into the longitudinal pattern of the vitality loss rate r, the heterogeneity term s, the challenge exposure rate λ and the average challenge magnitude β.

4.1 Data Source and Method

To illustrate the capability of the model to resolve mortality patterns, I first employ Swedish mortality data for both females and males from period year 1800 to 2007 (data source: Human mortality database (HMD 2010)) in section 4.2. Sweden, having the longest history of reliable records in mortality data, is also among those countries that are most advanced in extending lifespan. Besides, an abundance of studies on Swedish mortality patterns (Heckscher 1950; Wall, Rosen et al. 1985; Himes 1994; Hemström 1999; Wilmoth, Deegan et al. 2000; Yashin, Begun et al. 2002; Curtis 2010) allows a thorough cross-validation and comparison of the model with other models. According to the maximum likelihood function eq. (2.14) used in the fitting algorithm, only age-specific survival rates are needed for parameter estimation. The data are extensive from the human mortality database, with one-year increments from 0 to age 110 in period years between 1800 and 2007 stratified by sex.

For section 4.3, a cross-country comparison is conducted. Other than Sweden, I select period survival data of Switzerland (1900-2006), Japan (1946-2006) and Chile (1992-2005) from Human mortality database (HMD 2010) to represent different ethnic groups.

Period Data vs. Cohort Data

It needs to be further clarified that the IEV framework was originally built on a cohort population in which each individual has its own vitality trajectory simultaneously

projecting to future from their birth year. Under such a circumstance, the IEV parameters are derived from the average life experiences of the cohort population. However, in this study instead of cohort data, I mainly use period data not only because they are available for longer longitudinal years and are more complete than cohort data (Preston, Heuveline et al. 2001), but also there is an essential difference in explaining the parameters estimated from period and cohort data which makes the model more appropriate to fit period data. For cohort data, the estimated parameters characterize the average properties of the population in successive years for both intrinsic and extrinsic conditions. Although it makes sense to represent the intrinsic chronic process by the mean, it is problematic to average the extrinsic acute process from several years especially when the external conditions vary from one year to another. In contrast, for period data, the population is hypothetical as if they live their entire life according to the rates of a single period. While r and s are the synthetic measures of vitality process averaged from all individuals who die at the same year, λ and β characterize the extrinsic conditions which the hypothetic cohort experiences in a specific year. Since the period population is very likely to be subject to the same acute conditions at their death year, applying constant λ and β to period data seems more appropriate than to cohort data.

I fit these period survival data with the six-parameter version of the IEV model. Parameters are estimated with a maximal likelihood optimization as developed by Salinger et al. (2003) and adapted by Li and Anderson (Li and Anderson 2009). For every year, a set of the 6 parameters is obtained. Longitudinal patterns for Swedish population data are depicted in Fig. 4.1-4.3 and the cross country comparisons are illustrated in Fig. 4.4. Corrections for the model approximations were applied to parameter r, s, λ and β

according to section 2.2.2, though the general trends in the parameters did not change after correction.

4.2 Longitudinal Patterns in Vitality Parameters for Swedish Population

4.2.1 Longitudinal Patterns

Average fraction of vitality loss per year, r

The parameter *r*, representing the average fraction of vitality loss per year, determines the rate of senescence-related degeneration. The reciprocal of *r* approximately indicates the average longevity in the absence of extrinsic mortality. The effects of vitality loss equally acts across the entire population, which means a change in *r* tends to shift the age of median survival but does not significantly change the general shape of the survival curve such that the survival curve slope about the median age is relatively constant (Li and Anderson 2009). Despite the fact that *r* mainly characterizes the intrinsic process, it is modifiable by behavior and extrinsic conditions, such as smoking status, nutrition level and physic activity which have accumulative effects on survival. In other words, changes in *r* reflect alterations in chronic processes that influence mortality.

Over history (1800-2007), the vitality loss rate consistently declined corresponding to an increasing longevity for both females and males (Fig. 4.1A). Prior to 1950, the decline in the rate was relatively slow accompanied by some variation. This continuous improvement was likely the result of better nutrition and shelter conditions associated with the agrarian and industrial revolution in Sweden over the 19th and the early 20th centuries (Sundin and Willner 2007). Values of *r* are very similar between female and male implying small sex differentials in the intrinsic process. From the second half of 20th century, the rate of decrease in the vitality loss rate accelerates for both sexes.

However, females exhibit slightly lower *r* values which might reflect differences in lifestyle choices such as the levels of smoking and alcohol consumption between men and women (Agren and Romelsj 1992; Bongaarts 2006; Preston and Wang 2006). Both activities have cumulative effects on health and so they should affect the mean rate of vitality loss over the population lifespan. Although it is not clear whether there is a leading factor responsible for the decline in *r* during this period, strong economic growth, leading to a significant increase in the standard of living plus advancements in healthcare, improved diet and behavior, likely contributed to delaying the onset of the senescence-related process (Sundin and Willner 2007).

Variability in intrinsic process, s

The parameter *s* characterizes variation in the rate of loss of vitality, i.e. it quantifies the stochastic variability in the intensity of the intrinsic process. Individuals are different at birth and differentiate further over time because of their unique experiences and innate physiology and genetics. These differences are generically referred to as population heterogeneity, which is an important factor in determining features of population survival. Once again note that the Gompertz model does not characterize heterogeneity in any form and extensions that have incorporated it are rather ad hoc. In the context of the IEV model, *s* has a crossover effect on survival in that lower value of *s* benefits population survival at early ages but is detrimental to survival at old age (Li and Anderson, 2009). That is to say, a more homogeneous population survives better at the beginning but dies out more quickly at the end.

The variability in the vitality process, *s*, incorporates both initial variation resulting from genetic heterogeneity and evolving variation acquired with age. However,

studies have shown that only about 20% of the variation in human survival is heritable (Gavrilov and Gavrilova 1991; McGue, Vaupel et al. 1993; Herskind, McGue et al. 1996) and human genetic variation is presumably stable over the study period (1800-2007). Therefore, historical changes in the pattern of *s* should largely be determined by historical changes in the rate of evolving heterogeneity. As demonstrated by Fig. 4.1B, *s* continuously decreases through the first half of the 20th century for both sexes. Plausible reasons for the decrease in heterogeneity include reductions in the inequalities in living standards due to the economic growth and the improved distribution in health resources associated with the development of public health (Sundin and Willner 2007). From the second half of the 20th century, the patterns of *s* significantly differentiate between males and females. While evolving heterogeneity in females continues to decline, the term increases in males between 1950 and 1980 and then declines about to the value for females. Several studies confirmed there was a trend of widening of social inequality in adult mortality among men but not among women from 1960s to the early 1980s (Diderichsen 1990; Vagero and Lundberg 1993; Diderichsen and Hallqvist 1997). These works investigated cohort mortality data stratified by occupation or social economic status and suggested that increasing class differences in smoking contributed to the increasing differentials in male adult mortality during this period. Compared to epidemiology studies that rely on detailed cohort data, the IEV model tracks trends in mortality heterogeneity from general population data. The model's ability to capture detailed transitory life history events from essentially raw mortality data is somewhat surprising and illustrates the identifiability of processes through the vitality framework.

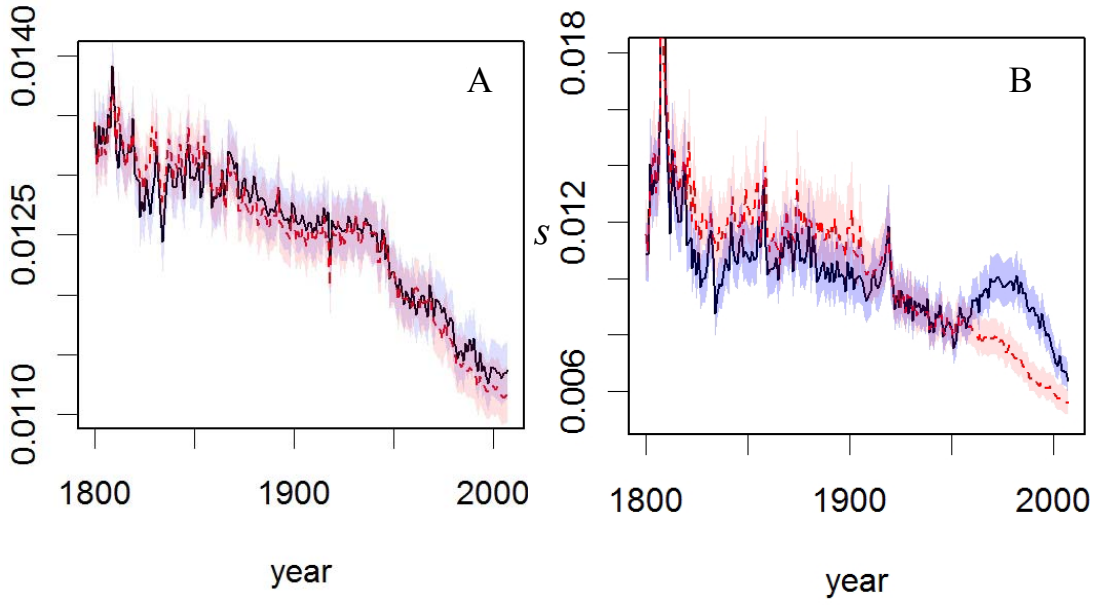

Figure 4.1: longitudinal patterns of vitality parameters for Swedish population (1800-2007): (A) fraction of vitality loss per unit time *r* and (B) variation of vitality spread *s*. Male and female patterns are depicted as solid and dash lines separately and the shade areas indicate 95% confidence interval.

Extrinsic challenge parameters, λ and β

The challenge frequency, λ, and the average challenge magnitude, β, generally reflect the acute extrinsic effects on post-adolescent mortality. Lower values in both parameters indicate a more favorable environment and consequently better survival. However, as discussed in chapter II, λ and β characterize the extrinsic mortality from two different aspects and shape mortality curve in distinct manners.

β quantifies the average magnitude in extrinsic challenges and primarily illustrates the period effects of environment on survival. Thus, it has close relationships with historical events, such as wars, famine and pandemics of infectious disease, which influence mortality of all age groups (Omran 1982). Meanwhile, the benefits from public health and the breakthroughs of medical technology that lead to overall mortality

reduction (Mason and Smith 1985; Frost 1995) are likely to be reflected in the change of β. The value of β is sensitive to the alteration of mortality at early and middle age, because the effects of challenge magnitude on survival are gradually diluted with ages. The underlying basis of this characteristic is intuitive. Larger β would impose notable impact on early age mortality but would not make a significant difference in older individuals when vitality level is low and any challenges can kill. Also note that β is a relative measure of environmental deleteriousness with respect to the society standards. For example, a disease like pulmonary tuberculosis was fatal about 100 years ago but is curable today because of medical technology. Although the absolute magnitude of the disease may not change, i.e. to what average degree it would damage the body, its relative detriments to human society has been greatly reduced corresponding to a large reduction in β.

The historical pattern of β exhibits a gradual decline but with significant departures that demonstrate correlations with environmental and cultural stages (Fig. 4.2A). Anomalously high values are associated with the Swedish-Finnish war in 1808 and 1809 and the influenza pandemic between 1918 and 1919 (Sundin and Willner 2007). Outsides these anomalies, the pattern of β can be roughly divided into three stages. The entire 19th century corresponds to the first stage where β is large and variable. I speculate that this variability in the magnitude of extrinsic challenges was driven by variability in year-to-year variations in environmental conditions. The second period, covering the first half of the 20th century, exhibits a dramatic decline in β. Many studies (Ryder 1965; Omran 1982; Riley 2001) proposed that medical interventions eradicated many infectious diseases over this period and the hypothesis is supported by the decline in β. Essentially,

the model indicates that the magnitude of challenge from infectious diseases was diminished by medical advancements. The recent 50 years constitute the third period in which the average challenge magnitude declined to a low asymptotic level.

Compared to β, the pattern of λ, the adult challenge frequency, is rather perplexing. Instead of an anticipated decline, λ exhibits a significant increase around 1950s for both sexes implying there are more challenges today than 100 years ago (Fig. 4.2B). This puzzling phenomenon requires additional discussion.

One potential explanation is that the rise in λ reflects a physical and tangible increase in the frequency of environmental stressors associated with modernization such as increased environmental pollution and carcinogens (Public Health Service, 1979), increased car accidents (Crimmins 1981), and increased exposure to disease associated with public transportation, e.g. air and subway travel (Colizza, Barrat et al. 2006).

Another possible explanation considers fixed environment conditions but a decline in the efficiency of the immune system. The changes in human behaviors, such as smoking, alcohol addiction and obesity, weaken the body defenses and thus raise the exposure rate to challenges (Ryder 1965). In particular, the epidemic of smoking has proved to be an important factor that influenced mortality in the 1960s in industrialized countries (Bongaarts 2006; Preston and Wang 2006).

Also, Yahsin et al.(2001; 2002) found a similar increase pattern in challenge frequency around 1950 using the Strehler and Mildvan general theory of mortality aging (Strehler and Mildvan 1960). Then they proposed a “theory of survival trade off” which suggests the organism can actively organize a defense against challenges balancing

between two different strategies: one is to refuse the stress and make the organism more robust and the other is to prompt the rate of damage repair. In our model, it implies that the increase in λ is because energy is allocated to reduce r.

The factors mentioned above may contribute to some increase of λ, but it is unlikely that they can fully account for the dramatic and simultaneous increase for both sexes within such a short period, i.e. between 1945 and 1951. Thus we also need to consider the possibility of model misspecification. As discussed in section 2.4.4, the estimation of λ would be biased when the model assumption cannot well describe the truly underlying processes. I will further explore the potential model misspecification and address this issue in Chapter VI.

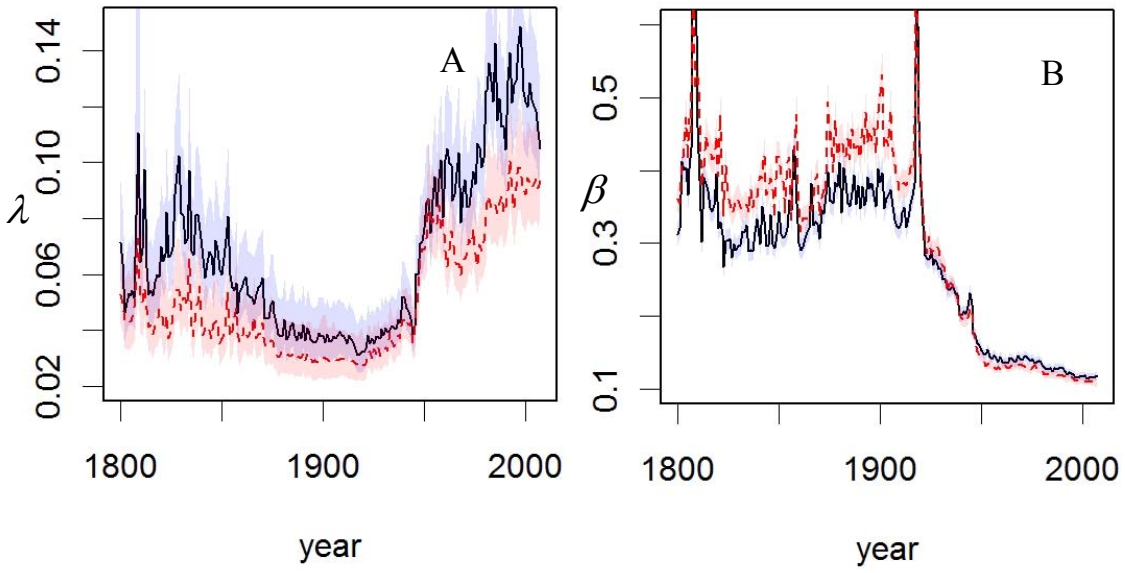

Figure 4.2: longitudinal patterns of vitality parameters for Swedish population (1800-2007): (A) frequency of adult challenge λ and (B) average magnitude of challenge β. Male and female patterns are depicted as solid and dash lines separately and the shade areas indicate 95% confidence interval.

Childhood mortality parameters, μ_0 and α

The childhood parameters μ_0 and α represent the high extrinsic mortality rate at age zero and its rate of decline with age respectively. The historical patterns of μ_0 and α for Swedish populations are straightforward (Fig. 4.3A-B). μ_0 has a general decreasing trend, but the decline is more rapid during two periods: the 19th century and the 1940s. In contrast, α is flat up through about 1875, increases steadily but to about 1950 and then increases over about 10 years to a high. The improvement in child mortality from the contributions of both components (μ_0 and α) seems to reach a plateau in recent years.

Comparing the patterns between males and females, female children have a consistently lower value of initial mortality rate, i.e., μ_0, whereas α in males and females

are similar indicating the duration of susceptibility to childhood mortality factors is similar in the sexes.

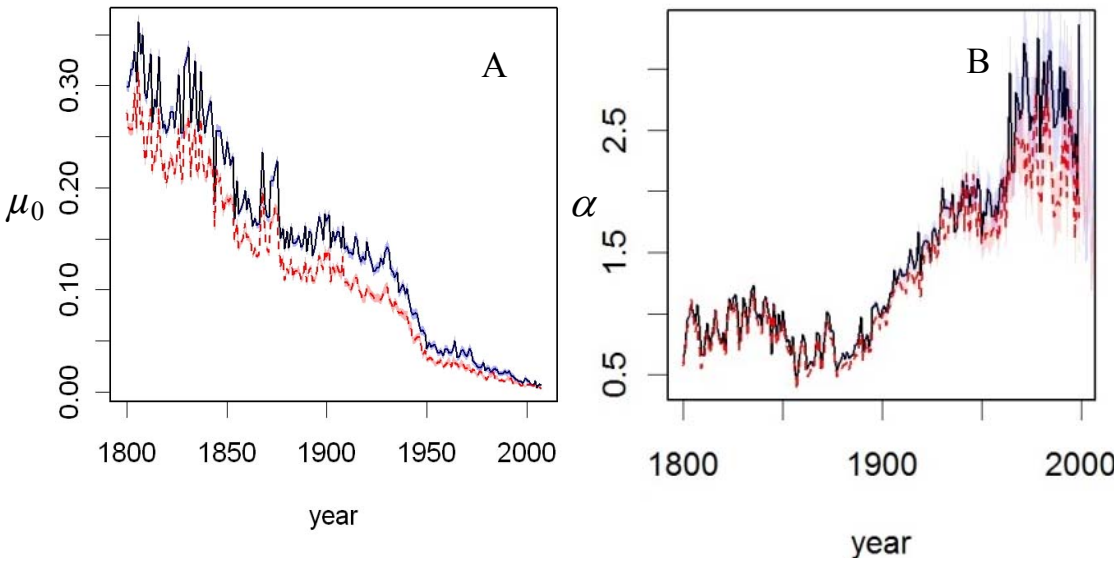

Figure 4.3: longitudinal patterns of vitality parameters for Swedish population (1800-2007): (A) initial mortality rate at age zero μ_0 and (B) the rate of mortality decline at childhood α. Male and female patterns are depicted as solid and dash lines separately and the shade areas indicate 95% confidence interval.

Summary

The value of the IEV model largely lies in describing the historical trends in terms of its biologically meaningful parameters. In particular, the model provides a quantitative description of the contribution from intrinsic chronic process and extrinsic acute process. According to the parameter patterns, the health transition in Sweden between 1800 and 2007 can be divided into three stages roughly corresponding to the division in epidemiological transition which is considered as one of the important theories in explaining the health transition (Omran 1977; Omran 1982; Fries 2005). The epidemiological transition depicts “the mortality declines as series of sea changes in the

leading causes of death, moving from an era of pandemic infectious diseases to an era in which chronic organ diseases dominate all causes of death" (Riley 2001). The first stage covering the entire 19th century is dominated by infectious diseases, famine and other extreme events. Thus, the survivorship largely depends on the natural environmental conditions characterized by high values of the average challenge magnitude β with large variation from year to year. Interestingly, there is essentially no change for β and only a slight decline for λ implying that the extrinsic acute effects on mortality haven't been much improved, despite the introduction of sanitary and public health projects. Meanwhile, a consistent decline in the intrinsic parameter r and s suggests that improvements in the standard of living accounts for most of the mortality reduction in this period. This finding largely agrees with the well-known work from McKeown (1976) who argued that a rising standard of living, especially better nutrition, mattered most in extending life expectance during the 19th century. Intuitively, a change of nutrition level mainly contributes through a chronic process, such that, its effects are reflected in r and s. The second stage of the epidemiological transition corresponds to a progressive decline in β indicating a large decline of infectious diseases in the first half of the 20th century. The rate of decrease in r diminishes and thus the leading contribution to mortality reduction in this period is the change of extrinsic acute conditions which are thought to have resulted from medical intervention and improvements in curative medicine (Sundin and Willner 2007) . The second stage is transitory, representing a change from an era dominated by infectious diseases to an era dominated by chronic diseases. In the third stage, corresponding to the last 50 years, both λ and β are gradually stabilized. The dominating

mortality factors in health transition switch back to the intrinsic ones as in the first period. However, at this stage the intrinsic processes are principally senescence-related diseases.

While each stage of the in health and epidemiological transition has been thoroughly studied (McKeown 1976; Omran 1977; Omran 1982; Kunitz 1986; Chesnais 1992; Riley 2001), the vitality model offers the prospect of quantifying trends in terms of its biologically meaningful parameters. The model uses essentially raw mortality data, independent of additional information, to track the historical patterns in the intrinsic and extrinsic processes of mortality. In particular, the model reveals patterns that are not evident in other studies. For example, while the fraction of vitality loss per year (r) has continuously declined over two centuries, the decline accelerated, representing a significant improvement in population vitality, after WWII. Meanwhile, in the last half century the extrinsic acute effects contributing to the increase of longevity reach a plateau; as denoted by stabilized λ and β. Finally, trends in population heterogeneity can be independently quantified through s. The decline in s tends to accelerate in recent years suggesting better sharing of health resources and technology.

4.2.2 Sex Differentials in IEV Parameters for Swedish Population

The ability to compare survival in terms of fundamental processes is also an advantage for the vitality model. The Swedish-female-and-male comparison reveals something interesting. Women and men have a similar intrinsic degenerative rate (r), but are different in other processes. The lower λ for women indicating a lower frequency in challenge events is possibly due to their physiologic robustness in resisting stresses, less reckless behaviors and less harsh working conditions (Wingard 1982; Waldron 1983; Nathanson 1984; Owens 2002; Crimmins and Finch 2006). However, both s and β exhibit

complicated patterns between the two sexes. Prior to the 20th century, female patterns indicate a higher degree of population heterogeneity and higher average challenge magnitude than males but the trends reverse in the recent 50 years. The high maternal mortality in 19th century may partially explain the larger value of β for females. Maternal mortality constituted about ten percent of all deaths among women in the 15-49 age group up until the latter stages of the 19th century (Sundin and Willner 2007). The dramatic fall in the risk of death during childbirth in the 20th century largely eliminated the survival differential between females and males. On the contrary, the increasing deaths from accidents caused by violence, alcohol consumption and so forth for men makes their average challenge magnitude surpass that of women after WWII. The larger variation among males in the second half of the 20th century has been explained previously as the wide differentials in smoking status among different occupation and social economic groups (Diderichsen 1990; Vagero and Lundberg 1993; Diderichsen and Hallqvist 1997). But the larger level of heterogeneity for females in 19th century is difficult to interpret. One potential explanation is that females were allocated less food than males when food resources were limited (Johansson 1984; Humphries 1991; Klasen 1998). Thus, the disparity in family economic status may have contributed to the model-identified differential in heterogeneity between males and females.

4.3 Mortality Comparison across Countries

In the previous section, I focused on the historical mortality patterns for a single country and demonstrated that the IEV model was useful for understanding health transitions and changes of mortality dynamics across time. Here I compare model parameters from different countries. In addition to Sweden, period survival data from Switzerland (1900-

2006), Japan (1946-2006) and Chile (1992-2005) are employed. The results are exhibited in Fig. 4.4, stratified by parameters and sexes. Only 4 adult parameters are shown.

The intrinsic parameter r and s for the three developed countries (Sweden, Switzerland, and Japan) are similar, but Japanese show some advantages in slowing down the rate of vitality loss in recent years (Fig.4.4A-B). Population heterogeneity increased around 1960s in Swedish and Swiss males (Fig. 4.4D), which is probably due to the effect of smoking as discussed in section 4.2.1. However, in the same period the influence of smoking is not evident in Japanese males. In comparison, Chile has higher values for both the rate of vitality loss and spread, but r starts to decline after 2000. The frequency of extrinsic challenge in males is similar across countries, but the patterns in females are different in the recent period (> 1980) (Fig. 4.4F). Chile females have the largest λ, females in Japan and Switzerland have the lowest values, and Swedish females have intermediate values (Fig. 4.4E). The average challenge magnitude, β, gradually converges for these countries, in particular for women (Fig. 4.4G-H). Again this suggests that modern medical technologies, which influence β, have become widespread.

4.4 Conclusion

In this chapter, the ability of the IEV model to track longitudinal mortality patterns was demonstrated in a descriptive manner. A more in depth analysis relating model parameters to quantitative measures of associated factors is highly feasible but is beyond the scope of this work. For example, relating model parameters to independent variables such as the index of economic development, measures of public health resources and levels of environmental quality should yield important information on the contributions to patterns of mortality. In the literature when there is no better way to summarize the

survivorship of a population, the life expectancy is largely in use. Other factors are related to the life expectancy to determine whether they have significant impacts on population mortality (Preston 1975; Rodgers 2002; Soares 2007). Nevertheless, the mortality process is so complex that a single dimension is inadequate to represent the whole system. More or less, information is lost when efforts concentrate on analyzing the life expectancy alone. The IEV model is an appealing way to represent mortality in terms of multiple biologically meaningful dimensions and thus is of great value.

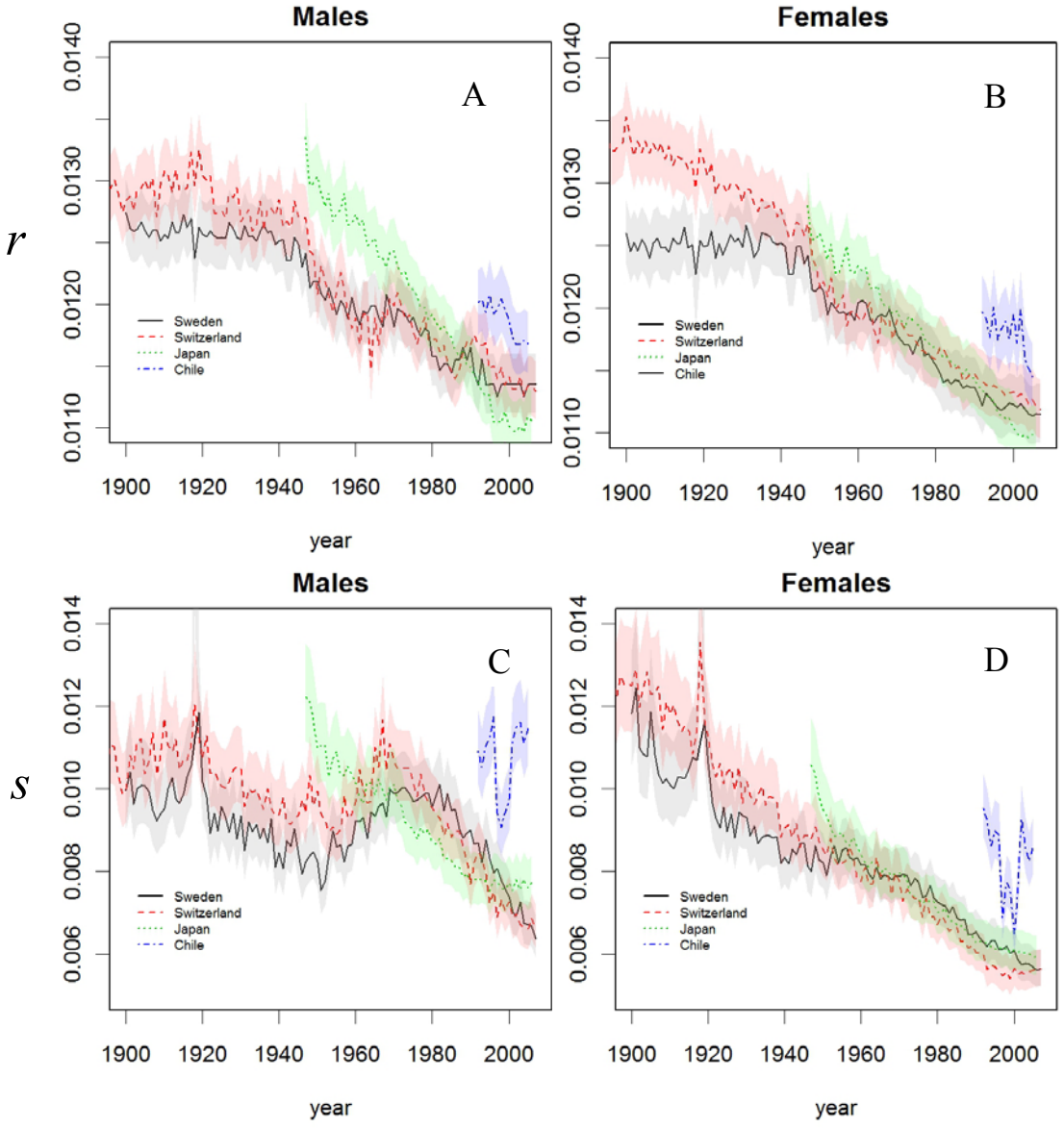

Figure 4.4: A cross-country comparison for the 4 adult parameters of the IEV model stratified by sex and parameters. Data are collected from Human Mortality Database (HMD 2010) including Sweden (1800-2007), Switzerland (1900-2006), Japan (1946-2006) and Chile (1992-2005). Approximated 95% confidence intervals are indicated by the shade areas.

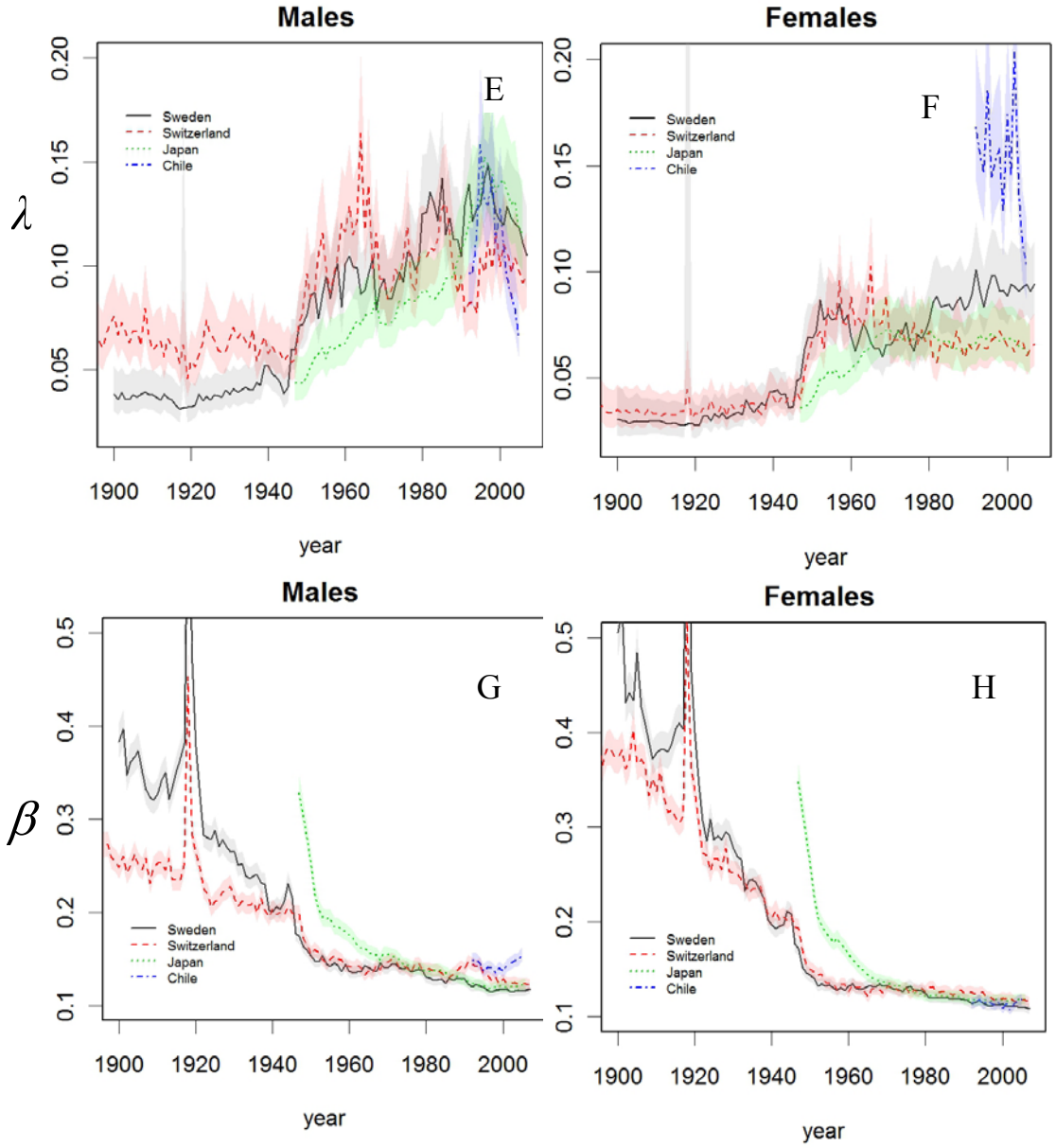

Figure 4.4 (cont.): A cross-country comparison for the 4 adult parameters of the IEV model stratified by sex and parameters. Data are collected from Human Mortality Database (HMD 2010) including Sweden (1800-2007), Switzerland (1900-2006), Japan (1946-2006) and Chile (1992-2005). Approximated 95% confidence intervals are indicated by the shade areas.

Chapter V: Comparison between the IEV and Other Mortality Models

In this chapter, I discuss how the IEV model compares to other mortality models, to illustrate some of its advantages in regards to its ability to fit data and understand mortality processes. The comparisons are with the Siler model (Siler 1979), the Heligman-Pollard (HP) mortality law (Heligman and Pollard 1980) and the Strheler-Mildvan (SM) general theory of mortality (Strehler and Mildvan 1960).

5.1 Comparing with the Siler model and the Heligman-Pollard (HP) mortality law

5.1.1 The Siler and the HP model

The Siler model (Siler 1979) and the HP mortality law (Heligman and Pollard 1980) represent a series of models that focus on fitting empirical age-specific mortality curves throughout the entire life span (Thiele 1872; Mode and Busby 1982; Mode and Jacobson 1984; Gage and Mode 1993). The two models are chosen here, because they are intensively discussed in the literature.

The Siler model, also known as the competing risk mortality model, was first proposed by Siler to model animal survival (Siler 1979) and then intensively applied to human mortality data by Gage and colleagues (1988; 1989; 1990; 1991; 1993). It is a five-parameter three-component competing hazards model, specified by

$$\mu_x = a_1 e^{-b_1 x} + a_2 + a_3 e^{-b_3 x} \tag{5.1}$$

The first additive component accounts for the decline in mortality with age during childhood which has the same child mortality function used in the IEV model. The

second component is defined by a single parameter a_2 corresponding to the Makeham's constant to denote the age-independent mortality. The third component follows the Gompertz law representing the senescent mortality suggested by Siler (1979) and Gage and Mode (1993). Finally, the total instantaneous mortality μ_x is defined as the additive effects of all three hazards.

The 8-parameter HP model also schedules mortality in terms of three competing parts: the child mortality, young adult mortality and the Gompertz-like component:

$$q_x = A^{(x+B)^C} + De^{-E(\log(x)-\log(F))^2} + \frac{GH^x}{1+GH^x} \qquad (5.2)$$

However, instead of modeling instantaneous mortality rate, the HP model uses q_x, the probability of dying within the interval. The mortality rate can be approximated from q_x as $\mu_x = \frac{q_x}{1-0.5q_x}$ when mortality rates are assumed to be linear across each age category and $\mu_x \approx q_x$ under small values of q_x (Preston, Heuveline et al. 2001). In the first component of the model, parameter A is nearly equal to q_1, which is the probability of dying during the second year of life. It is also analogous to a_1 in the Siler model and μ_0 in the IEV model. C characterizes the rate of decline in mortality with age, similar to b_1 and α in the Siler and IEV model respectively. The third parameter, B is an age displacement to account for mortality between age 0 and 1. The second component is designed to reflect the observed accident hump. This part contains three parameters, D, the intensity of young adult mortality, E, the spread of the accident hump and F, the location of the hump. Note that this component degenerates to Makeham's constant when E is 0. Finally, G and H characterize the Gompertz-like component.

The Siler and HP models are based on similar philosophies. Mortality results from three independent pieces in both models. They only differ in that HP has more parameters and thus yields better fits, in particular for child and young adult mortality. The arguments between the two models revolve around whether an accident hump is a universal feature of human mortality patterns (Heligman and Pollard 1980; Benjamin 1989; Gage and Mode 1993), since, for either empirical or theoretical applications, "the ideal model is one that precisely captures the characteristic features common to all human mortality curves while ignoring the idiosyncratic features and measurement error incorporated in a particular mortality curve" (Gage and Mode 1993).

Empirically, the mortality hump is indeed not universally observed through all data sets particularly for female mortality curves from industrialized countries, but this does not necessarily diminish the value of the HP model. When there is no significant hump, the second component in HP model is expected to converge to a Makeham's constant as allowed by its flexible structure. Interestingly enough, in reality, the HP model "mistakenly" adapts the curvature at later age, which corresponds to the later age "elbow" in the IEV model, through its "hump" component under such a circumstance. This problem has already been illustrated in Heligman and Pollard's original work (1980). They also found that a small amount of curvature at later age was consistently evident in other data they examined, such that they proposed two nine-parameter extensions to the original HP model from an empirical point of view, but they note these extended models are not biologically interpretable (Heligman and Pollard 1980; Gage and Mode 1993).

Gage (1993) compared model fits between the 8-parameter HP model and the 5-parameter Siler model using Australian mortality data. The Siler model had similar fits to

the HP model for all but one data set in which the early-age accident hump of the HP model "mistakenly" peaks at about age 54. Surprisingly, the HP model fit better under this condition, which suggests that both models miss some essential features related to the curvature occurring at late middle or early old age.

5.1.2 Comparing the IEV model to the HP and the Siler model

Theoretical comparison

Although the IEV model also assumes mortality results from competing forces, i.e. the intrinsic and extrinsic process, there are fundamental differences between the IEV model and the other two. Firstly, the two forces in IEV model are not completely independent from each other, but rely on common continuous processes acting across the entire life span. Secondly, the IEV model classifies mortality according to whether death occurs as a result of an instantaneous challenge or as a result of the exhaustion of survival capacity. In contrast, the other two models essentially partition mortality into age-dependent and -independent part. Thirdly, despite the fact that the child mortality component from the IEV model is the same as that in the Siler model and similar to that in the HP model, the IEV model yields a biological explanation for the shape within the conceptual framework. Furthermore, the IEV model is able to interpret the accidental mortality hump easily and is flexible enough to incorporate more complicated structures into the mortality curve. Finally, but most importantly, all parameters from the IEV model are process driven and are hence biologically meaningful. In contrast, parameters in the other two models are empirical and provide little insight into the underlying processes that shape mortality curves.

Comparison of model fit

Above I have discussed the theoretical advantages of the IEV model, but it is still necessary to compare the goodness of fit to empirical data among the three models. I follow Gage and Mode's method (1993) to use the root mean square error (RMSE), which is commonly used to assess how well models describe data. It is convenient to fit the survival fraction data (l_x), since both the algorithms of the IEV and Siler model are based on l_x (Gage and Mode 1993) and for the HP model, q_x can be easily transformed to l_x. Then RMSE is defined as

$$RMSE = \sqrt{\frac{\sum \left(y_x - \hat{y}_x \right)^2}{n}} \tag{5.3}$$

where y_x is l_x, $\hat{y}_x$ is the estimated survival fraction at age x from each of the three models and n is the number of data points. For a complete survival curve (0-110) from Human mortality database (HMD 2010) with 1-year age interval, n equals 111. To determine whether the additional parameters of a more complex model are statistically justifiable, I further compare the fit using an F test (Gallant 1987). The test statistic is

$$F = \frac{\left(SSE_r - SSE_f \right) / d}{SSE_f / \left(n - p \right)} \tag{5.4}$$

where SSE_r and SSE_f are the sums of the squared errors for the reduced (with less parameters) model and the full (more complex) model, respectively, n (= 111) is still the number of data points, p is the number of parameters in the full model, and d is the difference in the number of parameters between the two models. This procedure is similar to the F test commonly used to determine whether additional terms are justified in a linear regression model.

Data sets are chosen from Swedish females and Japanese females for selected period years (HMD 2010). Most of Swedish female mortality trajectories do not display significant mortality humps, whereas the Japanese female curves do. Results are summarized in Table 5.1.

Table 5.1 RMSEs for the 6-parameter IEV model, the 5-parameter Siler model and the 8-parameter HP model applied to Swedish and Japanese female data. * indicates that the *F* test is significant at 5% level. When the HP model has the smallest RMSE, the *F* test is conducted between the HP model and the second best model; When the IEV model has the lowest RMSE, the *F* test is used to assess whether the differences between the IEV and the Siler model is statistically significant (HP model with one more parameter than the IEV model is out of competition in this case). The number in the parenthesis is the age when the mortality hump peaks in the HP model.

	year	IEV	Siler	HP (age at hump)
Swedish female	1830	0.0038	0.0042	**0.0013* (37)**
	1880	0.0045	0.0028	**0.0006* (35)**
	1930	0.0065	0.0042	**0.0012* (30)**
	1960	0.0027	0.0040	**0.0025* (49)**
	1970	**0.0025***	0.0043	0.0032 (68)
	1980	**0.0018***	0.0044	0.0024 (72)
	1990	**0.0021***	0.0045	0.0034 (75)
	2000	**0.0013***	0.0058	0.0035 (81)
Japanese female	1950	0.0059	0.0050	**0.0011*(29)**
	1980	**0.0024***	0.0042	0.0027 (70)
	1990	**0.0023***	0.0050	0.0025 (65)
	2000	**0.0025***	0.0052	0.0032 (72)

Suggested by Table 5.1, the HP model fits early period data better, while the IEV model dominates all recent years. Compared to the other two, the Siler model does not stand out in any years and the *F* test does not indicates any advantages of having fewer parameters in the model. So I focus on comparing the HP and IEV model. In early period years, when the child and young adult mortality rate is high, the RMSE is more sensitive to the accuracy of model fits to early age. The HP model uses three parameters to capture the early age pattern of mortality compared to the two parameters used in the IEV model.

In addition, as discussed in chapters II and IV, the IEV model underestimates mortality at extremely old age for early period data. Therefore, the HP model gives better fits to the early period years. However, in recent years, when the early age mortality is low and more individuals survive to old ages, the RMSE is largely influenced by model performance at old ages. Since the IEV model has a better structure to characterize the early old age mortality elbow and the old age mortality plateau, there is no wonder that the IEV model performs better during these periods.

In Table 5.1, also contains the peak age of the HP model accident hump. The peak occurs at young and middle age up through 1960 but the model shifts the hump to old age for recent period data, which is against the original intent of representing risky behavior in early to middle adulthood. Fig. 5.1 illustrates this issue. Essentially, the location of accident hump is controlled by two competing processes: 1) fitting the parabolic shape in young adult mortality and 2) fitting the middle to late age mortality elbow. As demonstrated in Fig. 5.1A, when the peak of the young-adult hump and the elbow are relatively close to each other, the HP model adapts both features and fits data well. However, when the elbow and hump are distant, the HP model has troubles in simultaneously capturing both features and hence yields a relatively poor fit (Fig. 5.1B). Because the old age mortality is more important under such a condition, the model tends to locate the hump at an old age. As discussed before, this suggests that the HP model structure has unstable properties making it inadequate to characterize the old age survival.

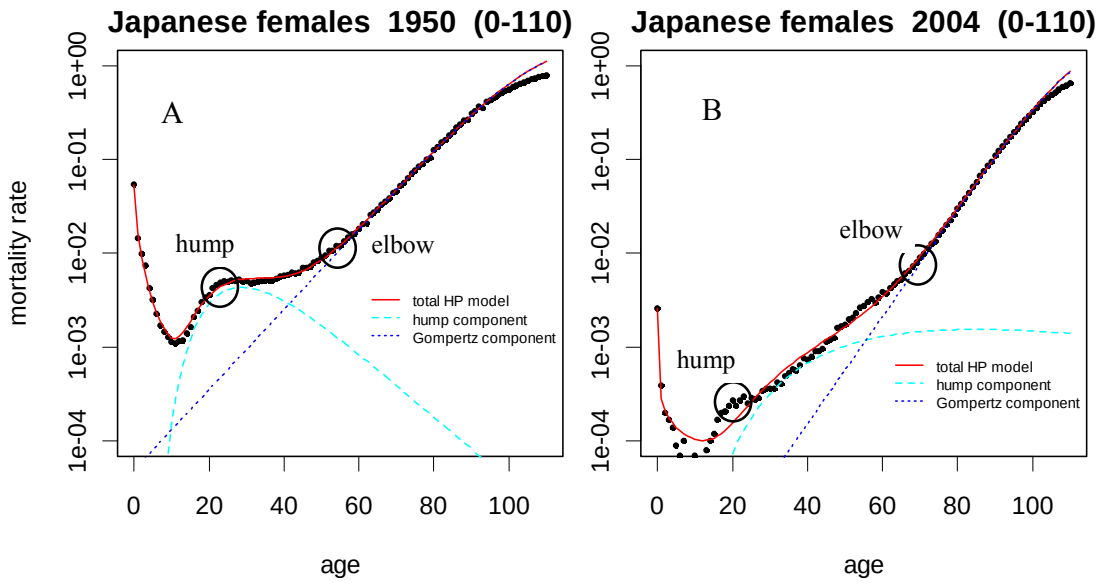

Figure 5.1: the 8-parameter HP model fits to mortality rate from Japanese females at period year 1950 and 2004.

Cohort mortality data

Note that the comparison in the previous section is based on period mortality data only. As discussed in chapter IV, the IEV model is more appropriately applied to period data, since individuals who die in the same year are more likely to be subject to the same extrinsic conditions characterized by constant λ and β. In contrast, the extrinsic process derived from a cohort population characterizes some weighted average of the extrinsic conditions across the cohort's lifespan. However, in reality individuals in the cohort can experience very different extrinsic processes depending on their ages of death. Thus, it is problematic to represent the extrinsic process of a cohort with fixed extrinsic parameters. But it is still interesting to examine mortality patterns from cohort data, in particular, to look at how patterns of extrinsic mortality differ in period and cohort data. Fig. 5.2 demonstrates two age-specific mortality curves from Swedish females for birth cohort year 1810 and 1905 separately. The shape of mortality curve in cohort year 1810 (Fig.

5.2A) is similar to that of most period data in a sense that the mortality rate in log scale between age 20 and 60 increases approximately linearly with age. Because the rate in this age interval is primarily controlled by the extrinsic processes, it indicates that the log extrinsic rate is linear over this segment. However, the pattern in cohort year 1905 is different (Fig. 5.2B). Except for a significant mortality hump in young adulthood, the extrinsic part seems constant with age, which raises a fundamental question whether the extrinsic death should be independent of age or not. This also illustrates the biggest difference between the IEV model and the other two models in defining the extrinsic mortality process.

Both the Siler and the HP models fit mortality curve from cohort year 1905 better than does the IEV model, because they require a constant extrinsic mortality rate, which matches the empirical pattern for cohort year 1905. In contrast, the IEV model requires an age-increasing trend in the extrinsic mortality. Albeit a poorer fit than the other two models, the IEV model could provide an essential way to examine the period effects of extrinsic detriments on cohort mortality. Note that the Swedish females from birth cohort 1810 spend most of their lives in the 19^{th} century when the extrinsic conditions are relatively stable according to my findings in Chapter IV. Thus, for this cohort the assumption of constant extrinsic parameters, λ and β, is realistic. The 1810 cohort mortality pattern mainly reflects the aging effects on extrinsic death as is the case with most of the period data. In contrast, for cohort year 1905, individuals experience the first half of 20^{th} century when a dramatic improvement in extrinsic conditions occurred as indicated by a remarkable decline of β (Fig 4.2B). Therefore, the pattern of extrinsic mortality from the 1905 cohort also incorporates the period effects resulting from rapid

changes in the environment which invalidates the assumption of constant extrinsic parameters. In effect, the time varying extrinsic parameters confound the effects of aging which leads to a leveling off of the extrinsic mortality rate. Fig 5.3 illustrates this effect plotting the extrinsic rate components (lines) derived from fitting the model to different period years on the 1905 cohort mortality curve. The effective age-dependent extrinsic mortality rates at cohort ages 15, 30, 45, 60 and 75 correspond to extrinsic mortality rates derived from period mortality curves in years 1920, 1935, 1950, 1965 and 1980. Each of the dashed lines represents the extrinsic mortality trajectory at the specific period year. The lines all follow an increasing trend with age.

Comparing the trajectories of period extrinsic mortality between year 1920 and 1935 implies that if the environmental detriments of period year 1935 were the same as that of period year 1920, the cohort-mortality rate at age 30 would be significantly higher (point *b*) than the current observed mortality rate (point *a*) and vice versa. This suggests that the seemingly constant extrinsic mortality with age from cohort data results from combined effects of intrinsic aging and extrinsic environmental change. After year 1950, the period extrinsic trajectories converge indicating the environmental factors have stabilized and the extrinsic rate no longer significantly changes.

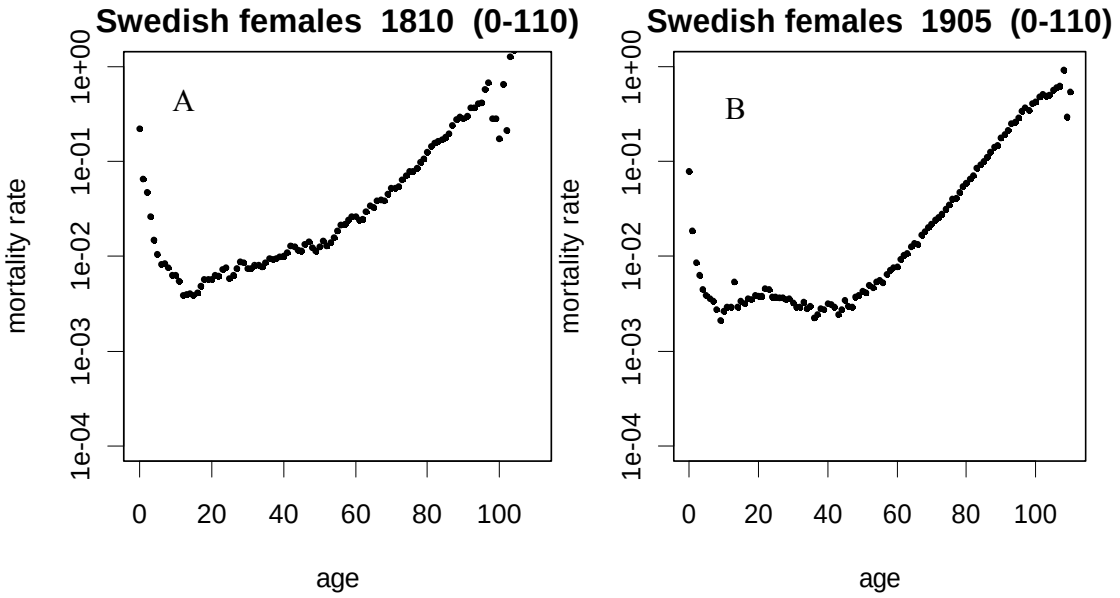

Figure 5.2: Age-specific mortality rate in log scale from cohort year 1810 and 1905 of Swedish female (data source: Human mortality database (HMD 2010)).

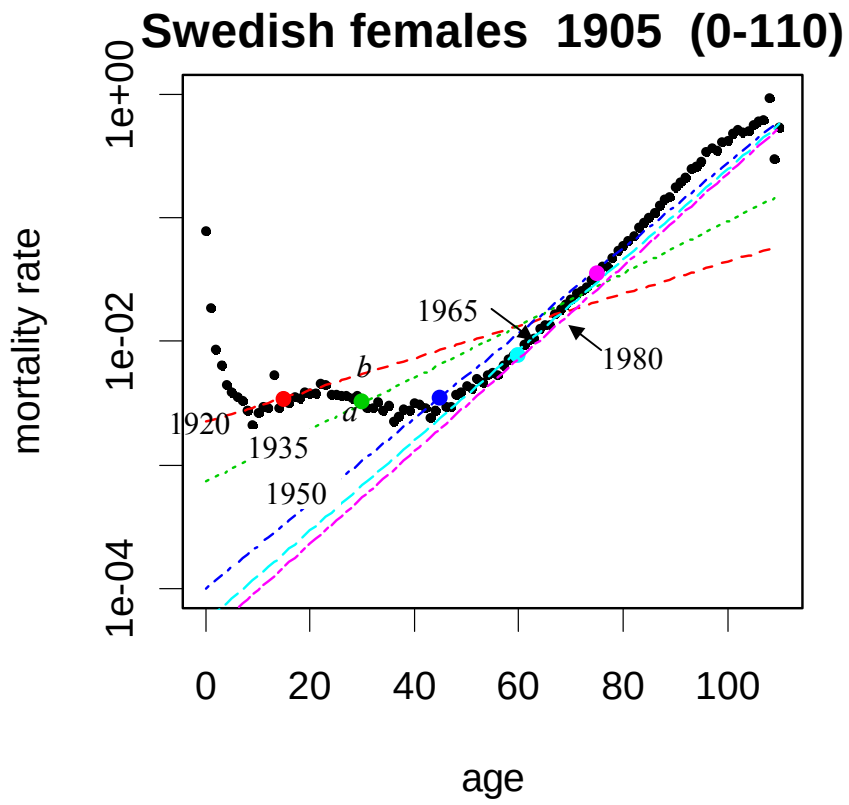

Figure 5.3: An illustration of period effects of extrinsic conditions on cohort mortality patterns.

Conclusion

There is no doubt that the 8-parameter HP model fits early age mortality better than the 6-parameter IEV model, but the IEV model performs better in fitting old age mortality, in particular for recent years' data. However, fitting to data is just one side of the story. One the other side, the IEV model is theoretically superior to the other two models in that it provides insight into why the model fits and when it doesn't. Most of all, the IEV model provides biological insights into mortality processes that help understand the underlying mechanisms of death and aging.

5.2 Comparing with the Strehler-Mildvan (SM) general theory of mortality and aging

5.2.1 The SM general theory of mortality and aging

Strehler and Mildvan (1960) developed a significant explanation for the biological basis of the Gompertz law, known as the SM general theory of mortality and aging. The SM theory and IEV model are similar in many ways. Both build on the abstract term, "vitality", to indicate the capacity or the energy reserves of an individual organism to stay alive. The SM theory borrows an idea from chemical kinetics (Golubev 2009) to explain that the increase in the age-specific mortality rate results from the interaction between the internal energy reserves of living beings, i.e. *vitality*, and the external energy demands from environmental insults. To be specific, vitality is assumed to linearly decline with age and death occurs when the energy demands from external challenges, which follow a Maxwell-Boltzmann distribution, exceed the vitality level. While SM theory uses concepts from physics and chemistry, in essence the killing process is the same as the extrinsic mortality in the IEV model. Therefore, the mortality rate of the SM model yields the same expression as the individual extrinsic mortality in the IEV model shown in eq. (2.9). But because the rate of vitality loss is deterministic in the SM theory, the vitality process is linearly transformed to the ageing process with no approximation involved. Then the SM mortality rate expressed in terms of the IEV model is

$$\mu_{SM}(x) = \lambda e^{-v_x/\beta} = \lambda e^{-(1-rx)/\beta} = \lambda e^{-1/\beta} e^{rx/\beta} = ae^{bx} \tag{5.5}$$

where r still indicates the fraction of vitality loss per unit time and λ and β again characterize the environmental challenge frequency and average challenge magnitude

respectively, and a and b are the standard Gompertz parameters. But since the SM theory does not include the intrinsic killing, the intrinsic parameter r cannot be directly disentangled from the environmental effect. In other words, eq. (5.5) only has two degrees of freedom and converges to the two-parameter Gompertz model. The Gompertz parameters, a and b, maintain a relationship with the IEV process parameters, r, λ, and β as below

$$\begin{cases} a = \lambda e^{-1/\beta} \\ b = r/\beta \end{cases} \Rightarrow \log a = \log \lambda - b/r \tag{5.6}$$

Eq. (5.6) demonstrates the well-known negative relationship between Gompertz coefficients that log a linearly declines with b under fixed values of r and λ. With a and b known, eq. (5.6) has two degrees of freedom, but there are three independent process parameters. Note that in the original paper (1960), SM parameters B, K, and D_ε are used instead of r, λ and β, but they share the same biological meanings.

However, there are two fundamental differences between the SM theory and the IEV model: 1) the stochastic structure of the IEV model allows heterogeneity in mortality within a population; 2) the killing process demonstrated in the SM theory accounts for all the deaths whereas the similar extrinsic process in the IEV model is only responsible for part of the deaths. I believe these distinctions make the IEV model incrementally more realistic than the SM theory and thus provided a better explanation and fit of mortality data. A comparison of parameters between the two models is listed in Table 5.2.

Table 5.2 Comparison of parameters

IEV parameters	IEV expression	representation	note	Equivalent SM expression
r	$\beta / \vec{v}_0$	normalized fraction of vitality loss per unit time, or drift rate	1/r approximately indicates the maximal life expectancy of the population	B / V_0
s	$\sigma / \vec{v}_0$	normalized variability in the rate of loss of vitality, or spread rate	s measures the evolving variation of the vitality among a population	*none*
λ		challenge frequency	characterize acute environmental condition	K
β	$D_\varepsilon / \vec{v}_0$	average challenge magnitude	the rate of the extrinsic mortality increasing with the vitality; characterizes acute environmental condition	D/V_0

5.2.2 Explaining the paradox in estimating fraction of vitality loss (*r*) in SM theory

Because of the expanded model framework, the IEV model can directly estimate all the parameters while the SM theory can only estimate the process parameter r ,λ and β upon some assumptions. The fraction of vitality loss per unit time r is a focal term because 1/r is a measure of the expected life span or the age of expected zero vitality (Zheng, Yang et al. 2011). Without direct estimation in the SM theory, r can be estimated by two methods proposed by Strehler and Mildvan (1960). The first method sets $\lambda = 1$, such that eq. (5.6) becomes $\ln a = -b / r$ and r can be derived from $-b / \ln a$ (Strehler and Mildvan 1960). Zheng et al. (2011) recently calculate r from 42 countries following this method. Perplexingly, the analysis revealed that Central American and South-East Asian countries had lower r, i.e., higher age of expected zero vitality, than most developed countries. This begs the question, do presumably harsher environmental conditions of these countries produce advantages in survival, or is the assumption on λ unrealistic?

Rearranging eq. (5.6) $-\frac{\ln a}{b}=\frac{1}{r}-\frac{\ln \lambda}{b}$ and combining $\hat{r}=-b/\ln a$ from the restricted estimation, yields

$$\frac{1}{\hat{r}}=\frac{1}{r}-\frac{\ln \lambda}{b} \tag{5.7}$$

The difference between the estimated age at zero vitality and the true age depends on the ratio of the challenge frequency term $\ln \lambda$ to the Gompertz coefficient b. Using simulations I accessed whether a bias exists or not. Survival curves were generated according to the IEV model death process, because the vitality structure is flexible enough to assign any values to each of the 4 parameters. The method for simulating survival trajectories is described in Chapter II. All the parameter values chosen for simulation were within a reasonable range for human mortality, i.e. $0.011<r<0.014$, s = 0.01, $\lambda = 0.12$, and $0.1<\beta<0.2$. Note that in the simulation I did not include the childhood component, because the simple Gompertz model is only designed to capture the senescence-related part. The Gompertz model ($\mu(t)=ae^{bt}$) was fitted to the entire simulation survival curves giving the estimated age at zero vitality from $1/\hat{r}=-\ln \hat{a}/\hat{b}$. I also tried to fit the Gompertz model to the truncated simulation survival curves with varying starting ages, such as 30 and 40. It turns out the truncating age has little influence on the patterns of the estimated age at zero vitality against average challenge magnitude. So I only showed the results from fitting the entire survival curves in Fig. 5.4.

The plot depicts the estimated age at zero vitality against the challenge magnitude term β with fixed challenge frequency, λ. A pattern emerges where the estimated age of zero vitality ($1/\hat{r}$) tends to be larger for populations with higher average challenge

magnitudes. However, in actuality all simulations represented in a single line (Fig. 5.4) were fixed with the same age of zero vitality ($1/r$). Thus, it is likely that the Central American and South-East Asian countries do not have lower senescence rates, r, relative to developed countries. I therefore speculate that the estimated difference in age of zero vitality in the Central American countries reflects a higher level in environmental stresses, β. That is $1/\hat{r}$ is more exaggerated for the developing countries compared to developed countries as a result of harsher living conditions in developing countries. Although this analysis does not exclude possibilities that there were real genetic and physical advantages in the Central American and South-East Asian countries, the vitality framework provides a plausible explanation that the estimated longer life expectance may be a mathematic misrepresentation because of unrealistic restriction on parameters in SM theory.

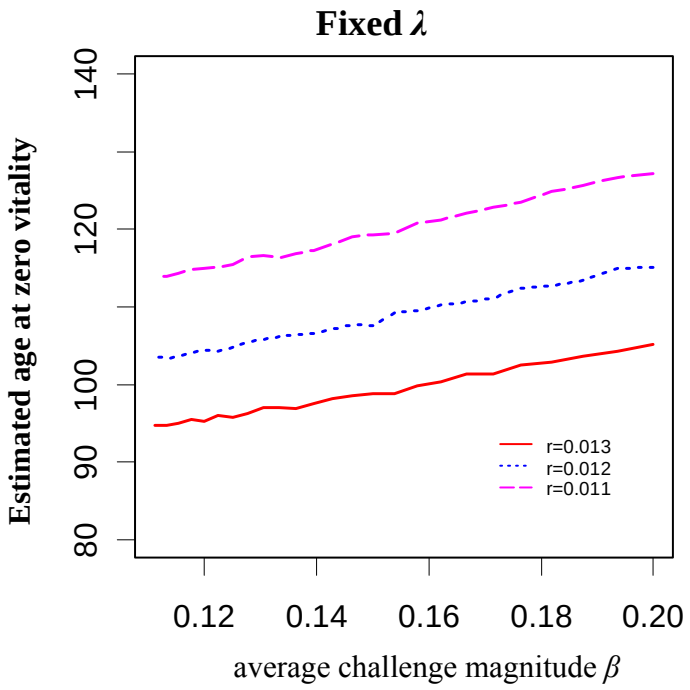

Figure 5.4: Estimated age at zero vitality against average challenge magnitude under fixed challenge frequency $\lambda = 0.12$. Each line represents a single true vitality loss rate that was used for generating the survival curves. All curves have the same background variance structure in vitality: $s = 0.01$.

5.2.3 Explaining SM correlation patterns

Another method for estimating the fraction of vitality loss per year r from SM theory relies on the regular relationship of Gompertz coefficients expressed by eq. (5.6). To estimate r from the Gompertz coefficients requires a linear relationship between $\ln a$ and b, in that the slope of the relationship is $1/r$ according to eq. (5.6). Thus, r actually represents the averaged fraction of vitality loss per year over a series of longitudinal survival curves constructed from a sequential series of years. The success of the method depends on a stable linear relationship, which would imply that eq. (5.6) is valid. Early studies confirm a stable pattern for adult mortality from the year 1900 to 1986 in the US (Riggs 1990) and other developed countries, including overall mortality trends in

industrialized countries (Riggs and Millecchia 1992; Prieto, Llorca et al. 1996). However, in recent period and cohort mortality data the stable linear relationship in the pattern is not evident in countries like France, Japan, Sweden and the US (Yashin, Iachine et al. 2000; Yashin, Begun et al. 2001; Yashin, Begun et al. 2002; Yashin, Ukraintseva et al. 2002). To be specific, for period data, "hooks" emerge in the $\ln a$ vs. b relationship for those countries in the second half of the 20^{th} century. The approximately constant negative slopes (1859-1960) reverse sign and flatten for France, Sweden and the US starting around 1960 and for Japan round 1980. For cohort data, only Sweden exhibits a linear relationship over the length of data. The other countries have complex patterns in which the slope changes sign multiple times over the years of data. The important point here is that the SM theory assumptions break down for the years where the curves change slope and flatten (Fig. 5.5).

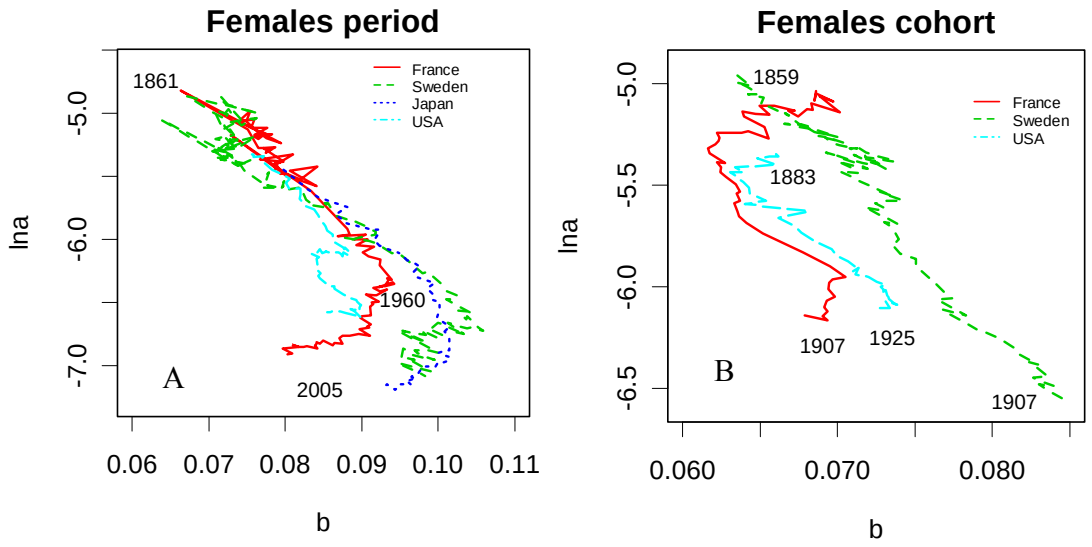

Figure 5.5: (A) period patterns of SM correlation for females in France (1861~2005), Sweden (1861~2005), Japan (1950~2000) and the US (1938~2005); (B) cohort patterns of SM correlation for females in France (1859~1917), Sweden (1821~1915) and the US (1883~1927). All mortality data are from the human mortality data base (Wilmoth and Shkolnikov 2010) and I use mortality for ages between 40 and 80.

The unstable patterns shake the root of the SM theory. As suggested by Yashin et al. (2001), new concepts need to be developed. In the following section I demonstrate that the IEV model readily provides an explanation for the variable patterns observed in Fig. 5.5. The approach again is to first simulate survival curves with a numerical form of the vitality model (Chapter II) using typical parameter ranges: r = 0.01 to.014, s = 0.01, β = 0.111 to 0.20 and λ = 0.05 to 0.2. Next the Gompertz model is fit to the simulated data to estimate Gompertz coefficients a and b ($\mu(t) = ae^{bt}$). The estimates of $\ln a$ and b from the simulated survival curves are shown in Fig.5.6.A under a fixed challenge frequency λ with variations in r and β and Fig. 5.6.B under a fixed average challenge magnitude β with variations in r and λ. In both plots, points on each lines tending from upper left to lower right, are estimated ($\ln a$, b) pairs generated with fixed r. In plot A λ is fixed and β

decreases and in plot B β is fixed and λ decreases. Also in both plots, each of the horizontal line, tending right to left, illustrates changes in ln *a* and *b* for decreasing *r* and fixed values in λ and β (plot A and B). Together these plots illustrate how ln *a* and *b* change as *r*, λ and β change. As *r* decreases, *b* decreases but ln *a* is relatively unchanged, while as either β or λ decrease, *b* increases and ln *a* becomes more negative. Now consider the patterns in Fig. 5.5 in terms of these relationships.

A stable negative linear pattern of the Gompertz coefficients from about 1860 to 1960 (Fig. 5.5) can be interpreted in terms of changes in the extrinsic parameters λ or β dominating changes in *r*. Correspondingly, a reversal and flattening in the ln *a* vs. *b* curve reflects the intrinsic parameter, *r*, dominating the extrinsic parameters λ or β. Thus in terms of the IEV model, over the first half of the 20th century, improvements in the developed countries period survival were the result of improvements in the environment, either through reducing the challenge frequency or average magnitude or both. The break in the linear trend about 1960 and the subsequent bending backwards of the pattern can be interpreted as the result of a gradual shift to the dominance of intrinsic chronic improvements, over environmental acute improvements.

Theoretically, the SM theory fails to explain the correlation patterns because it attributes all deaths to one killing process. Although it tries to connect death with an intrinsic process, artificial restrictions on parameters are required. Thus, it lacks power to resolve the differences between improvement in chronic aging-related process and improvement in the environmental acute process. From this aspect, including two death processes is of great necessity.

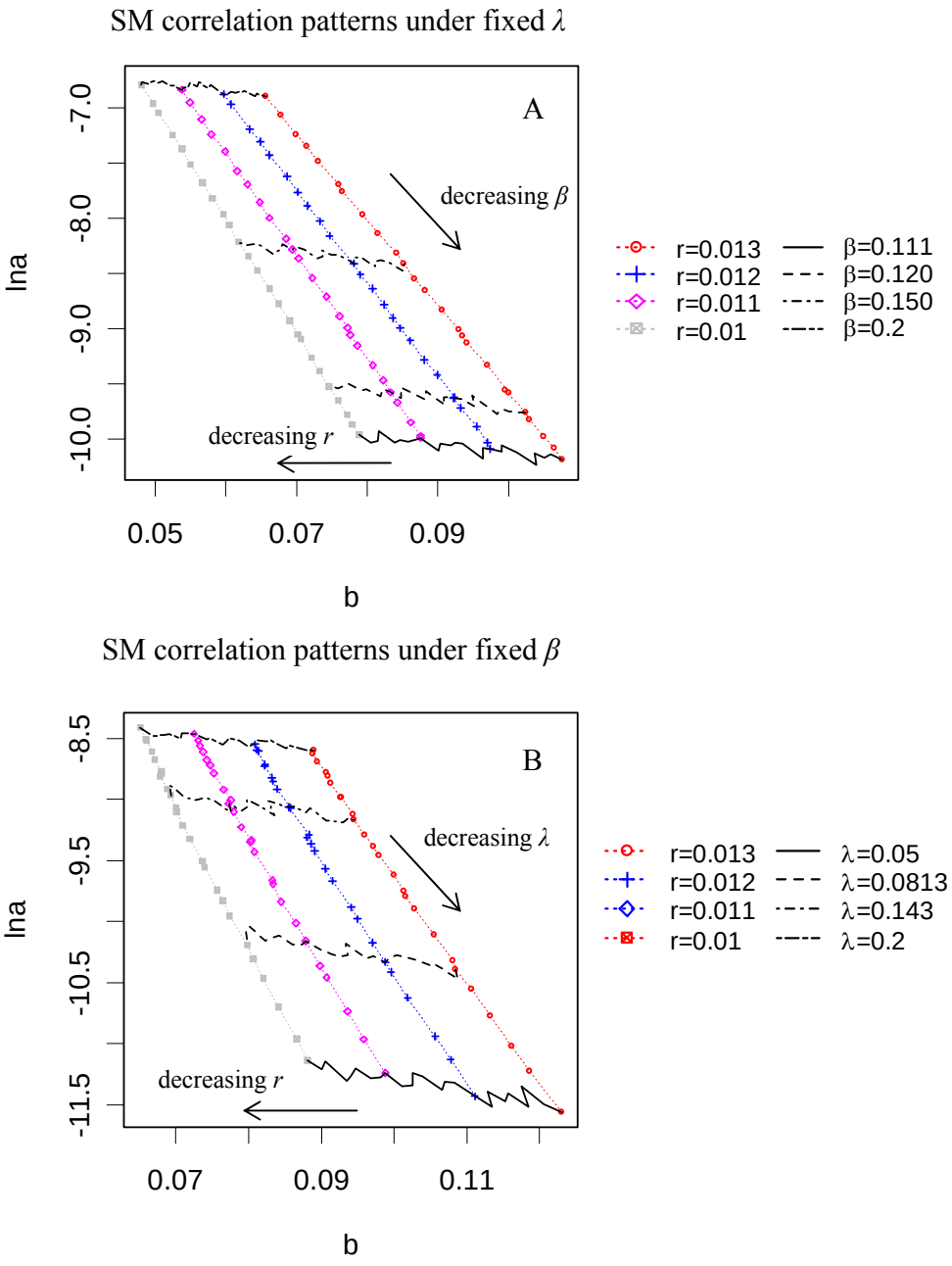

Figure 5.6: Simulated SM correlation patterns: (A) Survival curves are all simulated under fixed challenge frequency term $\lambda = 0.12$; (B) Survival curves are all simulated under fixed average challenge magnitude term $\beta = 0.125$. For both (A) and (B), curves all have the same background variance structure in vitality: $s = 0.01$.

This chapter helps further clarify the IEV framework through comparing the model with other established models including the Siler model, the HP mortality law and the SM general theory of aging and mortality. The comparison focuses on two perspectives, the model fit and the biological explanation of mortality patterns. Although the IEV model does not provide consistently better fit, it is much more biologically interpretable than any of the previous models.

Chapter VI: Exploration of Model Misspecifications

6.1 Potential Model Misspecifications

The basic IEV model relies on several rigorous assumptions on the underlying mortality processes, such as: 1) all vitality trajectories follow the Wiener Process with a linear decline in mean vitality; 2) the occurrence of extrinsic challenges follows a Poisson process; 3) the challenge magnitude has an exponential distribution; and 4) all parameters (r, s, λ and β) that characterize the processes are assumed to be constant through the entire adulthood. It is well expected that the real process is much more complex and all of the assumptions are violated to some degree. If the misspecification is manageable, the basic IEV model still captures the mortality patterns through representing the average effects of the processes. For instance, the vitality process can go up and down or have a non-linear trend, but a linear approximation to the process works well when fluctuations are relatively small. While all of the four parameters can vary with age, their general effects can still be approximated through their mean values across the entire life span. However, in other situations, the model's misspecifications to the underlying processes can have notable impacts on the mortality patterns, i.e., the predicted mortalities from the model deviate from the true mortality curves or the estimated model parameters from real data have irregular patterns that are not well explained.

Although the IEV model captures the important features in age-specific mortality patterns, it has two weak points as discussed in previous chapters. First, in Swedish populations the IEV model slightly underestimates the old age mortality rate for period data previous to year 1945 (Fig. 2.7A-B). Secondly, the longitudinal patterns for the challenge frequency, λ, exhibit a dramatic increase between period year 1945 and 1951

(Fig. 4.2A). These two anomalous phenomena may point to the same potential misspecification of the model. That is, the assumption of the exponential distributed challenge magnitudes may fail for early period years. In this chapter, I will mainly discuss this potential misspecification in the extrinsic process and assess how this would possibly affect the mortality patterns and the estimated parameter values.

6.2 The Extrinsic Challenge Space

As defined in Chapter II, the extrinsic process, describing the dynamic of challenge events, is characterized by two essential elements: the occurrence rate and the magnitude of a challenge. To illustrate the process, we introduce a plot in challenge space (Fig. 6.1) which simultaneously depicts the occurrence time and the magnitude for each event.

Each dot in Fig. 6.1A represents a single challenge event with x-coordinate indicating the occurrence age and y-coordinate indicating the challenge magnitude. This plot fully determines the challenge space and consequently determines the extrinsic process that leads to acute mortality. In theory, the distribution of events in the challenge space can be random, but the regularity of overall mortality suggests it follows certain patterns that have persisted across decades. However, these patterns can be very complex since they are determined by the combined effects from age, cohort and period. The IEV model makes relatively simple assumptions to characterize the patterns in two marginal spaces: the distribution of challenge magnitude (Fig 6.1B) and the age-specific pattern of challenge frequency (Fig 6.1C), but at the expense of potentially mis-specifying the underlying structures at certain degree.

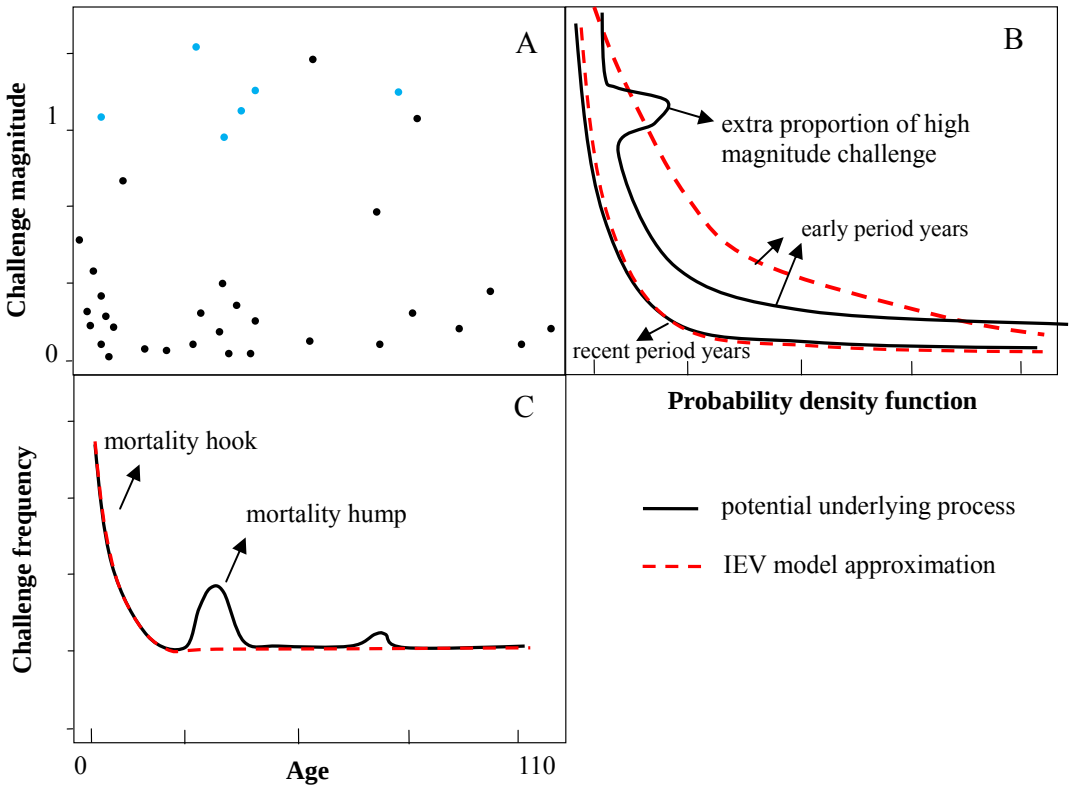

Figure 6.1: Plots of challenge space. A: each dot represents a single challenge event with y-axis indicating the magnitude and x-axis indicating the age of occurrence; B: the distribution of challenge magnitude; C: the age-specific shape of challenge frequency.

6.2.1 The Age-specific Pattern of Challenge Frequency

The IEV model assumes a constant challenge frequency for adults and adds an exponential shape to capture the high mortality at childhood (dashed line in Fig 6.1C), which potentially misses the high frequency for young adults and other fluctuations caused by age effects. Also, the shape of the age-specific challenge frequency is assumed to be maintained over all the period years. To be specific, only the values of parameters change with period years but the age patterns of frequency, i.e. an exponential decrease for children and a constant for adults, is kept stable. In reality, both period and cohort effects would have notable impact on the period shape. For instance, cohorts experiencing tobacco epidemics would be more susceptible to extrinsic challenges and

consequently have higher λ. This effect would result in a hump in challenge frequency at middle or late ages for corresponding period years when deaths largely happen in these cohorts. However, it is extremely difficult to disentangle the effects among age, period and cohort on the shape of challenge frequency which varies from one year to another. In this sense, as long as the deviation from a constant event frequency does not dominate in a long age span, a single λ should be a stable representation of adult frequency across years, and most importantly should not bias other processes in the model, which is in fact suggested by simulations. I also tested that no matter how the simulated age-specific shape of λ varied over period years, a dramatic increase in estimated λ as observed in Fig. 4.2A could not be achieved without artificially increasing the mean λ over these years. In other words, if the environment does not generate more challenges for recent years, the irregular increase in the estimated λ should not be attributed to the misspecification of the shape of λ. While including a complex pattern of event in frequency, such as a high challenge frequency to capture the mortality hump for young adults is possible, but adding such structures should done cautiously; otherwise the additional component can introduce artificial effects that become confound with other parameters. In conclusion, the assumption in the IEV model is conservative, but in many cases it reasonably represents the challenge event frequency pattern across years.

6.2.2 The Distribution of Challenge Magnitude

The IEV model uses an exponential distribution to approximate the challenge magnitude following the convention from the Strehler and Mildvan general theory of aging and mortality (1960). In the original SM theory, the distribution is derived from the Maxwell-Boltzmann distribution. It is analogous to energies among molecule in a sense that the

higher the energy needs, the less likely the event occurs. This distribution is assumed to be invariant to both age and period years. For age effects, there is no strong evidence that the distribution significantly varies with age, and therefore the model characterizes a representative distribution of challenge magnitude across the lifespan. For period data, the model assumes that only the scale parameter, i.e. the average challenge magnitude β, changes across years while the exponential shape of the magnitude distribution is maintained. However, whether this assumption is valid over all the time period is doubtful.

For data from the 19th and early 20th centuries, it is possible that the proportion of challenges with high magnitude (e.g. $\beta > 1$) were much greater than what was predicted from an exponential distribution. A century ago, a harsh environment with recurrent famines and diseases would be expected to produce a larger proportion of extreme events that resulted in greater levels of extrinsic death than can be represented by an exponential distribution. An example is demonstrated in Fig. 6.1B. If the real distribution of challenge magnitude (solid line) has a significant hump representing large magnitude challenges, the model's exponential distribution (dashed line) adjusts its scale to capture the high proportion of the extreme challenges and consequently overestimates the occurrence of the intermediate ones. To compensate for the artificially high proportion of intermediate challenges, the model has to decrease the estimated challenge frequency λ. Advancement in disease and other extreme events control in the 20th century effectively reduces large magnitude challenges resulting in a more exponential-like distribution in challenge magnitude. (see Chapter IV). In essence, this argument contends that improved living conditions and advanced medical technologies not only reduced the average challenge

magnitude, but also mediated the distribution of challenge magnitude. Furthermore, because health science first directed its efforts to the most fatal diseases, the health programs in effect selectively reduced higher magnitude challenges while ignoring the low and intermediate challenges that produce mortality mainly in the very old ages. Therefore, in the later 20th century the distribution of challenge magnitude becomes more analogous to an exponential distribution and the estimated λ and β more accurately reflect the underlying process.

Simulations were conducted to investigate the above hypothesis that changes in magnitude distribution affect the schedules of estimated parameters in the IEV model and in particular λ. Simulated survival curves were generated from the method described in section 2.3.2 except that an additional proportion of extreme events were added. A variable p, varying varies from 0 to 0.5%, quantifies the extra proportion of extreme challenges while the other parameters, $r = 0.011$, $s = 0.006$, $\lambda = 0.2$ and $\beta = 0.12$ were kept stable. All the values were within a reasonable range for generating survival curves similar to those characteristics of human beings. Note that in this simulation β still characterizes the standard exponential distribution, but does not represent the average magnitude which also needs to account for the extra extreme challenges expressed by p. The results are depicted in Fig. 6.2 where the estimated parameters from the IEV model over their true values are plotted against p. As suggested by the figure, the extra proportion of challenge magnitude does not significantly influence r and s, although r declines a little as the extreme challenges are reduced. In other words, the intrinsic parameters are relatively robust under the IEV model. In contrast, λ approaches its true value as the contribution of extreme challenges decrease. The pattern of λ matches our

speculation that the IEV model underestimates λ when the exponential distribution does not capture the challenge magnitude distribution which has an anomalous pattern of extreme challenges. The simulated pattern for estimated β also supports the hypothesis. The estimated β represents the mean magnitude averaging both the standard exponential distribution and extra extreme challenges. As the contribution of extra high magnitude challenges decline, β converges to the mean that represents for standard exponential distribution.

This simulation analysis suggests that a reduction in the harshness of the environment between 1945 and 1951 decreased the high magnitude challenges, which the IEV model was expressed as an increase in λ (Fig. 4.2A) and a decrease in β. Consequently the post 1950 estimates of λ and β should be relatively unbiased while the pre-1945 years of λ and should be underestimated. Also for early period years (1800-1945), underestimated λ results in the model under predicting mortality rate at very old ages because old age mortality is sensitive to λ (see Fig. 2.8C). In other words, since the fitting algorithm is more influenced by younger age fitting errors for early period years, the algorithm takes less care of fitting old age mortality. In conclusion, we show that the misspecification of the distribution of challenge magnitude has significant impact on the extrinsic parameters but not on the intrinsic ones. The two phenomena that cannot be well predicted by the basic IEV model, i.e., an underestimation of extremely old age mortality for early period years and a dramatic increase in λ, are then reasonably explained as the results of the underestimation of large magnitude challenges for early period years.

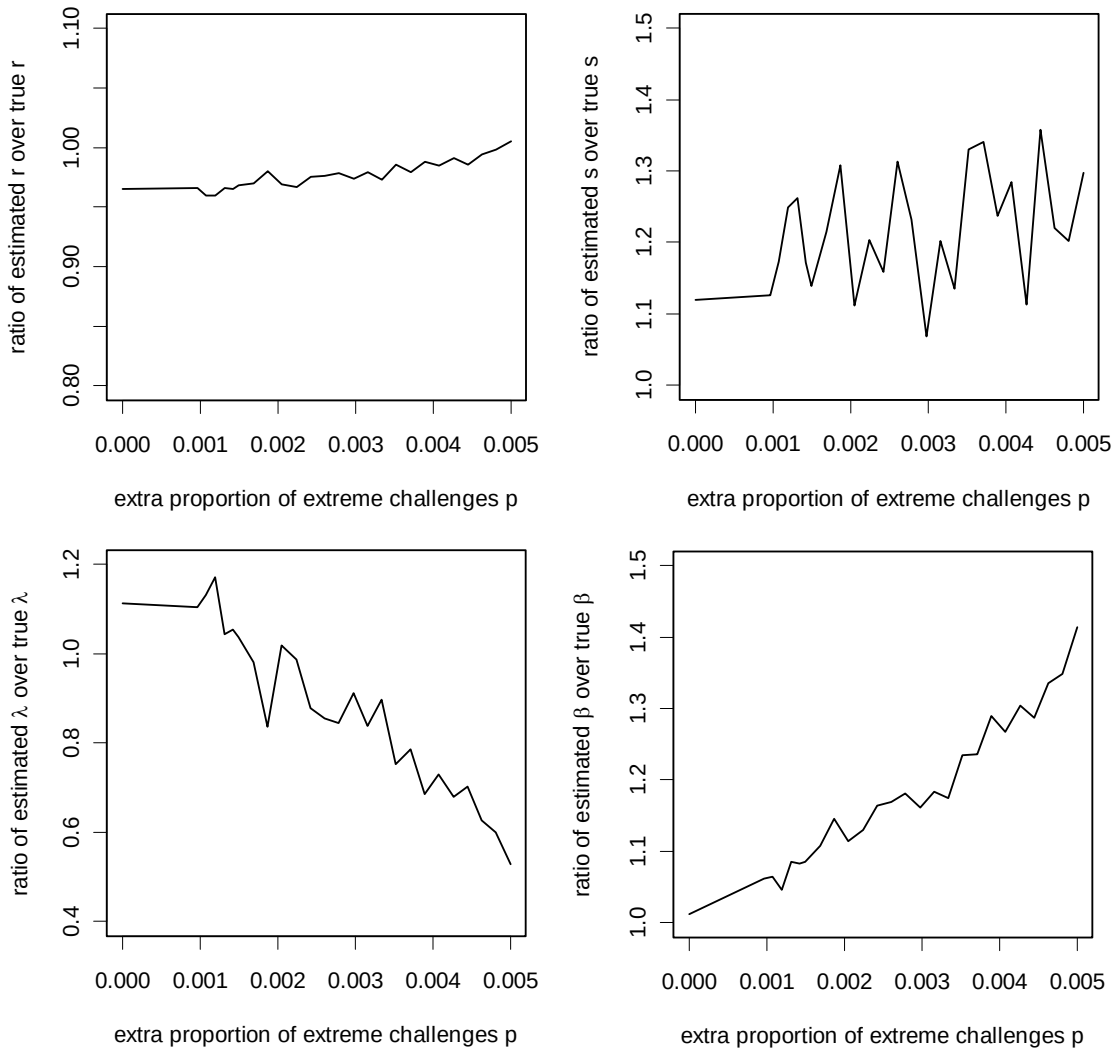

Figure 6.2: Estimated parameters from IEV model over their true values against the extra proportion of extreme challenges in additional to a standard exponential distribution (scale parameter $\beta = 0.12$).

6.2.3 Methods for Correction and Their Problems

A simple extension of the IEV model can be developed to correct the underestimation of extrinsic killing from high magnitude challenges, especially for early period years. The challenges with extremely high magnitude are usually non-recoverable in a sense that as long as they occur, individuals cannot survival irrespective of their vitality level. In other

words, the killing rate of such challenges is independent of age but only relies on the occurrence rate of the events. We could add a constant frequency term to account for the additional high proportion of such challenges, such that the magnitude of remaining challenges could be better approximated by a standard exponential distribution. An age-independent mortality component has been added to the mortality equations since the Makeham model (1861) and it also long exists in the 3-parameter vitality model developed by Anderson (1992, 2000, 2008), but here we reintroduce the term with a different philosophy. In this new extension of the model, this constant term more stands for the additional proportion (or frequency) of extreme challenges that are not captured by the exponential distribution. In essence, in the IEV model no mortality event is independent of age but some challenge events are so large that they result in mortality independent of the amount of vitality the individual possesses. Consequently these events can be represented by an age-independent term.

The extended model with one extra term indeed improves the data fit for all period years. However, the new term also introduces potential confounding effects with other model parameters in particular for recent period years when the exponential distribution for challenge magnitude is adequate to represent the underlying process. The parameter *r* becomes unstable and drops to very low values for many period years and the across year patterns of other parameters are also affected. These irregular patterns may be caused by model over-parameterization. Of course, more complex models can represent the challenge space, but they all face the same problem that data sets have limited power to distinguish model parameters. As such, more complex models may fit mortality data well but they may do so with a nearly random allocation of parameter values. To resolve

this problem additional information is essential. We could either take confident information from other sources in determining the critical properties of challenge and vitality spaces or apply prior information on the processes in a Bayesian estimation framework.

6.3 Conclusion

This Chapter mainly explores potential misspecifications of the IEV model in its challenge space. With manageable fluctuations in the shape of age-specific challenge frequency, the parameters estimated in the IEV model are relatively robust, while a poor approximation to the underlying distribution of magnitude causes estimation bias in extrinsic parameters. Introducing a more complex structure to describe the challenge space is possible but the estimation algorithm may become unstable. So what have we learned from this chapter?

Firstly, since the real underlying process of mortality has many dimensions, it is almost impossible to thoroughly capture all the perspectives and represent them through a model with manageable complexity. The IEV model presented in this dissertation makes relatively simple assumptions on both the intrinsic vitality and extrinsic challenge spaces. Although these assumptions are more or less violated in the real world, the model still provides a parsimonious, yet relatively stable, representation of the processes and maintains the major characteristics found in patterns of human mortality across centuries. In particular, the model seems to describe relatively well period data for recent years, possibly because the distribution of events in the challenge space is reasonably characterized by the model. Also, all the properties of the model discussed in previous chapters, such as the interpretations of features in mortality pattern (Chapter II), the

variance structure, the mortality partition (Chapter III) and the explanation of SM coefficient (Chapter V) still hold, in spite of the potential misspecification in challenge space. Thus, the IEV model is still of great value for both fitting data and providing a conceptually intuitive framework (vitality and challenge spaces) in which to view the complex mortality processes.

Secondly, it is well understood in the society of mathematics and statistics that "All statistical models are wrong, but some are useful"[1]. Achieving a balance between a better representation of the data and over-parameterization is essential. The goodness of fit is very important to assess a model, however, when the ultimate goal is to explore the underlying dynamics, the primary criterion, is whether the model provides consistent interpretations for both the data and the parameter patterns. Instead of pursuing perfect fit for mortality data, we are more concerned about developing a consistent mechanism that explains general patterns. A strong mechanistic foundation is also critical for projecting future patterns of mortality and longevity. Reliable projections should be based on biologically meaningful mechanisms, not merely on a good-fit model whose parameters may not be consistent across years.

Finally, the IEV model is a specific construction within the two-process framework that provides an efficient way to investigate the mortality system through intrinsic vitality and extrinsic challenge spaces. The concept that mortality patterns are determined by the shape and interaction of these two spaces is unique and allows great flexibility for exploring the underlying mechanisms of mortality.

---

[1] Quote from George E. P. Box, Emeritus Professor of statistics, University of Wisconsin at Madison

Chapter VII: Discussion and Future Directions

7.1 Conclusion

Over life, the accumulation of small day-to-day processes associated with behavior, nutrition, health care, stress and other events contribute, in sum, to mortality. A biology-motivated mathematical framework is developed to quantify these contributions through two stochastic processes: an intrinsic process, defining the survival capacity (i.e. vitality) of an organism, declines stochastically to a zero-boundary and an extrinsic process representing the occurrence of external stresses and how the stresses alter the intrinsic vitality trajectory. This vitality based model is designed to reflect both the biological and external processes that result in mortality or disease, and consequently differentiates 1) cumulative effects resulting from behavior, health care, nutrition and other environmental factors and 2) acute, short-duration challenges presented by disease, accidents and comparatively brief periods of extreme stress. Both of these components are represented parsimoniously using relationships that strongly reflect the general mechanisms underlying the killing processes.

This model is based on a stochastic process point-of-view which has been developed by a few scholars over the past 50 years. As early as 1956, Sacher and Trucco (1956; 1962) first used the Wiener process to characterize the internal physiological deterioration subject to random fluctuations. The temporal shape of mortality was derived from the presumed distribution of time (i.e., inverse Gaussian) when the internal physiological conditions (vitality) reach a threshold. Chhikara and Folks (1989) thoroughly explored the inverse Gaussian distribution as well as the associated stochastic process and applied this framework to some other studies such as the duration of strikes

and the frequency of using a word. Anderson (1992; 2000; Anderson, Gildea et al. 2008) was the first to propose a two-process model version in which a constant extrinsic killing process was added to the original intrinsic diffusion process to characterize organism survival. The intrinsic-part-only model was independently addressed by Aalen and Gessing (2001) along with other Markov process models in explaining survival patterns. Its mathematical properties, in particular the quasi-stationary distribution in capturing the old age plateaus were intensely studied by Weitz and Frazer (2001) and Steinsaltz and Evans (2004; 2007). A recent advance was suggested by Li and Anderson (2009) to include the initial population heterogeneity in the simple two-process model. The efforts made by these scholars propose a fundamental way to look at the underlying mechanisms of mortality and set up a good foundation of this work. The contribution of this dissertation is to develop a more sophisticated two-process model by including a vitality-dependent extrinsic process, such that the model realistically captures human mortality patterns and explain the regarding phenomena in death and aging.

This new framework demonstrates several essential merits over existing models. First of all, it fits mortality data over entire human lifespan and provides biologically meaningful explanations for the age-specific mortality patterns, in particular for the observed anomalies from the classic Gompertz law. The ability to investigate mortality under a consistent framework is an important contribution, because death is more likely to result from continuous processes than piecewise forces. Secondly, the model has an inventory structure to incorporate population heterogeneity. The effects of heterogeneity on population survival have been long underrepresented. In spite of an explicit consideration in the frailty model (Vaupel, Manton et al. 1979), population variation only

fits in through an ad hoc manner, i.e. additional coefficients have to be added to the mortality rate. In contrast, the IEV model admits variation through a stochastic process of vitality diffusion and thus in a more natural way. The variation structure proves to be critical in explaining the old age plateau and mortality curve crossover. Thirdly, all the model parameters are process-driven, such that age-specific mortality curves can be elegantly summarized in a low dimension parameter space. Each dimension represents a single biologically-meaningful element that contributes to the death process. Hence, the model provides a convenient and insightful approach for describing mortality trends, comparing survival and making forecast.

The mortality process is so complex that it involves many different factors driving the system in distinctive manners from both inside and outside of the body. The IEV model helps resolve the complexity of death from a process point of view. It links the macro observation of population mortality rate to a micro biology-motivated process through a parsimony structure. Despite a relatively low dimension of parameter space, the model provides a flexible structure to account for complexities. For instance, age-dependent functions can be assigned to the challenge frequency term, λ, to justify the high level of child mortality and the mortality hump at young adulthood. Nevertheless, adding flexible structures to the model parameters only demonstrates one perspective of how the framework can be extended. The next section will discuss two major potential extensions to the model: 1) to adopt different schedules of vitality trajectories and challenge spaces and 2) to apply the stochastic structure to new contexts other than mortality.

7.2 Potential Model Extensions

7.2.1 Different schedules of vitality trajectories

The model developed in this work is restricted to a relatively simple and fixed structure in a sense that not only the basic parameters are presumably constant across the entire lifespan, but also the vitality process is assumed to stick to a general linear declining trend with small random deviation. In fact, the vitality trajectories can have different schedules upon various physiologic stages and life experiences. For example, human beings would be likely to experience a building process in vitality, i.e. having vitality increase, at the early stage of life as the development of immune system and other physical functions. This can be applied to partially explain the early-age high mortality rate, which has been briefly illustrated in Chapter II.

Interventions would also cause a significant deviation of vitality trajectory from the linear decline trend. Although death does not happen, interventions would either induce long-term damages or chronic benefits to the system such that the vitality trajectory would not return to its original track. Understanding how early time interventions affect later time survival through altering the vitality trajectories has huge implications.

One ongoing project, with Professor James Anderson and one of his Ph. D. students, Jennifer Gosselin, at University of Washington, is to model the effects of intermittent heat shock on longevity using studies on C. elegans (Wu, Rea et al. 2006; Wu, Cypser et al. 2009) and fish (Gosseling 2010). This work is an expansion of the model to characterize effects of time-varying intrinsic vitality on cross-life survival

patterns. The individual animal would either die fast because of the damage caused by the thermal stress, or become adapted and gain an extended life span because of the generated heat shock proteins helping repair damages and prevent further deterioration (Cypser, Tedesco et al. 2006). The vitality framework provides an approach to examine both detrimental and beneficial effects through explicitly modeling the changes of vitality trajectories under both situations. Thus, it is able to explain the observed stepped-like survival curves as the mix effects of debilitation and hormesis introduced by the intervention (Yashin, Cypser et al. 2001; Cypser, Tedesco et al. 2006; Olsen, Vantipalli et al. 2006; Wu, Rea et al. 2006).

Another prominent perspective of applying the vitality framework with interventions lies in disease modeling, in particular for studying HIV (this project is currently collaborated with Professor James Anderson, Professor Samuel Clark and a Ph.D. student Gregor Passolt at University of Washington). The immune-deficient disease, i.e. HIV, would not result in mortality directly, but make the patients much more susceptible to secondary infections that usually lead to death. The vitality framework has the advantages to represent a disease's effect on reducing either the challenge threshold or the recovering capacity through lowering the vitality trajectory. Moreover, the framework can also be used to evaluate the effects of treatment on reversing the decline of vitality caused by disease progression.

As discussed in Chapter VI, the challenge space is also complex and can vary from years to years. We could introduce different schedules of the challenge space to better capture the underlying processes among different years.

In general, the framework is flexible enough to account for different survival conditions. It is not necessary to bring all the complexity together at all the time, but to adopt different versions of the model according to the data sets and the specific questions that need to be addressed.

7.2.2 New Application Context

Death is the primary outcome of the vitality process, but the framework can be applied to a different context where the occurrence of an event other than death serves as the endpoint. Modeling the incidence rate of aging-related diseases using a similar stochastic structure would be one promising application in which disease is the primary outcome.

Among all the chronic diseases, cancer is in particular of interest. Although it has been long recognized that cancer occurs predominantly among older persons, the relationship between cancer and aging is still vague at both biologic and demographic perspectives (Cohen 2007). The similarity in age patterns between the overall cancer incidence rate and the all-cause mortality rate for human beings, i.e. a peak during early childhood, an exponential increase trend during adolescence and deceleration at old ages (Arbeev, Ukraintseva et al. 2005), strongly suggests a consistent framework that accounts for the mechanisms of both all-cause mortality and cancer progression. Especially, the aging process needs to be incorporated into cancer progression beyond the epidemic consideration. The two-process structure with aging-disease interaction can be well applied to model the cancer incidence trajectory. Under such a circumstance, the intrinsic process could still represent the aging-related deterioration of the survival system, while the extrinsic process is designed to indicate the multistage carcinogenesis. Cancer then results when the intrinsic survival capacity is inadequate to suppress the progression to

malignancy. A preliminary study (Li and Anderson 2010)(draft available) has shown that the model fits the entire all-cancer incidence trajectory well. More important, it provides a tool for exploring the differences in cancer patterns among the two sexes and varying regions with regard to the impact of genetic, physical, social and environmental factors on aging and carcinogenesis process.

Essentially, all the flexibilities of the model framework are based on a process point of view of the whole system which is a much more fundamental approach to explore different dynamics including mortality, aging and disease. I believe this approach will play an increasingly important role on the study of health and mortality in the near future.

7.3 Limitations and Future Directions

The IEV model established in this work does have several limitations.

First of all, to achieve an analytic solution of mortality function, an approximation to the extrinsic killing has to be involved. Although a correction can be applied to the estimated parameters via simulations, it weakens the model assumption with regard to the heterogeneity of extrinsic mortality. A future step would be to develop a fitting algorithm that does not require a closed form of the mortality function, such that the estimated parameters would directly reflect the underlying process. However, great efforts on mathematical and computational development are needed.

Secondly, there is a potential issue on parameter identifiability. As discussed in chapter IV and VI, when the underlying processes are not correctly specified, the model parameters may interact among each other, which makes it difficult to accurately

disentangle their effects. In addition, without extra information on intrinsic survival, the effects of internal and external factors on high child mortality cannot be fully resolved. A possible way out of this problem of resolving the pattern of model parameters is through additional biological information such as the trajectory of biomarkers indicating the aging-related intrinsic process or the efficiency of the immune system. It is possible to develop a two-stage model in the near future with one stage explicitly modeling the age-specific trajectory of biomarkers and the other stage characterizing the mortality or disease outcomes at a macro level. An underlying stochastic process is still the key to connect the two stages.

Thirdly, the IEV model only has a single parameter, s, to indicate the population heterogeneity. It represents the combined effects of genetic (initial) and acquired (evolving) variation, the former of which usually refers to the population differences in pre-existing conditions associated with genetics and prenatal care, whereas the later one denotes the differences gained through varying life experiences and living environments. Differentiating the two sources of variation has huge implications, in particular for understanding the role of genetic factors and the force of natural selection on later life mortality. However, the IEV model fails to accurately disentangle the two types of variation by adding one more parameter as previously conducted in the simple two-process vitality model (Li and Anderson 2009). It is likely that the IEV model has too many perspectives to characterize, such that it has limited power left in clarifying the heterogeneity structure. A solution to the problem also relies on gaining additional information on the biological processes. Auxiliary data may help identify the effects of

different factors on mortality and thus makes it possible to further clarify the model structure and disentangle the parameters.

The IEV model, in many ways, is an idealized construction subsuming various mechanisms into a single abstract measurement. With limited dimensions obtained from overall mortality data only, it cannot solve all the mysteries in the mortality and aging process, but it helps to break the complexity down. This dissertation work focuses on building the model concept, exploring the model properties and illustrating some preliminary applications, but there are much more to do with the vitality framework in the future.

Future directions might primarily cover five areas: 1) mathematical development to overcome some of the model limitations and further illustrate the model properties such as how to disentangle the cohort and period effects on mortality; 2) studies to explore how environmental, genetic, behavioral and social-economic factors affect the mortality process through the model parameters; 3) studies on the effects of early-age interventions on later-age survival with an extended model; 4) studies to model different disease processes, such as HIV and cancer; and 5) studies incorporating biological measurements for a more complex multi-stage process model. Overall, I believe the idea of looking at morbidity, mortality and aging through a process point of view has a brilliant future yet more theoretical developments are needed.

Reference

Aalen, O. O. and H. K. Gjessing (2001). "Understanding the shape of the hazard rate: a process point of view." Statistical Science **16**(1): 1-13.

Acsádi, G. and J. Nemeskéri (1970). History of human life span and mortality. Budapest, Akadémiai Kiadó.

Agren, G. and A. Romelsj (1992). "Mortality in alcohol-related diseases in Sweden during 1971?0 in relation to occupation, marital status and citizenship in 1970." Scandinavian Journal of Public Health **20**(3): 134.

Anderson, J. J. (1992). "A vitality-based stochastic model for organism survival." Individual-based models and approaches in ecology: populations, communities and ecosystems. Chapman & Hall, New York: 256-277.

Anderson, J. J. (2000). "A vitality-based model relating stressors and environmental properties to organism survival." Ecological Monographs **70**(3): 445-470.

Anderson, J. J., M. C. Gildea, et al. (2008). "Linking growth, survival, and heterogeneity through vitality." Am Nat **171**(1): E20-43.

Arbeev, K., S. Ukraintseva, et al. (2005). "Mathematical models for human cancer incidence rates." Demographic Research **12**(10): 237-260.

Ashok, B. T. and R. Ali (1999). "The aging paradox: free radical theory of aging." Experimental Gerontology **34**(3): 293-303.

Beckman, K. B. and B. N. Ames (1998). "The free radical theory of aging matures." Physiological Reviews **78**(2): 547.

Beisel, W. R. (1996). "Nutrition and immune function: overview." Journal of Nutrition **126**(10 Suppl): 2611S.

Benjamin, B. (1959). "Actuarial aspects of human lifespans." The Life Span of Animals **5**: 2–20.

Benjamin, B. (1989). "Demographic aspects of ageing." Annals of human biology **16**(3): 185-235.

Benton, T. G., S. J. Plaistow, et al. (2006). "Complex population dynamics and complex causation: devils, details and demography." Proceedings of the Royal Society B **273**(1591): 1173.

Berkman, L., B. Singer, et al. (1989). "Black/white differences in health status and mortality among the elderly." Demography **26**(4): 661-678.

Bongaarts, J. (2006). "How long will we live?" Population and Development Review **32**(4): 605-628.

Bonneux, L. (2003). "COMMENTARY: Benjamin Gompertz revisited." European Journal of Epidemiology **18**(6): 471-472.

Boyce, M., C. Haridas, et al. (2006). "Demography in an increasingly variable world." Trends in Ecology & Evolution **21**(3): 141-148.

Carey, J. and P. Liedo (1995). "Sex-specific life table aging rates in large medfly cohorts." Experimental Gerontology **30**(3-4): 315-325.

Carey, J., P. Liedo, et al. (1992). "Slowing of mortality rates at older ages in large medfly cohorts." Science **258**(5081): 457.

Carey, J. R., P. Liedo, et al. (1992). "Slowing of mortality rates at older ages in large medfly cohorts." Science **258**(5081): 457.

Carnes, B. A., L. R. Holden, et al. (2006). "Mortality partitions and their relevance to research on senescence." Biogerontology **7**(4): 183-198.
Carnes, B. A. and S. J. Olshansky (1997). "A biologically motivated partitioning of mortality." Experimental Gerontology **32**(6): 615-631.
Carnes, B. A., S. J. Olshansky, et al. (1996). "Continuing the search for a law of mortality." Population and Development Review **22**(2): 231-264.
Chandra, R. (1997). "Nutrition and the immune system: an introduction." American Journal of Clinical Nutrition **66**(2): 460S.
Chesnais, J. C. (1992). The demographic transition: stages, patterns, and economic implications: a longitudinal study of sixty-seven countries covering the period 1720-1984, Oxford University Press, USA.
Chhikara, R. S. and L. Folks (1989). The inverse Gaussian distribution: theory, methodology, and applications, CRC.
Clarke, R. (1950). A bio-actuarial approach to forecasting rates of mortality. Proceed Cent Assem Inst Act.
Coale, A. J. and E. E. Kisker (1986). "Mortality Crossovers: Reality or Bad Data?" Population Studies: A Journal of Demography **40**(3): 389-401.
Cohen, H. (2007). "The cancer aging interface: a research agenda." Journal of Clinical Oncology **25**(14): 1945.
Colizza, V., A. Barrat, et al. (2006). "The role of the airline transportation network in the prediction and predictability of global epidemics." Proceedings of the National Academy of Sciences of the United States of America **103**(7): 2015.
Congdon, P. (1993). "Statistical graduation in local demographic analysis and projection." Journal of the Royal Statistical Society. Series A (Statistics in Society) **156**(2): 237-270.
Cox, D. R. and H. D. Miller (1965). "The theory of stochastic processes." London: Methuen: 225.
Crimmins, E. (1981). "The changing pattern of American mortality decline, 1940-77, and its implications for the future." Population and Development Review **7**(2): 229-254.
Crimmins, E., J. K. Kim, et al. (2010). "Biodemography: New approaches to understanding trends and differences in population health and mortality." Demography **47**(S): S41-S64.
Crimmins, E. M. and C. E. Finch (2006). "Commentary: Do older men and women gain equally from improving childhood conditions?" International journal of epidemiology **35**(5): 1270.
Curtis, S. (2010). "Social Change and Health in Sweden: 250 Years of Politics and Practice (review)." Journal of Social History **43**(2): 509-512.
Cutler, D., A. Deaton, et al. (2006). "The determinants of mortality." The Journal of Economic Perspectives **20**(3): 97-120.
Cypser, J. R., P. Tedesco, et al. (2006). "Hormesis and aging in Caenorhabditis elegans." Experimental Gerontology **41**(10): 935-939.
Dellaportas, P., A. F. M. Smith, et al. (2001). "Bayesian analysis of mortality data." Journal of the Royal Statistical Society: Series A (Statistics in Society) **164**(2): 275-291.

Diderichsen, F. (1990). "Health and social inequities in Sweden." Social Science & Medicine **31**(3): 359-367.
Diderichsen, F. and J. Hallqvist (1997). "Trends in occupational mortality among middle-aged men in Sweden 1961-1990." International journal of epidemiology **26**(4): 782.
Eakin, T. and M. Witten (1995). "A gerontological distance metric for analysis of survival dynamics." Mechanisms of ageing and development **78**(2): 85-101.
Eakin, T. and M. Witten (1995). "How square is the survival curve of a given species?" Experimental Gerontology **30**(1): 33-64.
Engen, S., R. Lande, et al. (2003). "Demographic stochasticity and Allee effects in populations with two sexes." Ecology **84**(9): 2378-2386.
Finkelstein, M. (2007). "Aging: Damage accumulation versus increasing mortality rate." Mathematical Biosciences **207**(1): 104-112.
Fox, G. and B. Kendall (2002). "Demographic stochasticity and the variance reduction effect." Ecology **83**(7): 1928-1934.
Frenk, J., J. L. Bobadilla, et al. (1991). "Elements for a theory of the health transition." Health transition review: the cultural, social, and behavioural determinants of health **1**(1): 21.
Fried, L. P., C. M. Tangen, et al. (2001). "Frailty in Older Adults: Evidence for a Phenotype." The Journals of Gerontology Series A: Biological Sciences and Medical Sciences **56**(3): M146.
Fries, J. F. (2005). "The compression of morbidity." Milbank Quarterly **83**(4): 801-823.
Frost, W. H. (1995). "The age selection of mortality from tuberculosis in successive decades." American Journal of Epidemiology **141**(1): 4.
Gage, T. and C. Mode (1993). "Some laws of mortality: how well do they fit?" Human biology; an international record of research **65**(3): 445.
Gage, T. B. (1988). "Mathematical hazard models of mortality: an alternative to model life tables." American Journal of Physical Anthropology **76**(4): 429-441.
Gage, T. B. (1989). "Bio mathematical approaches to the study of human variation in mortality." American Journal of Physical Anthropology **32**(S10): 185-214.
Gage, T. B. (1990). "Variation and classification of human age patterns of mortality: analysis using competing hazards models." Human biology; an international record of research **62**(5): 589.
Gage, T. B. (1991). "Causes of death and the components of mortality: Testing the biological interpretations of a competing hazards model." American Journal of Human Biology **3**(3): 289-300.
Gage, T. B. (1993). "The decline of mortality in England and Wales 1861 to 1964: decomposition by cause of death and component of mortality." Population Studies **47**(1): 47-66.
Gallant, A. R. (1987). Nonlinear statistical models. New York, John Wiley.
Gavrilov, L. A. and N. S. Gavrilova (1991). The biology of life span: a quantitative approach, Harwood Academic Publishers, Chur [Switzerland]; New York.
Gavrilov, L. A. and N. S. Gavrilova (2001). "The reliability theory of aging and longevity." Journal of theoretical Biology **213**(4): 527-545.
Gavrilov, L. A. and N. S. Gavrilova (2004). "The reliability-engineering approach to the problem of biological aging." Annals of the New York Academy of Sciences

1019(Strategies for Engineered Negligible Senescence: Why Genuine Control of Aging May Be Foreseeable): 509-512.
Gavrilov, L. A., N. S. Gavrilova, et al. (1978). "The main regularities of animal aging and death viewed in terms of reliability theory." Journal of General Biology [Zhurnal Obschey Biologii] **39**: 734-742.
Golubev, A. (2004). "Does Makeham make sense?" Biogerontology **5**(3): 159-167.
Golubev, A. (2009). "How could the Gompertz-Makeham law evolve." Journal of theoretical Biology **258**(1): 1-17.
Gompertz, B. (1825). "On the nature of the function expressive of the law of human mortality, and on a new mode of determining the value of life contingencies." Philosophical Transactions of the Royal Society of London **115**: 513-583.
Grubeck-Loebenstein, B. and G. Wick (2002). "The aging of the immune system." Advances in immunology **80**: 243-284.
Gurven, M. and A. Fenelon (2009). "Has actuarial aging "slowed" over the past 250 years? A comparison of small-scale subsistence populations and european cohorts." Evolution **63**(4): 1017-1035.
Hacker, J. D. (1997). "Trends and determinants of adult mortality in early New England: reconciling old and new evidence from the long eighteenth century." Social Science History **21**(4): 481-519.
Haldane, J. B. S. (1990). The causes of evolution, Princeton Univ Pr.
Halley, E. (1694). "An estimate of the degrees of the mortality of mankind, drawn from curious tables of the births and funerals at the city of Breslaw; with an attempt to ascertain the price of annuities upon lives. ." Philosophical Transactions (1683-1775) **17**: 596-610.
Hamilton, W. D. (1966). "The moulding of senescence by natural selection." Journal of theoretical Biology **12**(1): 12-45.
Heckscher, E. (1950). "Swedish population trends before the industrial revolution." The Economic History Review **2**(3): 266-278.
Heligman, L. and J. Pollard (1980). "The age pattern of mortality." JIA **107**: 49-80.
Hemström, Ö. (1999). "Explaining differential rates of mortality decline for Swedish men and women: a time-series analysis, 1945-1992." Social Science & Medicine **48**(12): 1759-1777.
Herskind, A., M. McGue, et al. (1996). "Untangling genetic influences on smoking, body mass index and longevity: a multivariate study of 2464 Danish twins followed for 28 years." Human Genetics **98**(4): 467-475.
Himes, C. L. (1994). "Age patterns of mortality and cause-of-death structures in Sweden, Japan, and the United States." Demography **31**(4): 633-650.
HMD (2010). The Human Mortality Database.
Holt, P. and C. Jones (2000). "The development of the immune system during pregnancy and early life." Allergy **55**(8): 688-697.
Horiuchi, S. and J. R. Wilmoth (1998). "Deceleration in the age pattern of mortality at older ages." Demography **35**(4): 391-412.
Humphries, J. (1991). "'Bread and a pennyworth of treacle': excess female mortality in England in the 1840s." Cambridge journal of economics **15**(4): 451.
Janzen, V., R. Forkert, et al. (2006). "Stem-cell ageing modified by the cyclin-dependent kinase inhibitor p16INK4a." Nature **443**(7110): 421-426.

Johansson, S. R. (1984). "Deferred infanticide: Excess female mortality during childhood." Infanticide: Comparative and evolutionary perspectives: 463-485.
Johnson, N. E. (2000). "The racial crossover in comorbidity, disability, and mortality." Demography **37**(3): 267-283.
Kendall, M. G., A. Stuart, et al. (1977). The advanced theory of statistics, C. Griffin.
Khazaeli, A. A., L. Xiu, et al. (1995). "Stress experiments as a means of investigating age-specific mortality in Drosophila melanogaster." Experimental Gerontology **30**(2): 177-184.
Kirkwood, T. and R. Holliday (1979). "The evolution of ageing and longevity." Proceedings of the Royal Society of London. Series B, Biological Sciences **205**(1161): 531-546.
Kirkwood, T. B. L. and S. N. Austad (2000). "Why do we age?" Nature **408**(6809): 233-238.
Klasen, S. (1998). "Marriage, bargaining, and intrahousehold resource allocation: Excess female mortality among adults during early German development, 1740-1860." Journal of Economic History **58**(2): 432-467.
Krementsova, A. V. and A. A. Konradov (2001). "Historical dynamics of life-span distribution of Man." Advances in gerontology= Uspekhi gerontologii/Rossi skai a akademii a nauk, Gerontologicheskoe obshchestvo **8**: 14.
Kunitz, S. J. (1984). "Mortality change in America, 1620-1920." Human biology; an international record of research **56**(3): 559.
Kunitz, S. J. (1986). Mortality since Malthus, Oxford.
Lerner, M. (1973). "Modernization and health: A model of the health transition." American Public Health Association, San Francisco.
Li, T. and J. J. Anderson (2009). "The vitality model: A way to understand population survival and demographic heterogeneity." Theoretical Population Biology **76**(2): 118-131.
Li, T. and J. J. Anderson (2010). "The explanation of age-specific patterns in cancer incidence rate by the vitality model (draft)."
Makeham, W. M. (1860). "On the law of mortality and the construction of annuity tables." Journal of the Institute of Actuaries **8**: 301?310.
Makinodan, T. and W. H. Adler (1975). Effects of aging on the differentiation and proliferation potentials of cells of the immune system.
Manton, K. G., E. Stallard, et al. (1991). "Limits to human life expectancy: Evidence, prospects, and implications." Population and Development Review **17**(4): 603-637.
Mason, W. M. and H. L. Smith (1985). Age-Period-Cohort analysis and the Study of Deaths from Pulmonary Tuberculosis. Cohort analysis in social research: beyond the identification problem. W. M. Mason and S. E. Fienberg. New York, Springer-Verlag.
McGlnnis, J. M. and W. H. Foege (1993). "Actual causes of death in the United States." JAMA **270**(18): 2208.
McGue, M., J. Vaupel, et al. (1993). "Longevity is moderately heritable in a sample of Danish twins born 1870-1880." The Journal of Gerontology **48**(6): B237.
McKeown, T. (1976). The modern rise of population, Edward Arnold London.

Miller, R. A. (1996). "The aging immune system: primer and prospectus." Science **273**(5271): 70.
Milne, E. M. G. (2010). "Dynamics of human mortality." Experimental Gerontology **45**(3): 180-187.
Min, K. and M. Tatar (2006). "Drosophila diet restriction in practice: do flies consume fewer nutrients?" Mechanisms of ageing and development **127**(1): 93-96.
Mitnitski, A. B., J. E. Graham, et al. (2002). "Frailty, Fitness and Late-Life Mortality in Relation to Chronological and Biological Age." BMC geriatrics **2**(1): 1.
Mode, C. J. and R. C. Busby (1982). "An Eight-parameter Model of Human Mortality: The Single Decrement Case." Bulletin of Mathematical Biology **44**(5): 647-659.
Mode, C. J. and M. E. Jacobson (1984). "A Parametric Algorithm for Computing Model Period and Cohort Human Survival Functions." International journal of bio-medical computing **15**(5): 341.
Mueller, L. D., M. D. Drapeau, et al. (2003). "Statistical tests of demographic heterogeneity theories." Experimental Gerontology **38**(4): 373-386.
Nathanson, C. A. (1984). "Sex differences in mortality." Annual Review of Sociology **10**: 191-213.
Neafsey, P. (2008). "A mathematical modeling approach to characterize hormesis, caloric restriction and toxicity in mortality data from toxicity studies." American Journal of Pharmacology and Toxicology **3**(1): 80-92.
Oeppen, J. and J. W. Vaupel (2002). "Demography: enhanced: broken limits to life expectancy." Science **296**(5570): 1029.
Olsen, A., M. C. Vantipalli, et al. (2006). "Lifespan extension of Caenorhabditis elegans following repeated mild hormetic heat treatments." Biogerontology **7**(4): 221-230.
Olshansky, S. and B. Carnes (1997). "Ever since Gompertz." Demography **34**(1): 1-15.
Omran, A. R. (1977). "Epidemiologic transition in the United States: the health factor in population change." Population Bulletin **32**(2): 1.
Omran, A. R. (1982). Epidemiologic transition. International encyclopedia of population. New York, The Free Press**:** 172-183.
Owens, I. P. F. (2002). "Sex differences in mortality rate." Science **2002**(297): 2008-2009.
Passos, J. F., G. Saretzki, et al. (2007). "DNA damage in telomeres and mitochondria during cellular senescence: is there a connection?" Nucleic Acids Research **35**(22): 7505.
Pletcher, S. D., D. Houle, et al. (1998). "Age-specific properties of spontaneous mutations affecting mortality in Drosophila melanogaster." Genetics **148**(1): 287.
Preston, S. (1975). "The changing relation between mortality and level of economic development." Population Studies **29**(2): 231-248.
Preston, S., P. Heuveline, et al. (2001). "Demography: measuring and modeling population processes." Population and Development Review **27**(2): 365.
Preston, S. H. and H. Wang (2006). "Sex mortality differences in the United States: the role of cohort smoking patterns." Demography **43**(4): 631-646.
Prieto, M., J. Llorca, et al. (1996). "Longitudinal Gompertzian and Weibull analyses of adult mortality in Spain (Europe), 1900-1992." Mechanisms of ageing and development **90**(1): 35-51.

Prieto, M. D., J. Llorca, et al. (1996). "Longitudinal Gompertzian and Weibull analyses of adult mortality in Spain (Europe), 1900-1992." Mechanisms of ageing and development **90**(1): 35-51.
Promislow, D., M. Tatar, et al. (1996). "Age-specific patterns of genetic variance in Drosophila melanogaster. I. Mortality." Genetics **143**(2): 839.
Rauser, C. L., L. D. Mueller, et al. (2006). "The evolution of late life." Ageing research reviews **5**(1): 14-32.
Riggs, J. E. (1990). "Longitudinal Gompertzian analysis of adult mortality in the US, 1900-1986." Mech. Ageing Dev **54**: 235?247.
Riggs, J. E. and R. J. Millecchia (1992). "Using the Gompertz-Strehler model of aging and mortality to explain mortality trends in industrialized countries." Mechanisms of ageing and development **65**(2-3): 217.
Riley, J. C. (2001). Rising life expectancy: a global history, Cambridge Univ Pr.
Rodgers, G. (2002). "Income and inequality as determinants of mortality: an international cross-section analysis." International journal of epidemiology **31**(3): 533.
Rose, M. R. (1991). Evolutionary biology of aging, Oxford University Press, USA.
Rose, M. R., M. K. Burke, et al. (2008). "Evolution of ageing since Darwin." Journal of genetics **87**(4): 363-371.
Ryder, N. B. (1965). "The cohort as a concept in the study of social change." American sociological review **30**(6): 843-861.
Saccheri, I. and I. Hanski (2006). "Natural selection and population dynamics." Trends in Ecology & Evolution **21**(6): 341-347.
Sacher, G. and E. Trucco (1962). "The Stochastic Theory of Mortality." Annals of the New York Academy of Sciences **96**(Mathematical Theories of Biological Phenomena): 985-1007.
Sacher, G. A. (1956). "On the statistical nature of mortality, with especial reference to chronic radiation mortality." Radiology **67**(2): 250.
Salinger, D., J. Anderson, et al. (2003). "A parameter estimation routine for the vitality-based survival model." Ecological Modelling **166**(3): 287-294.
Schofield, R., D. S. Reher, et al. (1991). The decline of mortality in Europe, Oxford University Press, USA.
Service, P. M. (2000). "Heterogeneity in individual mortality risk and its importance for evolutionary studies of senescence." The American Naturalist **156**(1): 1-13.
Service, P. M. (2004). "Demographic heterogeneity explains age-specific patterns of genetic variance in mortality rates." Experimental Gerontology **39**(1): 25-30.
Shock, N. W. (1957). "Age changes in some physiologic processes." Survey of Anesthesiology **1**(6): 619.
Shryock, H. S., J. S. Siegel, et al. (1980). The methods and materials of demography, Dept. of Commerce, Bureau of the Census: for sale by the Supt. of Docs. US Govt. Print. Off.
Siler, W. (1979). "A competing-risk model for animal mortality." Ecology **60**(4): 750-757.
Soares, R. (2007). "On the determinants of mortality reductions in the developing world." Population and Development Review **33**(2): 247-287.
Sprott, R. (1997). "Diet and calorie restriction." Experimental Gerontology **32**(1-2): 205-214.

Steinsaltz, D. and S. N. Evans (2004). "Markov mortality models: implications of quasistationarity and varying initial distributions." Theoretical Population Biology **65**(4): 319-337.
Steinsaltz, D. and S. N. Evans (2007). "Quasistationary distributions for one-dimensional diffusions with killing." Transactions-American Mathematical Society **359**(3): 1285.
Strehler, B. L. and A. S. Mildvan (1960). "General theory of mortality and aging." Science **132**(3418): 14-21.
Sundin, J. and S. Willner (2007). "Social change and health in Sweden: 250 years of politics and practice."
Thiele, P. N. (1872). "On a mathematical formula to express the rate of mortality throughout the whole of life." Journal of the Institute of Actuaries **16**: 313?329.
Ungvari, Z., G. Kaley, et al. (2010). "Mechanisms of vascular aging: new perspectives." The Journals of Gerontology Series A: Biological Sciences and Medical Sciences **65**(10): 1028.
UNICEF. (2010). "Why are millions of children and women dying?", from http://www.unicef.org/health/index_problem.html.
Vagero, D. and O. Lundberg (1993). Socio-economic Mortality Differentials Among Adults in Sweden: Towards an Explanation, Swedish Institute for Social Research.
Vaupel, J. (2010). "Biodemography of human ageing." Nature **464**(7288): 536-542.
Vaupel, J., K. Manton, et al. (1979). "The impact of heterogeneity in individual frailty on the dynamics of mortality." Demography: 439-454.
Vaupel, J. W. (2004). "The biodemography of aging." Population and Development Review **30**: 48-62.
Vaupel, J. W., J. R. Carey, et al. (1998). "Biodemographic trajectories of longevity." Science **280**(5365): 855.
Vaupel, J. W. and A. I. Yashin (1985). "Heterogeneity's ruses: some surprising effects of selection on population dynamics." The American Statistician **39**(3): 176-185.
Waldron, I. (1983). "Sex differences in human mortality: the role of genetic factors." Social Science & Medicine **17**(6): 321-333.
Wall, S., M. Rosen, et al. (1985). "The Swedish mortality pattern: a basis for health planning?" International journal of epidemiology **14**(2): 285.
Wang, H. and S. H. Preston (2009). "Forecasting United States mortality using cohort smoking histories." Proceedings of the National Academy of Sciences **106**(2): 393.
Weismann, A. (1891). Essays upon heredity and kindred biological problems, Clarendon press.
Weitz, J. S. and H. B. Fraser (2001). "Explaining mortality rate plateaus." Proceedings of the National Academy of Sciences **98**(26): 15383.
Wiegel, D., W. Beier, et al. (1973). "Vitality and error rate in biological systems: some theoretical considerations." Mechanisms of ageing and development **2**(2): 117.
Wilmoth, J. R., L. J. Deegan, et al. (2000). "Increase of maximum life-span in Sweden, 1861-1999." Science **289**(5488): 2366.
Wilmoth, J. R. and V. Shkolnikov (2010). The Human Mortality Database.
Wingard, D. L. (1982). "The sex differential in mortality rates: demographic and behavioral factors." American Journal of Epidemiology **115**(2): 205.

Wittstein, J. (1883). "The mathematical law of mortality." Journal of the Institute of Actuaries **24**: 152-173.

Wu, D., J. Cypser, et al. (2009). "Multiple mild heat-shocks decrease the Gompertz component of mortality in Caenorhabditis elegans." Experimental Gerontology **44**(9): 607-612.

Wu, D., S. L. Rea, et al. (2006). "Visualizing hidden heterogeneity in isogenic populations of C. elegans." Experimental Gerontology **41**(3): 261-270.

Yashin, A. I., A. S. Begun, et al. (2001). "The new trends in survival improvement require a revision of traditional gerontological concepts." Experimental Gerontology **37**(1): 157-167.

Yashin, A. I., A. S. Begun, et al. (2002). "New age patterns of survival improvement in Sweden: do they characterize changes in individual aging?" Mechanisms of Ageing and Development **123**(6): 637-647.

Yashin, A. I., J. R. Cypser, et al. (2001). "Ageing and survival after different doses of heat shock: the results of analysis of data from stress experiments with the nematode worm Caenorhabditis elegans." Mechanisms of Ageing and Development **122**(13): 1477-1495.

Yashin, A. I. and I. A. Iachine (1997). "How Frailty Models Can Be Used for Evaluating Longevity Limits: Taking Advantage of an Interdisciplinary Approach." Demography **34**(1): 31-48.

Yashin, A. I., I. A. Iachine, et al. (2000). "Mortality modeling: a review." Mathematical Population Studies **8**(4): 305-332.

Yashin, A. I., S. V. Ukraintseva, et al. (2002). "Individual aging and mortality rate: how are they related?" Social Biology **49**(3/4): 206-217.

Yashin, A. I., S. V. Ukraintseva, et al. (2001). "Have the oldest old adults ever been frail in the past? A hypothesis that explains modern trends in survival." Journals of Gerontology Series A: Biological and Medical Sciences **56**(10): 432.

Yin, D. and K. Chen (2005). "The essential mechanisms of aging: Irreparable damage accumulation of biochemical side-reactions." Experimental Gerontology **40**(6): 455-465.

Zens, M. S. and D. R. Peart (2003). "Dealing with death data: individual hazards, mortality and bias." Trends in Ecology & Evolution **18**(7): 366-373.

Zheng, H., Y. Yang, et al. (2011). "Heterogeneity in the Strehler-Midvan General Theory of Mortlaity and Aging (Accepted)." Demography **47**.

Appendix A: *R* ® Code for Model Parameter Estimation (6-parameter version)

Based on the code of Salinger et al. 2006 for the 3- parameter model of Anderson (2000)

```
#======function for data preparation==================================

dataPrep<-function(time,sdata,datatype,rc.data)
#
#  Function to deal with NAs, right truncated data and datatype cumulative survival or
#  incremental motality.
{
        #check for and remove NAs from data
         if (any(is.na(time))) {
          naT=is.na(time)
                    time  =time[!naT]
                    sdata =sdata[!naT]
                    warning(message="WARNING:  NAs found in data and removed.")
          }
          if (any(is.na(sdata))) {
                   naT=is.na(sdata)
                    time   =time[!naT]
                    sdata =sdata[!naT]
                    warning(message="WARNING:  NAs found in data and removed.")
          }

          if(length(time) < 5) {
                   stop(message="ERROR:  not enough data.")
         }

          if(!all(0<=sdata) || !all(sdata<=1)) {
                    stop("ERROR:  survival fraction data outside range.")
          }
# end data checking
   maxx2 <-max(time)  #for right-censored data and for plotting
# === check data type (CUMulative or INCremental.  If CUM, create INC ===
if (datatype == "CUM") {
          #====== survival assumed =1 at time 0 ===
          if (time[1] > 0) {
                    time <-c(0,time)
                    sdata <-c(1,sdata)
          }
          else {
                    if (sdata[1] < 1) {
                              sdata<-sdata/sdata[1]
                              warning(message="Initial survival < 1.  Data scaled so that initial
                                        survival =1.")
                    }
          }

          #------------------------
          sfract <-sdata
```

```
        len<-length(time)
        #  ...set up data for MLE fitting of incremental survivorship...

        # --------- right censored data?
        if (rc.data != T) {
                if (rc.data == F) {
                        #check if final sdata indicates full mort
                        if (sfract[len] != 0) {
                                warning("WARNING: Survival data may be right censored...")
                                rc.data<-"TF"
                        }
                        else {
                                #standard setup
                                x1 <-c(time[1:(len-1)],0)
                                x2 <-c(time[2:len],0)
                                sfract1 <-c(sfract[1:(len-1)],0)
                                sfract2 <-c(sfract[2:len],0)
                        }
                }
                if (rc.data == "TF") {
                        #setup: add zero sruv and short time step  ("TF" option)
                        x1 <-time
                        x2 <-c(time[2:len],2*time[len]-time[len-1])
                        sfract1 <-sfract
                        sfract2 <-c(sfract[2:len],0)
                }

        }
        else {                  #if rc.data == T
                x1 <-time
                x2 <-c(time[2:len],10*maxx2)        #testing...
                sfract1 <-sfract
                sfract2 <-c(sfract[2:len],0)
        }
        # -----------------  end of dealing with right censored data options

        Ni <-sfract1-sfract2     #incrimental survival fraction

        #  ...end conversion of cumulative survivorship to incremental mortality

}

else {
        if (datatype == "INC") {
                lent<-length(time)
                #should be no t=0 data.  Eliminate if necessary.
                if(time[1] == 0) {
                        time  <-time[2:lent]
                        sdata <-sdata[2:lent]
                        lent  <-length(time)
                }
                #check for right censored data
                if (rc.data != T) {
                        if (rc.data == F) {
                                if(sum(sdata) < 1) {
                                        rc.data <-"TF"
```

```
                                        warning("WARNING: Survival data may be right
                                            censored...")
                                }
                                else {
                                        #standard setup
                                        Ni <-sdata
                                        x1 <-c(0,time)[1:lent]
                                        x2 <-time
                                }
                        }
                        if (rc.data == "TF") {
                                #setup: add zero sruv and short time step  ("TF" option)
                                Ni <-c(sdata,1-sum(sdata))
                                x1 <-c(0,time)
                                x2 <-c(time,2*time[lent]-time[lent-1])
                            #final time interval assumed same as prev.
                          }

                }
                else {      #if rc.data == T
                        Ni <-c(sdata,1-sum(sdata))
                        x1 <-c(0,time)
                        x2 <-c(time,10*maxx2)    #final time interval large
                }

                # Build cumulative data
               sfract<-NULL
                for (i in 1:length(Ni)) {
                        sfract <-c(sfract,1-sum(Ni[1:i]))
                }

        time<-c(0,time)
             len<-length(time)   #check
             print(c(length(sfract),length(time),length(Ni),length(x1),length(x2),lent))

        }
    else {
                stop("ERROR:  bad datatype specification")
        }
}

    return(data.frame(time,sfract,x1,x2,Ni,rc.data))
}

#=============survival function  l(x) = l_i(x) l_e(x) ==========================
SurvFn.2p<-function(xx,r,s,lambda,beta,mu0,alpha)
 #  The cumulative survival distribution function.
{
          yy<-s^2*xx
          # pnorm is: cumulative prob for the Normal Dist.
          tmp1 <- sqrt(1/yy) * (1 - xx * r)    #  xx=0 is ok.  pnorm(+-Inf) is defined
          tmp2 <- sqrt(1/yy) * (1 + xx * r)

          # --safeguard if exponent gets too large.---
          tmp3 <- 2*r/(s*s)
```

```
        if (tmp3 >250) {
                q <-tmp3/250
                if (tmp3 >1500) {
                        q <-tmp3/500
                }
                valueFF <-(1.-(pnorm(-tmp1) + (exp(tmp3/q) *pnorm(-tmp2)^(1/q))^(q)))*exp(-
                        lambda*exp(-1/beta)/(r/beta)*(exp(r*xx/beta)-1) +mu0/alpha*(exp(-
                        alpha*xx)-1))
        }
        else {
                valueFF <-(1.-(pnorm(-tmp1) + exp(tmp3) *pnorm(-tmp2)))*exp(-lambda*exp(-
                        1/beta)/(r/beta)*(exp(r*xx/beta)-1)+ mu0/alpha*(exp(-alpha*xx)-1))
        }
        if ( all(is.infinite(valueFF)) ) {
                warning(message="Inelegant exit caused by overflow in evaluation of survival
                        function. Check for right-censored data. Try other initial values.")
        }

        return(valueFF)
}

#=============incremental survival probability==============================
survProbInc.2p<-function(r,s,lambda,beta,mu0,alpha,xx1,xx2)
# calculates incremental survival probability
{
        value.iSP <--(SurvFn.2p(xx2,r,s,lambda,beta,mu0,alpha) –
                SurvFn.2p(xx1,r,s,lambda,beta,mu0,alpha))
        value.iSP[value.iSP < 1e-18] <-1e-18   # safeguards against taking Log(0)
        value.iSP
}

#=============likelihood function ======================================
logLikelihood.2p<-
function(par,xx1,xx2,NNi)
{
        #returns the log likelihood
        # --calculate incremental survival probability--- (safeguraded >1e-18 to prevent log(0))
        iSP <-  survProbInc.2p(par[1],par[2],par[3],par[4],par[5],par[6],xx1,xx2)
  loglklhd <--NNi*log(iSP)
  return(sum(loglklhd))
}

#==========Newton-Ralphson method for MLE=========================
fit.nlm.2p<-nlminb(vector of initial parameter values, obj=logLikelihood.2p,lower=c(0,-1, 0, 0, 0,
0),upper=c(100,50,100,1000,10,10),xx1=x1,xx2=x2,NNi=Ni)

#==========Example=============================================
#==========Data=============================================
age<-(0:110)            #age from 0 to 110 with time interval equal 1
sdata<-c(1.000,    0.995, 0.994, 0.994, 0.994, 0.994, 0.994, 0.994,        0.993, 0.993, 0.993, 0.993,
        0.993, 0.993, 0.993, 0.992, 0.992, 0.992, 0.992, 0.991, 0.991, 0.991, 0.990, 0.990, 0.990,
        0.989, 0.989, 0.988, 0.988, 0.988, 0.987, 0.987, 0.986,           0.986, 0.985, 0.985, 0.984,
        0.983, 0.983, 0.982, 0.981, 0.980, 0.979, 0.978, 0.976, 0.975, 0.973, 0.971, 0.969, 0.967,
        0.965, 0.962, 0.959, 0.957, 0.954, 0.951, 0.946, 0.943, 0.938, 0.932, 0.927, 0.921, 0.915,
        0.909, 0.901, 0.894, 0.885, 0.876, 0.865, 0.853, 0.842, 0.828, 0.812, 0.796, 0.778, 0.758,
```

```
        0.736, 0.712, 0.686, 0.657, 0.624, 0.589, 0.554, 0.514, 0.475, 0.433, 0.391, 0.347, 0.306,
        0.263, 0.221, 0.184, 0.149, 0.118, 0.091, 0.068, 0.050, 0.035, 0.024, 0.016, 0.010, 0.006,
        0.004, 0.002, 0.001, 0.001, 0.000, 0.000, 0.000,        0.000, 0.000)
        #survival rate data, fraction of survival at each age

#==========Data preparation=========================================
rc.data<-F            #if survival data are censored rc.data<-T, otherwise rc.data<-F
datatype="CUM"  #"CUM" means data are survival fraction data

dTmp<-dataPrep(age,sdata,datatype,rc.data)
#use data preparation function to obtain clean data-frame dTmp
time<-dTmp$time
sfract<-dTmp$sfract
x1<-dTmp$x1
x2<-dTmp$x2
Ni<-dTmp$Ni
rc.data<-dTmp$rc.data

fit.nlm.2p<-nlminb(c(0.01,0.01,0.1,0.2,0.01,0.1), obj=logLikelihood.2p,lower=c(0,-1, 0, 0, 0,
0),upper=c(100,50,100,1000,10,10),xx1=x1,xx2=x2,NNi=Ni)

fit.nlm.2p$par    #gives the parameter estimation

#compare model fit with original data from plot
par(cex=1.8,lwd=1.8,mar=c(4.5,4,2,1))
plot(time,sfract,main=paste("Survival curve"),type="n",ylab="Survival rate",xlab="age")
points(time,sfract,cex=0.7,pch=20)
lines(time,SurvFn.2p(time,fit.nlm.2p$par[1],fit.nlm.s2p$par[2],fit.nlm.2p$par[3],fit.nlm.2p$par[4],fit.nlm.2
p$par[5],fit.nlm.2p$par[6]),col=2,lwd=2)
```

Note:

1. Choosing appropriate initial values for parameters is critical to obtain reliable parameter estimations. If the initial parameters are far from the real values, the likelihood estimation would probably get stuck in local minimum or even not converge. If nlminb report errors, in most case it means the MLE does not converge. Choose another set of initial values and try again.

2. If sdata is incremental mortality (rather than cumulative survival), set datatype=”INC”.

3. Choosing time scale for the original data should be careful. If the time scale is too small (eg. days for the population which can survival over 60 years), the estimated r and s would be too tiny to be precise.

Appendix B: *R* ® Code for Conducting Simulations

```
#=========generate survival curves from simulated vitality trajectories===============
#function for generating single vitality trajectory from the Wiener process
gen<-function(r,s,T){
       i=1
       v0<-rnorm(1,1,0)      #generate initial vitality, in this case all individuals start from value 1
       vt<-rep(0,T)
       vt[1]<-v0
       w.t<-rnorm(T,0,1)    #generate white noise for each step
       while(vt[i]>0&i<T){
            vt[i+1]<-vt[i]-r+s*w.t[i]    #update vitality for each age according to Wiener process
            i=i+1
      }
      return(vt)
}

#function for generating survival curves
genSurvFn<-function(rr, ss, alpha, beta, TT, L, pplot=F){
     v1<-sapply(1:L,function(r,s,T)  gen(rr,ss,TT))
     #generate vitality trajectories for a population of L with r = rr, s = ss and age from 0 to TT-1
     r.temp2<-rep(1,L)
     sum.temp1<-rep(L,100)
     for(t in 2:TT){
          r.temp1<-rbinom(n=L,size=1,exp(-alpha/2*(exp((-v1[t,])/beta)+exp((-v1[t-
                    1,])/beta))))*r.temp2              #extrinsic killings
          r.temp2<-r.temp1*(v1[t,]>0)
          sum.temp1[t]<-sum(r.temp2)
      }
     time<-(0:(TT-1))
     sfract<- sum.temp1/L
     if(pplot==T){
          plot(time,sfract, xlab="time", ylab="survival fraction", main="generated survival curve")
     }
     return(data.frame(time,sfract))
}

#====================example=================================
set.seed(1982)          #set a random seed
data.surv<-genSurvFn(0.012,0.012,0.1,0.2,100,10000,pplot=T)
```

VITA

Ting Li was born in Chengdu, China and spent most of her life before age 18 in that beautiful city. Then she moved to Beijing and earned a Bachelor of Science in Statistics after four years' study at Peking University. Seattle became her second hometown afterwards where she spent five and half years. During that period, she got a Master of Sciences from the program of Quantitative Ecology and Resource Management at University of Washington. In 2011 she finished her study at the University of Washington and earned a Doctor of Philosophy.